CZECH TECHNICAL UNIVERSITY IN PRAGUE

Faculty of Civil Engineering

Experimental Centre

Cement Composites Used for Radioactive Waste Deposition

Cementové kompozity pro ukládání radioaktivního odpadu

HABILITATION THESIS – COLLECTION OF PUBLISHED SCIENTIFIC PAPERS

Ing. Jan Zatloukal, Ph.D.

Prague, 2025

I declare that this thesis and the work presented in it are my own and has been generated by me as the result of my own original research. Wherever contributions of others are involved, every effort is made to indicate this clearly, with due reference to the literature, and acknowledgement of collaborative research and discussions.

Prague, 12. 5. 2025

…….

Jan Zatloukal

Acknowledgement

Large portions of this work were performed as parts of research project TK01030058: Non-solid radioactive waste permanent disposal technology, funded by TA CR, Technology Agency of the Czech Republic, under the Theta programme.

Abstract

Presented work summarizes course of work during development of solidification matrix based on special cement binder designated for solidification of liquid radioactive waste before final reposition in near-surface underground repository. Expected utilization of the matrix is during conditioning of low- and intermediate-level radioactive waste, originating during normal operation of nuclear reactors. Such waste consists mainly of evaporator concentrates, produced in processing of primary coolant of the reactor and their radioactive inventory consists mostly of isotopes Cs-137 and Co-60. Requirements for their safe disposition usually does not exceed 500 years, during which the radionuclides contained in the waste decay to safe level at which there is no further risk of radioactive contamination of the environment. Suitable material was developed as a result of research project TK01030058: Non-solid radioactive waste permanent disposal technology, enabling solidification of evaporator concentrated with their high content od boric acid and other chemicals, usually preventing solidification of ordinary Portland cement.

The thesis takes form of compilation of impacted papers, published in journals during research work performed on the project. Each chapter deals with specific field of the investigated topic.

Keywords: radioactive waste management, repository, evaporator concentrate, cement composite, radionuclides´ immobilization

Abstrakt

Předkládaná práce shrnuje postup vývoje solidifikační matrice na bázi speciálních cementů, určené pro ztužování kapalných radioaktivních odpadů před jejich definitivním uložením v přípovrchovém podzemním úložišti. Předpokládané užití matrice je při zpracování nízko a středněaktivních radioaktivních odpadů, vznikajících při běžném provozu energetických reaktorů. Jedná se především o odparkové koncentráty, vznikající při úpravě chladiva primárního okruhu, obsahující především Cesium-137 a v male míře I Kobalt-60. Požadavek na jejich bezpečné uložení obvykle nepřesahuje 500 let, během nichž obsažené radioizotopy vymřou na bezpečnou úroveň a dále již nehrozí kontaminace prostředí radioaktivními látkami. V rámci řešení výzkumného projektu TK01030058: Technologie pro trvalé ukládání netuhých radioaktivních odpadů byl vyvinut material, umožňující ztužení těchto odparkových koncentrátů pomocí speciálních cementů, i přes vysoký obsah kyseliny borité a dalších chemikálií v koncentrátu, které by jinak zabraňovaly ztuhnutí běžného portlandského cementu.

Práce má formu kompilátu odborných článků v impaktovaných žurnálech, které byly během řešení projektu publikovány. Jednotlivé kapitoly jsou zamřené vždy na jeden konkrétní aspekt problematiky.

Klíčová slova: zpracování radioaktivních odpadů, podzemní úložiště, odparkové koncentráty, cementový kompozit, imobilizace radionuklidů

Table of contents

List of Figures

List of Tables

Introduction

American journalist David Dietz in his book “Atomic energy”, published in 1947, described his vision of future with abundant energy due to utilization of then very recently discovered nuclear energy. In his vision, the future world of atomic energy was to be as different from his present, as much as mid-twentieth century was from ancient Egypt. He described world with nearly unlimited natural resources due to availability of clean, cheap energy, provided by nuclear power plants, allowing for extraction of every possible raw material from seawater and ores containing only trace amounts of desired material. Transportation in the age of nuclear energy was to be cheap, fast and reliable, with unlimited range of supersonic aircraft with nuclear propulsion and land vehicles requiring refuelling only once a year. Weather manipulation would be possible due to use of nuclear energy, either by removing clouds using heat or creation of nuclear-powered artificial suns, used for heating in otherwise inhospitable areas – in this case Dietz notes, that working nuclear source of heat and light would require some form of shielding against deadly radiation, originating in the fission process, but is sure, that future engineers will surely deal with such setback. This vision of abundance of energy and resources led Dietz to assumption, that there will be no more need for competition for oil, coal and other commodities, thus leading to the end of all wars. What a lovely vision. Unfortunately, one tiny little problem stood in its way.

Soon after discovery of nuclear fission, it was found, that not only breath-taking amounts of energy emerge from the split fissionable nucleus, but also some undesirable waste material is produced. The fission products were found to be highly radioactive and dangerous if not treated properly. Not only the fission product themselves, but also other, previously harmless materials, exposed to stream of neutrons emerging from nuclei splitting, were found to be radioactive and thus harmful to living beings. Previous experience with x-ray machines and radium showed, that ionizing radiation has great potential to cause severe health issues and even death, as experienced by the pioneers of the field of radiation physics: Marie Curie died of radiation induced aplastic anemia, her daughter Irene Joliot-Curie died of radiation induced leukemia, workers of the Undark corporation, that painted watch dials and hands with self-luminous radium containing paint died of radiation poisoning. These known health issues, related with radiation exposure indicated that this newly discovered phenomena must be treated with care and respect, as long as ionizing radiation itself is undetectable by human senses (except for extremely severe cases) and uncontrolled release of radioactive substances into the environment is very dangerous.

The problem of safe disposal of radioactive waste emerged together with the implementation of industrial-scale plants for fissile material production. Early on, during the period of Manhattan project, the fissile material was intended for military use. This consisted of highly enriched weapons-grade uranium with about 90% content of ^{235}U isotope and ^{239}Pu produced in reactors. During the early era of industrial production of fissile material, the only priority was to produce as many nuclear bombs as possible in the shortest amount of time, with other concerns, like safety and waste management, being side-lined. This led to serious accidents and even without such accidents, to accumulation of considerable quantities of radioactive waste material at the sites of weapons-grade uranium and plutonium production, considering dealing with it a problem for future generations. During these early days, the measures to prevent leaks of radioactive materials to the environment were inadequate, resulting in release of radioactive substances in the air, soil and water. These leaks resulted into statistically significant increase in cancer rate in population surrounding these areas.

In USA themselves several such sites were located, where untreated radioactive waste was stored: most famous the Hanford Site, where the production of plutonium took place and the Oak Ridge K-25

uranium enrichment facility, later in the 1950's accompanied with Savannah River Site facility for refining weapons-grade nuclear materials.

The United Kingdom also has its famous radiation-leaking facility, the Sellafield reprocessing plant, built on the site of Windscale plutonium producing air-cooled graphite reactor, which caught fire in 1957, releasing fission products in the air, resulting in approximately 250 fatal cancer cases in the following years. By the time of the accident, little was known about Wigner effect, where dislocations occur in crystalline structure of material bombarded by neutrons, resulting in potential energy build-up, which can be released in form of spontaneous pulse of heat. Such burst of energy overheated the reactor, resulting in graphite fire.

Still, the worst radiation incident in the history (except for Chernobyl disaster) took place, by no surprise, in the Soviet Union, few days before the aforementioned Windscale fire of 1957 in the, by no surprise, plutonium production facility Chelyabinsk-40, also known as Mayak complex. This incident, referred to as the Kyshtym disaster, was a storage tank explosion, that released about 4.4 exabecquerels (about 75-90 % as Chernobyl) of radioactivity into the environment. About 270 000 people were affected, with about 200 having died of acute radiation syndrome and number of fatal cancer cases being thoroughly covered up by the USSR. Even without the explosion, radiation contamination of the surrounding environment of the Mayak complex was very severe, as the radioactive waste was untreated dumped in the Techa river. After the disaster, the practice of dumping radioactive waste into the river ceased and the waste was dumped in nearby lakes instead. Lake Karachay, right next to the facility, is to this day the most radioactive place in the world, in some spots capable of dealing lethal dose of radiation to human in about 30 minutes of exposure. In 1968 the shallow lake temporarily dried up and wind carried dust form the lake bed, irradiating approximately half million people in the area.

Radiotoxic incidents outside weapons production and most famous power plant-related accidents, such as Chernobyl, Three Mile Island and Fukushima disasters are almost exclusively of two kinds: medicinal radiotherapy incidents, when patients receive miscalculated dose of radiation during their treatment and incidents with orphaned or mishandled radiation sources. Vast majority of these incidents involve gamma sources with ^{60}Co and ^{137}Cs, as these radioisotopes are most common and easily available. There is wide spectrum of medical and industrial applications, utilizing ionizing radiation, from simple measuring of thickness of materials, detecting level of liquids, radiography, medical diagnostics and treatment and even disinfection and food preserving. Cobalt sources are in this respect less dangerous, because cobalt comes in metal form and the source itself is a solid metal pellet. Even when removed from its protective shielding, killing everything in sight, the source can be recovered without causing excessive contamination of its surroundings. On the other hand, caesium, being alkali metal with melting point of 28.5 °C and other amicable properties, typical for alkali metals, like tendency to ignite on contact with air or explode on contact with water, is mostly used in the form of caesium chloride, which is chemically stable, but water soluble. It means that while extracted from its protective shielding it will not only kill everything in sight, but when exposed to water, caesium chloride will dissolve and wash away, contaminating enormous amounts of anything it touches. Exactly such scenario happened in Brazil in Goiânia accident of 1987, where 93 grams of caesium chloride from stolen radiotherapy source from closed hospital killed 4 people, harmed 249 more and contaminated soil and structures, resulting in demolition of 7 houses and removal of 3500 m^3 of material. Some of the victims were irradiated by coming to see "strange blue glowing powder" and carrying some home with them, presuming supernatural properties of the substance. Still, such decontamination effort only accounted for about 85 % of the radioisotope, the rest being impossible to recover and was left to decay naturally, with half-life of ^{137}Cs being 30.17 years.

Previous paragraphs demonstrate one important fact: radioactive material needs to be properly treated, especially when in non-solid form. Treatment of radioactive waste does not involve only spent nuclear fuel, which represents category of engineering science itself, but also other classes of waste, from nearly harmless to very dangerous and insidious, like caesium chloride contaminated rubble from Goiânia or radioactive dump from lake Karachay. Two major sources of non-solid radioactive waste exist: waste from industrial processes, that is stored on site and awaits treatment, conditioning and safe disposal and waste emergent from incidents, mostly involving caesium SRS (Spent Radiation Source). Such incidents are not as rare as one might think, two such incidents happened in the first half of 2023 alone, one in Australia and one in Thailand, with Australian caesium capsule being successfully recovered, but Thai capsule apparently being smelted with scrap metal into steel.

Industrial processes, generating non-solid radioactive waste are in most cases related to nuclear power generation. Contaminated material from primary circuit need to be disposed of safely. The most important source, in terms of quantity of generated waste, is treatment of reactor coolant – ion exchange resins used to filter impurities in the coolant and liquid waste in the form of evaporator concentrate. This waste form is created as residue after boiling off water and concentrating mix of chemicals, present in the coolant – most significantly boric acid, hydroxides and salts. Also, inventory of radionuclides is present, either leaked fission products or activation products of impurities carried through the reactor core by the coolant. Most activity of the evaporator concentrate is represented by ^{14}C, ^{63}Ni, ^{137}Cs and ^{60}Co, with activity in the order of kBq/l or more, with by orders of magnitude smaller amounts of other radioisotopes. Provisions for handling such liquid waste are present at the sites of generation, i.e. inside nuclear power plants, where the waste is stored in controlled environment in large tanks with capacity sufficient to last for the design service life of the power plant. As the service life needs to be extended for the plant to remain profitable, the liquid waste needs to be taken care of. It is not allowed to dispose of waste in non-solid form in geological repositories, as the risk of leak and environment contamination is higher than with solid wastes. The liquid waste is therefore not disposed of, but only stored in temporary packaging, like steel drums or similar easy to handle devices. For long term disposal of liquid waste, solidification of the waste needs to be done, usually by means of mixing the waste with some kind of solidifying agent. Even in solid form, there are still some engineering challenges connected with the treated waste, limiting durability of the finished solid waste package. Together with usual material degradation, well described and understood by material science, there are specific issues connected with radioactive waste. Most notably there is radiolytic degradation of materials, caused by exposure of the material to gamma radiation emitted from the waste, also there is thermal action connected with radioactive decay of the waste and very importantly radiolytic release of hydrogen, capable of embrittlement of metals.

In this work, the process of designing solidification matrix for evaporator concentrate is described, in the form of collection of five papers, published in impacted journals over the course of four years. First paper describes different kinds of radioactive waste and brings summary of state-of-the-art techniques of its treatment. In the second paper there is investigation of effect of gamma irradiation on mechanical properties of cementitious composites used as solidification matrix for liquid radioactive waste. The third paper describes changes of microstructure of matrix materials due to irradiation, fourth deals with radiolysis and release of gases due to irradiation. The final paper investigates caesium leaching from the solidified matrix and evaluates the designed matrix in terms of durability in underground repository.

Chapter 1: State-of-the-art

This paper was published in the Journal of Environmental Radioactivity (Journal Impact Factor 2.4), volume 178, page 147-155, DOI 10.1016/j.jenvrad.2017.08.012. As of may 2025, the paper has been cited 74 times in WoS collection. The paper provides background for further study of the topic of radioactive waste management and presents comprehensive summary of radwaste treatment technologies, with special focus on use of cement-based matrices.

The radioactive waste is classified according to IAEA guidelines in five categories, depending on activity and half-life of radionuclides present in the waste. Most dangerous waste, in terms of quantity, activity and longevity is spent nuclear fuel, classified as high-level waste (HLW), containing fission products, which require safe disposal capable of enduring tens of thousands of years and also due to high initial activity, cooling of the waste is required for several years before further processing is possible. The topic of spent nuclear fuel is engineering discipline by itself and is not further discussed in this work, as the primary focus of this study is non-solid intermediate lever waste (ILW). The following text explains methods of waste management, utilised in various countries for dealing with ILW – its processing, treatment and conditioning, immobilization of non-solid wasteforms, packaging of the treated waste, as processes leading to safe transport and disposal of such waste.

Special attention is given to the use of cementitious composites as means of treatment of intermediate level waste, suitability of such materials is described, with strengths and weaknesses of such approach described in chapter 3 of the paper. Cementitious materials are used in two major modes on radwaste deposition, as immobilizing agent of non-solid waste and as part of engineered barrier of the disposal site. For each of these applications, examples of actual use are given.

1. Concrete and cement composites used for radioactive waste deposition

By Jaroslava Koťátková, Jan Zatloukal, Pavel Reiterman and Karel Kolář

Abstract

This review article presents the current state-of-knowledge of the use of cementitious materials for radioactive waste disposal. An overview of radwaste management processes with respect to the classification of the waste type is given. The application of cementitious materials for waste disposal is divided into two main lines: i) as a matrix for direct immobilization of treated waste form; and ii) as an engineered barrier of secondary protection in the form of concrete or grout. In the first part the immobilization mechanisms of the waste by cement hydration products is briefly described and an up-to date knowledge about the performance of different cementitious materials is given, including both traditional cements and alternative binder systems. The advantages, disadvantages as well as gaps in the base of information in relation to individual materials are stated. The following part of the article is aimed at description of multi-barrier systems for intermediate level waste repositories. It provides examples of proposed concepts by countries with advanced waste management programmes. In the paper summary, the good knowledge of the material durability due to its vast experience from civil engineering is highlighted however with the urge for specific approach during design and construction of a repository in terms of stringent safety requirements.

Keywords: *radioactive waste management, repository, concrete, cementitious materials, radionuclides´ immobilization*

1.1. Introduction

Sources of radiation are of beneficial use in many fields ranging from nuclear power, to medicine, scientific research, industry and agriculture. In all these applications radioactive waste with more or less radioactivity, in several forms and concentrations is produced. To ensure safe disposal of such hazardous waste a number of variables need to be considered, which lead to finding the most proper way for disposal of the particular radwaste type. There are a variety of the waste conditioning procedures and the final repositories systems. Concrete and cement composites, as one of these alternatives, are cheap and well goal-fulfilling materials used for radwaste immobilisation or serving as the secondary protection barrier between waste and the surrounding environment in the near surface repository. The experience of many years from use of cement and concrete in civil engineering provides broad knowledge about its technology, durability and performance in wide range of environments. The article is oriented to review the utilization of cement composites and concrete for radwaste solidification and final disposal with respect to the specifics of particular radwaste type management.

1.2. Radioactive waste classification

There are several schemes for radioactive waste classification, however the method of conditioning and the end point (i.e. transient storage or underground repository) rely on the level of radioactivity and lifetime of the radwaste. Therefore, the International Atomic Energy Agency (IAEA) has established a generally recognised classification scheme based on two parameters: radionuclide half-life and radioactivity content (International Atomic Energy Agency, 2009). There are two categories considering the lifetime of radionuclides: long-lived and short-lived radioactive waste, while the threshold level is established to be the half-life of ^{137}Cs (30.17 years). The general term “radioactivity content” includes more parameters: activity concentration, specific activity and total activity. The higher the radioactivity content, the higher the requirements on multi-barrier protection system. A special category is the exempt waste (EW), which contains such small concentrations of radionuclides, that it does not need any protection barrier and can be disposed in conventional landfills. Exemption

levels were established for both concentration and total amount of radionuclides based on the individual and collective dose and can be found in the International Basic Safety Standards for Protection against Ionizing Radiation and for the Safety of Radiation Sources (International Atomic Energy Agency, 1996). Besides exempt waste there are five categories of radwaste according to IAEA:

a) very short-lived waste (VSLW) – usually radionuclides with very short half-lives from medicine and research
b) very low-level waste (VLLW) – typically soil and rubble with low levels of activity concentration
c) low level waste (LLW) – radionuclides of higher activity than VLLW, but with limited concentrations of long-lived ones, requires engineered barriers for isolation in near-surface repositories for periods up to a few hundreds of years
d) intermediate level waste (ILW) – higher amounts of long-lived radionuclides, requires more advanced isolation from the environment in higher depths (tens to a few hundreds of meters) but with no or limited provisions to heat dissipation
e) high level waste (HLW) – waste with very high concentrations and/or high amount of long-lived radionuclides, typically spent nuclear fuel (SNF) and facilities and activated components from decommissioning of nuclear power plants, needs disposal in deep stable geological formations in depths of hundreds of meters.

The IAEA classification scheme does not give exact limits of concentrations for particular radionuclides to classify them into the appropriate classes; these are set in the domain of national regulatory bodies.

The process of radwaste management relies on its characterization, which includes the category and its form (solid or liquid). After characterization, the radwaste is processed, stored and ultimately disposed. Processing is composed of pre-treatment, treatment technologies (such as volume reduction, chemical modification, evaporation etc.) and conditioning. Conditioning transforms the waste into a form suitable for handling and storage including immobilization. Immobilization ensures safe embedding of radwaste into a matrix, preventing the leakage of radionuclides into the environment. Such solidified waste is further packaged in a system of barriers according to its class. A general scheme of radioactive waste management is presented in Figure 1-1 and an example of radwaste treatment in Slovakia is given in Figure 1-2. Cement matrix is well used for immobilization of VLLW, LLW and ILW waste thanks to the combination of its low cost and the suitability for radionuclide encapsulation due to physical and chemical bonds. Concrete serves as secondary barrier for LLW and ILW in the form of packages, which are further disposed in the appropriate repository.

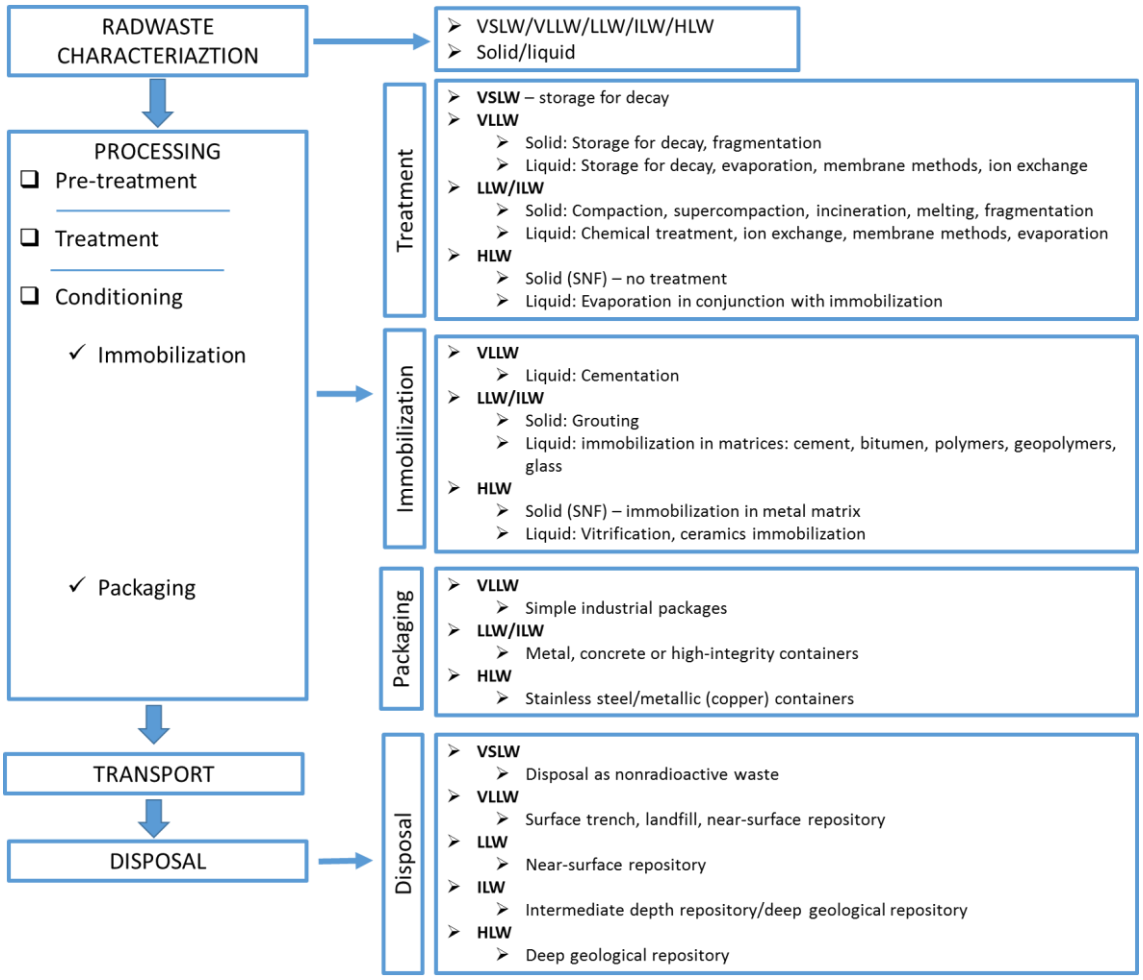

Figure 1-1: Scheme of radioactive waste management

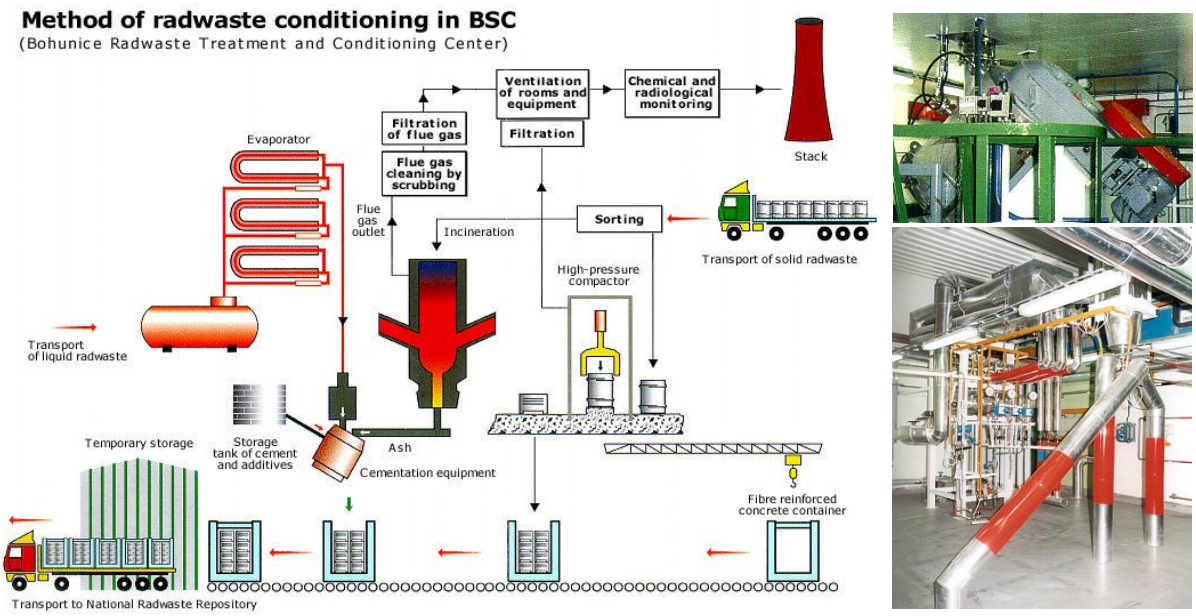

Figure 1-2: Processing of radwaste in Slovakia: a scheme (left-hand side) and examples of cementation (top right-hand side) and evaporation technique (bottom right-hand side) ***("Treatment and conditioning of radwaste in nuclear power plants," 2008)***

1.3. Immobilization of LLW/ILW by cement composites

1.3.1. Cement suitability for radwaste immobilization

The understanding of the immobilization mechanisms of radioactive waste in cement matrices is complicated due to the variety of alternatives of cementing agents, radionuclide nature and service environments. However, the retention potential of cementitious materials is very high thanks to its high sorption or uptake capacity (Chen et al., 2009; Mallants et al., 2016; McCulloch, 1985). The choice of the right matrix for immobilisation derives from the chemistry of both radioactive and inactive compounds present in the waste. For example, certain ion exchange resins are not compatible with the Ordinary Portland cement (OPC) environment, but also the presence of non-hazardous waste, such as cellulose may be problematic, as it degrades with time and thus generates gases, which may complex and solubilise actinides (McCulloch, 1985). These factors have to be considered in making prediction of changes in physical parameters, especially pH and Eh, due to the cement-waste interactions.

1.3.2.Immobilization mechanisms of cement

Cement in the immobilization process acts both chemically and physically. Physical action is mainly realized by surface sorption. The chemical mechanisms have not been up to now completely understood, but some analogues can be derived from experience of hazardous metal waste immobilization. The most published data relating the retention mechanisms is referred to Portland cement and can be summarized as follows (Ojovan, 2011):

a) surface and bulk sorption – prevailing mechanism for low species concentrations with low capacity, dependant on the surface area of hydration minerals, mainly of C-S-H gel
b) ion exchange – crystalline phases of hydrated cement offer anion and cation sites for uptake of radioactive species, e.g. Cl in AFm
c) characteristic phase formation – e.g. Ca-U-OH or $CaSn(OH)_6$ for U and Sn encapsulation respectively
d) oxy/hydroxyl precipitation – creation of usually metastable precipitates, e.g. $Cr(OH)_3$
e) combination of above mentioned mechanisms.

The particular processes of retention are controlled by hydrated minerals of cement paste. C-S-H gel due to its nanostructure, composed of small platelets and fibres, offers a variety of sites suitable for sorption of both cations and anions. Layered Portlandite with short Van der Waals forces does not exhibit high sorption ability due to the need of high energy to introduce compounds between its layers. AFm (alumina, ferric oxide, mono-sulfate) phase has similar structure to Portlandite, however with an unbalanced layer charge due to the presence of trivalent ions (Al, Fe) substituting the divalent calcium ion. This is compensated by anions presence in the interlayer space, which enlarge spacing between layers. Therefore, AFm phase offer capacity for ion exchange, regarding substitution of both anions from interlayer space by anions such as MoO_4^{2-} and cations of Al and Fe by trivalent radionuclides, such as Cr^{3+}. Ettringite (AFt, alumina, ferric oxide, tri-sulfate) has very open structure built of columns of alternating calcium and aluminium polyhedra and thus provides many opportunities for substitution of its main ionic components (calcium, aluminium and sulphate) by radionuclides such as Sr^{2+}, Ni^{2+}, Cl^-, IO^{3-} (Atkins and Glasser, 1992; Cornelis et al., 2008; Mallants et al., 2016; Tits et al., 2006).

In case of blended cements and use of mineral admixtures the chemistry is altered, which may provide additional possibilities for binding of radionuclides. Pozzolanic and latent hydraulic materials participate in hydration reaction consuming the low-sorptive Portlandite and producing minerals similar to the main products of cement hydration, C-S-H and C-A-H, which offer higher surface area for sorption and higher capacity for ion exchange.

Two essential facts should be noted: the prevailing mechanism depends on the concentration of radionuclide (i.e. sorption prevails for low concentration, while in high concentrations also the mechanisms acting in the whole volume take part); and the capacity of retention is dependent on the mechanism, while sorption usually presents lower capacity compared to ion exchange or phase transformation (Ojovan, 2011).

1.3.3. Cement-waste interactions

Naturally, the mechanisms of waste solidification influence the properties of fresh and hardened cement paste. Adsorption of solutes brought by the waste on the cement grains may slow down the setting of cement paste by blocking calcium silicate dissolution sites. Phosphates, usually present in the evaporator concentrates of effluent treatment stations, are known to retard the setting of cement paste and adversely influence its mechanical properties. Benard et al. (Benard et al., 2005) has dealt with phosphates' undesirable performance and proposed a solution, that by adding a small amount of hydroxyapatite to the binder, which acts as growth basis and manage the phosphate ion precipitation while decreasing their adsorption onto calcium silicate dissolution sites.

In case of high surface area of the solidifying waste, the adsorption of mixing water on the particles of waste during mixing may bring problems with workability, which can be solved by use of superplasticizer. But the choice of the right plasticizing agent has to be done with respect to the chemistry of the waste and its possible undesirable interactions with the waste. Acid wastes may result in decreasing the pH of the cement paste due to the its tendency to neutralize the acidity of the waste. When the pH decreases below 10.5 the hydrated phases become unstable and lose their integrity. Oxidation of some metals containing aluminium cause the generation of hydrogen bubbles leading to cracking. Problems in miscibility of some compounds (e.g. magnesium) may result in insufficient homogeneity of the matrix. This can be solved by producing a high-viscosity paste or by the adding surface-active molecules (CEA, 2009). All these factors have to be considered in stage of the design process of suitable matrix for waste solidification.

1.3.4. Alternative materials for immobilization

Next to Portland and blended cements, other materials are under research if being suitable for this application. These are geopolymers and special cements. Geopolymers, materials made from mixing of a source of silicates and aluminates (such as fly ash or metakaolin) and an alkali activator, have been claimed to be used by Egyptians for construction of pyramids (Davidovitz and Morris, 1988). This would talk in their favour, proving their long-term durability, but the statement is insufficiently validated. Next to the lack of knowledge about their long-term performance, the need of caustic Na/K(OH) as an activator brings about difficulties in handling. Although, apparently geopolymers have potential for good retention properties of alkalis, there is not enough data to make conclusions (Ojovan, 2011). However, investigations are currently in progress (Fernandez-Jimeneza et al., 2005; Khalil and Merz, 1994; Lichvar et al., 2013; Siemer et al., 2001; Xu and Deventer, 2000) and according to some authors (Xu and Deventer, 2000), geopolymers can be considered as analogues to metastable zeolites, i.e. complex aluminosilicates with three-dimensional network structure containing channels with high retention potential. When the crystallization of geopolymers is well controlled, they offer a perspective for immobilization of variety of contaminants. Examples of developing matrices based on geopolymers are "SIAL" developed in Slovak Republic (Lichvar et al., 2013), "hydroceramics" from Idaho National Engineering and Environmental Laboratory (INEEL, USA) (Siemer et al., 2001) or "ALUSIL" used in nuclear power plant Dukovany, Czech Republic. There is also an ongoing research in UJV Řež, a.s., a research centre in the Czech Republic, in cooperation with Chemcomex Praha a. s., dealing with immobilization of semi-liquid radioactive waste (such as sludge, ion exchange resins) in cement and

geopolymers. Figure 1-3 shows a device for testing of its solidification and an example of mixing the waste with geocement.

Figure 1-3: Testing of solidification of semi-liquid radioactive waste in UJV Řež in cooperation with Chemcomex Praha a. s., Czech Republic (Trtílek, 2017)

Special cements have better compatibility with certain types of waste due to their specific chemistry. Ion exchange resins, used for decontamination of water such as of reactor coolants, are usually rich in ^{137}Cs and ^{60}Co. In particular cases, ion exchange resins encapsulated with OPC suffer from strong expansion and potentially full disintegration. The use of blast furnace slag (CEM III/C) cement avoids the damage of the hardened paste, as the swelling of resins and induced stresses occur already in the stage of setting, while the paste is still plastic (Lafond et al., 2017).

Borate, lithium and zinc ions are difficult to be immobilized by Portland cement as they retard its hydration. However, it was found that in case of its solidification using sulfoaluminate cement (CSAC), no inhibition of hydration occurred even for high zinc concentrations of 1mol/L. Sulfoaluminate cements contain higher amounts of gypsum up to 20% (compared to 3-5% in case of Portland cement), yeelimite ($4CaO.3Al_2O_3.SO_3$), dicalcium silicate and a ferritic phase. The hydration products are mainly composed of ettringite and/or monosulfoaluminate hydrate with low content of C-S-H and C-A-H phases. This leads to its rapid setting and hardening and high early-stage strength (up to 30-40 MPa in 24 hours in specific conditions of high RH and temperature of 20°C) (CEA, 2009). Moreover, it has very high retention ability to zinc ions and is dimensionally very stable. In case of high concentration of borate and lithium ions in the waste, the immobilization process has been found to be feasible when a mixture of 70% of sulfoaluminate cement and 30% of Portland cement is used (Cau Dit Coumes et al., 2017; CEA, 2009). CSACs may also have a potential to stabilize waste streams with significant amounts of chloride and carbonate ions, including ^{36}Cl and ^{14}C long-lived radioactive isotopes. Also calcium aluminate cement (CAC) provides appropriate mineralogy for retention of particular radionuclides. The hydrated AH_3 phase offer high amount of sites for chemisorption and, in case of CAC hydration with ionic solutions, the AFm phase can bind nuclides through chemical reactions. The precipitation of AFm phase can be induced by the addition of gypsum (of about 15%) to the calcium

aluminate cement, as in case of the study of Toyohara et al. (Toyohara et al., 2002), which showed enhanced sorption of radioiodine compared to OPC matrix. Fryda et al. (Fryda et al., 1996) reached almost full entrapment of caesium nuclides in mixture of CAC with 40% of silica fume. The advantages of CACs and CSACs use for specific radwaste immobilization can be summarized:

a) their setting is far less influenced by strongly retarding radionuclides,
b) the retention capacity of specific species is enhanced by the hydration of high amounts of AFt, AFm and AH_3 phases
c) the corrosion of particular electropositive metals (e.g. aluminium) is inhibited due to low pH of the pore solution (Cau-dit-Coumes, 2013).

Magnesium phosphate cements, which are in civil engineering known for their rapid strength gain and thus used for repair works, have been investigated in terms of problematic mixed waste treatment, such as wastes containing ^{137}Cs, ^{99}Tc, Pu, or highly saline effluents (Mayberry et al., 1993; Singh et al., 1998; Wagh et al., 1999a, 1999b). The waste immobilization in magnesium phosphate cements is controlled by two processes: (i) by its physical entrapment in highly dense matrix and (ii) by the precipitation of particular radionuclides, e.g. poorly soluble phosphates. As in case of CACs and CSACs, also magnesium phosphate cement hydrate in a low-pH matrix, can be utilized for solidification of waste from reactor vessel decommissioning, which is rich in aluminium. A matrix named “ceramicrete” was developed in Argonne National Laboratory (USA) (Wagh et al., 1997), based on reaction of deadburnt MgO with monopotassium phosphate KH_2PO_4 in temperature above 65°C. Due to the rapid precipitation of the reactant ($MgKPO_4 \cdot 6H_2O$), boric acid was used as a retarding agent. A promising material for waste immobilization could also be calcium phosphate cements, even though the available forms, which were developed for dentistry and medicine, do not meet the requirements for use in nuclear waste management. When modified they can offer many advantages, such as the stability of hydration products (hydroxyapatite) up to 1000°C, the resistance to amorphization due to radiation damage, high chemical entrapment capacity through ion substitution and three to four times lower solubility in water (Cau-dit-Coumes, 2013; Cau-dit-Coumes et al., 2003).

The implementation process of above mentioned binders for immobilization still have to deal with these concerns (Cau-dit-Coumes, 2013):

Geopolymers:

a) hydration process highly sensitive to the activation conditions
b) difficult handling of large batches due to the presence of caustic activator
c) incompatibility with most of the common superplasticizers
d) insufficient knowledge about durability and interaction with waste species

CACs and CSACs:

a) need to control the heat generation during hydration
b) very rapid setting of CSAC, boric acid needed as a retarder
c) conversion of CAC hydration products in warm and humid environment
d) water loss of ettringite in case of CSAC presence in hot and dry conditions
e) insufficient knowledge about interaction with waste species

Phosphate cements:

a) cost and availability
b) variable specific surface area of deadburnt MgO having straightforward influence on reactivity
c) too rapid setting in case of magnesium phosphate cements, a retarding agent needed

d) slow setting and hardening of calcium phosphate cements at room temperature
e) high porosity affecting its strength
f) insufficient knowledge about durability and interaction with waste species.

Another way of the binder modification is the use of mineral admixtures. Liquid LLW and ILW waste, originating from chemical treatment of radioactive liquid effluents and reprocessing plant during concentration of HLW respectively, are the subject of long-term experiments of waste immobilization in India. LLW from chemical treatment usually contains complexing agents such as oxalic and citric acids and thus pozzolanic mineral admixtures, namely bentonite and vermiculite, were incorporated into the matrix for its ability to consume the highly alkaline and soluble Portlandite. ILW waste for storage in carbon steel tanks has been embedded in Portland cement and blast-furnace slag matrices also with and without admixtures of vermiculite (International Atomic Energy Agency, 2013). An investigation carried in South Africa aiming at immobilization of difficult waste streams (graphite fuel spheres, sludge, tritium, resins and organics such as oil) proposed a cement matrix with 4 % of bitumen as best alternative (International Atomic Energy Agency, 2013).

For monovalent radionuclides (e.g. ^{137}Cs) the capacity of surface sorption is rather low, therefore it is convenient to incorporate pozzolanic mineral admixtures with ion exchange potential into the matrix (Ojovan, 2011). The aforementioned vermiculite and bentonite are good sorbents with pozzolanic properties, as well as zeolites; other suitable admixtures are also fly ash, blast furnace slag and silica fume. Zeolites are temperature and radiation stable, compatible with cement matrix and have very good selectivity properties. El Kamash et al. (El-Kamash et al., 2006) studied the leaching of ^{137}Cs and ^{90}Sr radionuclides in the form of chloride salts, which were loaded in synthetic zeolite A and then solidified in OPC. Next to the significant reduction in leach rates achieved by the presence of zeolites in the matrices, the increase in compressive strength and decrease in setting time was achieved due to the zeolite incorporation. Caesium solidification was also the focus of a study (Goñi et al., 2006), showing good solidifying properties of fly ash belite cement. The leaching of ^{137}Cs from the matrix can be reduced by two orders, when 50% of cement is replaced by zeolite admixture. Zeolite- and bentonite-cement matrices were also studied in terms of ion-exchange resins and dry radioactive evaporator concentrate immobilization in Serbia (I Plecas et al., 2006; Plecas et al., 2004) as a part of a long-term project, which is supposed to provide data for design of encapsulation matrices in future Serbian radioactive waste disposal center. A study of Brough et al. (Brough et al., 2001) was aimed at the immobilization of highly alkaline low level radioactive waste with high concentrations of Na, Al, phosphate, carbonate, nitrate, and nitrite ions. The proposed binder was composed of cement, clay and almost 70% of fly ash to reduce the hydration heat and was adiabatically cured up to 90°C, which gave rise to zeolites next to the common hydration product C-S-H phase. By changing the curing conditions, the mineralogy of hydrated paste was significantly altered. Silica fume blended cements showed its good properties for Cs immobilization in the investigation of Bar-Nes et al. (Bar-Nes et al., 2008). When densified silica fume was used, the leachability of Cs ions was further reduced, which is believed to be the effect of additional Cs sorption by unreacted silica particles in the agglomerates. Solidification of liquid radwaste rich in ^{137}Cs ions in cement with rice husk ash admixture was studied by El-Dakroury and Gasser (El-Dakroury and Gasser, 2008). The investigation showed enhanced strength, leaching properties and durability of the matrix, which were accounted to the three factors: the filler effect, the acceleration of ordinary Portland cement hydration and the pozzolanic reaction with calcium hydroxide (CH).

1.4. Concrete as secondary barrier for LLW/ILW disposal

Low level waste should be deposited in the near-surface repositories, while intermediate level waste requires higher depths depending on its radioactivity content. Each disposal site is characteristic in its geochemistry and hydrological conditions. Some sites may be of high-salinity, while other may contain low-mineral water; the underground water may be running and corrosive. Near-surface repositories are influenced by rather short-term fluctuations, such as thermal cycling (including freezing), wet-dry cycling with episodic flooding caused preferably by climatic changes. On the other hand, deeper disposal sites are more affected by processes connected with waste and single barrier emplacement (e.g. temperature rise during masses of concrete hydration, temperature rise of waste with higher activity) and interactions between these materials and the host rock (e.g. swelling pressure of bentonite) etc. The design of engineering barriers of secondary protection should reflect all these factors and consider all possible scenarios of degradation mechanisms in long-term in the course of their operational phase, once again regarding the waste type, especially its lifetime (Adinarayana et al., 2013; McCulloch, 1985).

There are various concepts for short/long-lived LLW/ILW repositories. Sweden, Finland or France belong to countries with advanced waste management strategies and have developed their own disposal schemes. The typical overall waste package is composed of:

a) internal containers or primary waste package - metallic drums or concrete containers with conditioned and immobilized waste
b) external container or secondary waste package - usually made of concrete, may be reinforced
c) grouting for confinement of the outer waste package contents (Ojovan, 2011).

The gap between the waste package and the surrounding rock is filled by a backfill (unreinforced concrete, bentonite or other materials).

The purpose of an engineered barrier is to limit the groundwater inflow to the immobilized waste matrix and serve as a secondary protection against the diffusion of substances to and from the waste. The use of concrete is advantageous in terms of: (i) blocking the transport of liquid and thus making diffusion the main mechanism of transport of hazardous and corrosive substances, (ii) featuring good sorption properties of many radionuclides and low diffusion coefficient, (iii) providing alkaline environment of concrete creating a passivation layer of metallic containers (SKB, 2013). In some cases, the concrete container with specified dimensions and weight may be used also for transport and handling of radwaste, which is further disposed in the final repository and then serves as secondary barrier. Table 1-1 summarizes the requirements imposed on the concrete secondary packages used for both handling, transport and the final disposal. The following subchapters provide examples of proposed concepts.

Table 1-1: Requirements on concrete secondary packages for handling, transport and disposal

Concrete container for LLW/ILW

Disposal specific requirements:	Service-live specific requirements:
❑ Serve as mechanical protection of primary package ❑ Withstand the stresses created by backfill material, surrounding rock and hydraulic pressure of underground water ❑ Inhibit the transport of liquids and minimise the diffusion of hazardous and toxic substances ❑ Allowing the escape of hydrogen when generated by waste radiolysis	❑ Allowing handling and transport of primary containers prior to final disposal ❑ Protection of primary packages against aggressive environment ❑ Allowing the escape of hydrogen when generated by waste radiolysis ❑ Safe encasement during operational period, satisfactory thickness to provide shielding against β, γ radiation in case of ILW with higher activity ❑ Reversibility

1.4.1. French concept of waste package

A container with use for interim storage, handling, transport and final disposal has been developed jointly by The Alternative Energies and Atomic Energy Commission (CEA) and The National Radioactive Waste Management Agency (ANDRA) in France (Figure 1-4). The container has been designed in order to accommodate a variety of long-lived intermediate level waste, six types of primary packages (WP) to be encased in the container has been identified: activated metal WP, bitumenized sludge WP, cemented technological WP, cemented hulls and nozzles WP, compacted structural and technological WP, structural and technological WP. One container can bear four primary packages and the container itself fit in the arrangement of the disposal cell with 2 to 4 columns and 3 to 4 levels of containers. For the body and the lid of the container, different concrete mixture compositions were specified, due to the requirement on the lid to allow the escape of radiolytic gas through higher content of pores. Thus the lid concrete mixture contains higher amount of water and reduced content of silica fume. The reinforcement is made of stainless steel to limit corrosion and improve the container durability. The container is currently being tested to validate its performance in terms of mechanical behaviour, durability, hydrogen release and handling (CEA, 2009; Ojovan, 2011).

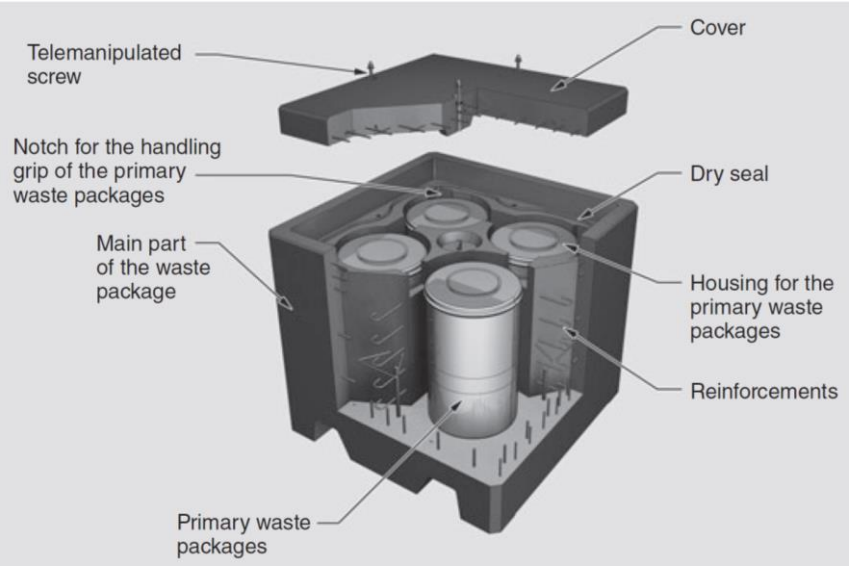

Figure 1-4: Scheme of French waste package concept ***(Ojovan, 2011)***

1.4.2. Silo concept

The concept of silo type repositories has been proposed in the disposal strategies of several countries, such as Sweden, Slovenia, Republic of Korea etc. The scheme is illustrated in Figure 1-5. The silo concept consists of a case in which disposal containers and waste packages are placed on top of each other in several levels and the remaining space is filled with a backfill. An experimental program of the silo concept development was carried out in the Republic of Korea, which contained characterization of cementitious and concrete materials, investigation of its durability, corrosion mechanisms of both concrete and steel reinforcement, radionuclide transport modelling and studies of silo closure options. A silo concept was also adopted by Slovenian national agency for radwaste management (ARAO) for low and intermediate level waste (LILW) repository at Krsko. The disposal site Krsko is situated in a demanding geological conditions, i.e. a saturated aquifer composed of silt with lenses of sand or clay, and so, the point of well-designed engineered barriers has gained on high importance. The experimental works has been aimed at development of suitable concrete mixture composition, investigation of its properties in both fresh and hardened state, durability (resistance to penetration of water, freeze/thaw resistance, resistance to groundwater), corrosion of reinforcement and degradation processes of concrete (International Atomic Energy Agency, 2013; Park et al., 2012).

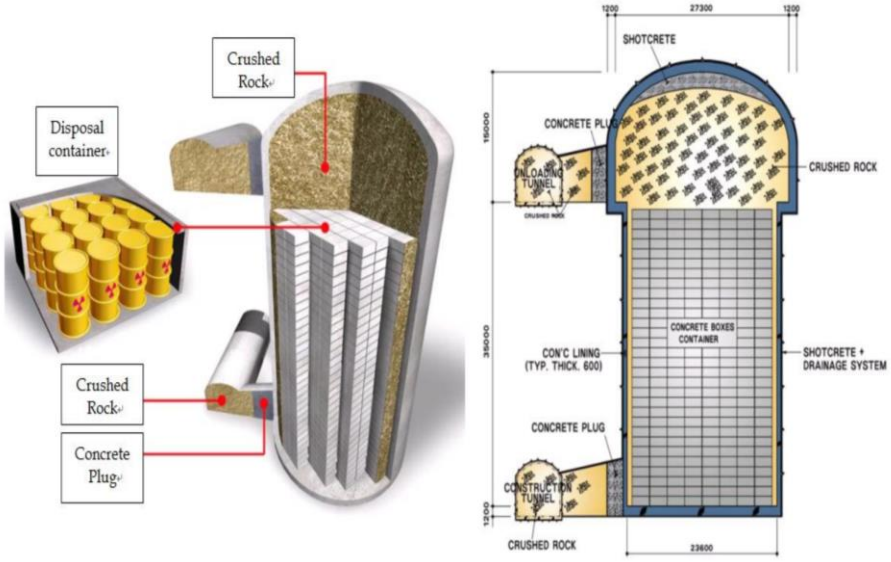

Figure 1-5: Example of silo concept at the Wolsong LILW Disposal Centre in the Republic of Korea (Park et al., 2012)

1.4.3. Swedish rock vault alternatives

Next to silo concept, Sweden proposed also alternatives for disposal in a rock vault. The assumed depth of the repository for long-lived LLW/ILW is about 300-500 metres. Figure 1-6 provides a scheme of the concept, while there are three alternatives of the backfill considered (number 2 in the figure) – concrete, bentonite or crushed rock. As mentioned above, the barrier made of concrete is convenient due to its ability to limit liquid water flow, fair capacity for sorption of radionuclides, high pH providing protection of the metal components against corrosion. However, these properties are highly dependent on the state of concrete, i.e. on the presence of cracks, voids etc. High risk in terms of crack creation is the corrosion of reinforcement and therefore, the concrete barrier was proposed to be without reinforcement, which results in much less load-bearing capacity. The second issue is the generation of gas, when the metallic containers start to corrode, which induces cracking of the concrete barrier. The use of stainless steel containers and the alkaline environment of concrete

significantly decelerate the corrosion rate, but the transport of gaseous oxidation products must be considered and technical solutions may need to be proposed (SKB, 2013).

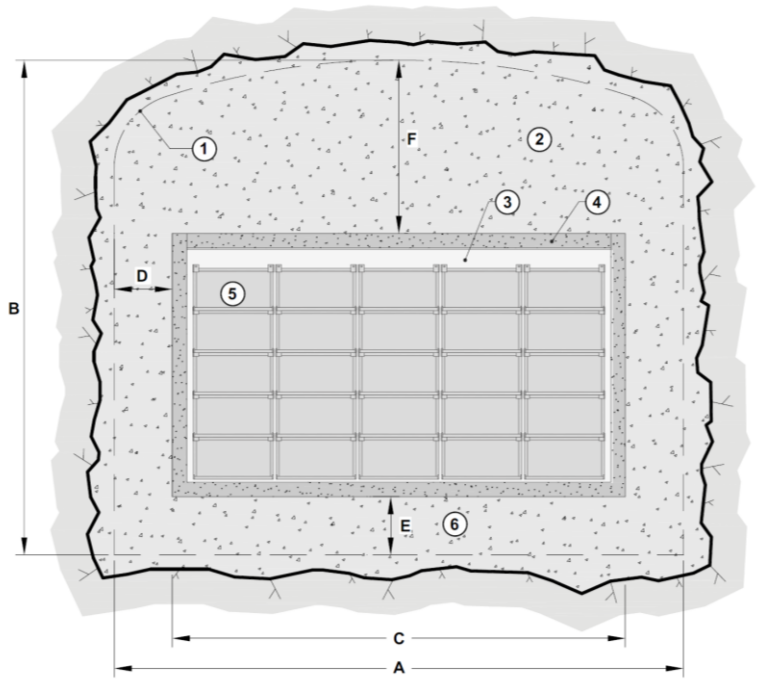

Figure 1-6: Example of Swedish concept of long-lived LLW/ILW repository ***(SKB, 2013)***

1) theoretical tunnel contour, 2) unreinforced concrete (eventually bentonite or crushed rock), 3) grout, 4) concrete structure for operation period, 5) waste packages, 6) unreinforced concrete (eventually bentonite or crushed rock); dimensions: A = 20 m, B = 17 m, C = 16 m, D = 2 m, E = 2 m, F = 5-10 m

1.5. Summary

Safe disposal of radioactive waste is of high priority and thus the development of secure engineered barriers needs to be paid with high attention. Cementitious binders for radwaste immobilization propose a reliable and cost-effective solution. The vast experience with cementitious materials from civil engineering ensures good knowledge of degradation mechanisms and durability. However, there are many specifics implicit from the waste nature and interactions with the matrix requiring vast additional research and experimental work. The proposed concepts of secondary barriers with the use of concrete needs verification of the material performance under such conditions and some undesirable factors must be dealt with. Nevertheless, concrete and cementitious binders have proved its wide range of utilization and certainly present an important and irreplaceable piece of chain in the disposal system waste management.

Chapter 2: Mechanical properties

This paper was published in Progress in Nuclear Energy (Journal Impact Factor 2.7), volume 127, article number 103437, DOI 10.1016/j.pnucene.2020.103437. As of may 2025, the paper has been cited 3 times in WoS collection.

In this paper, effects of gamma irradiation on mechanical properties of cement pastes ate studied. The mixtures used for irradiation were chosen after initial tests with evaporator concentrate simulator – mixture of chemicals identical in composition to actual radioactive waste, but using non-radioactive components. Chemical and physical properties of the simulator however are identical to those of actual radioactive waste and results of the tests are valid for actual mixture of binder and waste. Test specimens of the binder-waste mixture were prepared in laboratory of Experimental Centre in Prague and transported to CEA Saclay in France, where the irradiation experiment took place. Every set of specimens was tested before and after irradiation with reference set being kept in controlled environment during irradiation.

It was found, that gamma irradiation has no significant adverse effect on mechanical properties of the solidified matrix. Comparing specimens that did undergo irradiation cycle with reference specimens has shown, that after receiving dose of gamma rays comparable to expected dose during waste disposal, does not deteriorate mechanical properties of the composite. Crack formation, observed during the experiment was due to surface drying of the specimens, these cracks were only surface cracks without larger impact to tensile strength of the material. Some drying cracks were observed even in the sealed specimens, such water loss was probably not caused by drying, but by radiolysis of water.

2. Mechanical Properties of Irradiated Cement Pastes for Immobilization of Evaporator Concentrates

By Jaroslava Zatloukalová, Véronique Dewynter-Marty, Jan Zatloukal, Karel Kolář, Zbyněk Hlaváč and Petr Konvalinka

Abstract

The effects of gamma irradiation on the properties of concrete or cement composites have been investigated by several authors. However, the behaviour of composites immobilizing radioactive evaporator concentrates may be significantly affected by the altered chemistry of the matrix material. A newly proposed binder intended for the development of a composite immobilizing evaporator concentrates was investigated in terms of changes in its' mechanical properties due to gamma irradiation. Three kinds of cement pastes – a reference Portland cement paste (PC), a proposed binder as a mix of cements (NP) and a mixture "NP" containing a model evaporator concentrate (NP_C) - were irradiated by gamma source Co-60 in two subsequent experiments differing in conditions – on air and closed in a glass box. Surface cracks appeared on the NP and NP_C samples after the first irradiation experiment, i.e. in non-sealed conditions, due to drying effects supported by high ventilation in the irradiation chamber. In closed conditions, some smaller surface cracks also appeared probably due to radiolysis of water present in the material, however they did not have any effects on the integrity of the internal structure of the pastes observed by non-destructive measurements. Compressive strength was enhanced by irradiation in all cases, only flexural strength decreased due to the presence of surface cracks. It should be noted that surface cracks appeared also on non-irradiated NP_C samples when left on air to dry. Therefore, further development of the cement composites will be focused on the elimination of any volume changes due to drying.

Keywords: *evaporator concentrates, gamma irradiation, mechanical properties*

2.1. Introduction

The management of radioactive waste is nowadays very topical issue and it is gaining on importance. Many countries in the world are currently in some stage of planning the concepts of construction a long-term underground repository. The final long-term disposal must be safe, reliable, easily monitored and respect the environment. However, there are number of levels of the waste radioactivity and several types of the waste differing in its composition and safety requirements. High-level waste (HLW) requires a different solution than intermediate (ILW) or low-level waste (LLW). In every case, there has to be a multi-barrier system developed for each kind of the waste composed of a matrix with the immobilized waste in a primary package and several secondary barriers, each of them having its specific function. Cementitious materials are very suitable to be used for some of these barriers as these are durable, resistant to radiation and higher temperatures, low-cost and well-understood materials with good sorption capacity (Chen et al., 2009; Mallants et al., 2016; McCulloch, 1985).

Evaporator concentrates (EC) present an intermediate-level waste coming from the cooling system of the primary circuit of nuclear power plants. For this type of liquid waste, cementation may be a suitable way of its immobilization, however due to their complex chemistry, there are many issues which need to be dealt with. Due to the high concentration of borates, the setting and hardening of ordinary Portland cement is hindered (Bensted et al., 1991; Coumes et al., 2017; Demribas and Karslioglu, 1995; Lieber, 1973; Ramachandran and Lowery, 1992). Therefore, a composite with suitable binder needs to be developed and then tested, especially for its durability, leaching rates and radiation stability. The first task is to find a binder which sets and hardens in a reasonable time without the loss of the matrix long-term mechanical properties. The retardation mechanism of borates on the cement hydration has

not been fully understood yet. According to literature, the possible cause of the hindering effect may be the surface adsorption of borates on the cement grains and subsequent precipitation with calcium (Csenteyi et al., 1995). It was also reported (Masonnaye, 1993; Roux, 1989) that when pH is within the range of 4.5 – 12, polyboric anions ($B_3O_3(OH)^{4-}$, $B_3O_3(OH)_2^{5-}$) form an amorphous $2CaO.3B_2O_3.8H_2O$ which inhibits the cement hydration. However, at pH > 12 the borate ions precipitate into crystalized $CaO.B_2O_3.6H_2O$ or $CaO.B_2O_3.4H_2O$ which do not disturb the hydration of cement grains. Once having a suitable binder hydrating properly, there are other problems to deal with. Since evaporator concentrates are rich with dissolved salts, several corrosion mechanisms may appear. Cracking of the matrix needs to be avoided and the composite should incorporate materials with high sorption capacity of radionuclides, while maintaining the integrity of the matrix. Moreover, the composite must be radiation stable and durable. The resistance of concrete and cement composites to gamma radiation has been studied widely(Acher et al., 2016; Craeye et al., 2015; Hilsdorf et al., 1978; Hlaváč et al., 2018; ICHIKAWA and KOIZUMI, 2002; Kaplan, 1989; Kontani et al., 2012; Maruyama et al., 2017; McDowall, 1971; Reches, 2019; Soo and Milian, 2001; Vodák et al., 2011), but stated results in literature are not consistent. According to Hilsdorf (Hilsdorf et al., 1978) and Kaplan (Kaplan, 1989), gamma doses up to 108 Gy do not have any negative impact on the mechanical properties of concrete. Vodák (Vodák et al., 2005) observed minor deterioration of mechanical properties of concrete when exposed to doses 300 kGy, while Sommers (Sommers, 1969) observed 50 % loss of strength of concrete under an extreme dose over 1 GGy. However, at doses which can be expected in case of intermediate-level waste, the major effect of gamma radiation on cementitious materials is the accompanying heat having a negative impact on mechanical properties, volume and mass stability, which is moreover supported by the radiolysis of water from the cement paste (Maruyama et al., 2018; Reches, 2019). Studies which excluded the influence of radiogenic heating presented an increase in mechanical properties of hardened cement paste, especially in flexural strength, due to the formation of aragonite and vaterite as products of radiation induced carbonation (Maruyama et al., 2018). Composites containing evaporator concentrates have altered chemistry which may result in different degradation mechanisms and thus the verification of their resistance to gamma irradiation is needed.

This work is aimed at studying the changes in macro-mechanical properties of a proposed binder for immobilization of evaporator concentrates due to gamma irradiation up to doses 2 – 4.5 MGy. The target dose of 2 MGy was selected according to the study of Bykov et al. (Bykov et al., 2008), which reported that a cement paste with waste containing radionuclide Cs-137 with an activity 3.7×10^{10} Bq/kg (1 Ci/kg) would absorb 2 MGy of gamma radiation by the time the activity of the radionuclide decreased by a factor of 100. Although the total irradiation doses are comparable, the energy of irradiation with the Co-60 source (primary peaks at 1.17-1.33 MeV) is much higher than Cs-137 (primary peaks at 0.61-0.80 MeV). The source Co-60 was chosen due to its availability and time constrictions knowing that the effect of such accelerated testing will be more aggressive to the material than in real conditions, which makes a good safety margin.

2.2. Materials and experiments

The studied materials were cement-based pastes, which were previously studied as the suitable binder for composite immobilizing evaporator concentrates (Koťátková et al., 2018)). The binder paste (labelled as “NP”) is based on a mixture of Portland cement CEM I 52.5 R and non-gypsum cement (Ordinary Portland cement without added gypsum) with water/binder ratio 0.3 and a melamine-formaldehyde resin superplasticizer Melment F10 (supplied by Stachema spol. s.r.o., Czech Republic). In order to simulate the waste package chemistry, the second cement paste (“NP_C”) was made of “NP” binder mixed with a solution simulating the evaporator concentrate without radionuclides (SEC) substituting the mixing water. Its chemical composition is given in Table 2-3 (Szalo and Žatkulák,

2000a). The third cement paste ("PC") was selected as reference and was made of Portland cement CEM I 42.5 R with the same w/b ratio and superplasticizer (Table 2-1).

Table 2-1: Composition of studied materials

Composition	PC [g/1 kg of binder]	NP [g/1 kg of binder]	NP_C [g/1 kg of binder]
Portland cement CEM I 42.5 R	758	379	379
Non-gypsum cement	-	379	379
Superplasticizer Melment F 10	15	15	15
Water	227	227	227*

*in case of NP_C the prepared amount of water was then mixed with chemicals from Table 2-3 to prepare SEC, therefore the water/binder ratio was 0.3 for all mixtures

Table 2-2: Mineralogical composition of the used cements

Sample		Portland cement CEM I 42.5 R	Non-gypsum cement
C3S	% wt.	59.0	67.3
	standard deviation	0.3	0.3
C2S	% wt.	9.2	9.5
	standard deviation	0.3	0.2
C4AF	% wt.	11.5	9.6
	standard deviation	0.2	0.1
Calcite	% wt.	5.9	-
	standard deviation	0.1	-
Portlandite	% wt.	2.1	1.9
	standard deviation	0.1	0.1
Periclase	% wt.	0.5	1.5
	standard deviation	0.0	0.1
Arcanite	% wt.	0.6	0.6
	standard deviation	0.1	0.1
Aphthitalite	% wt.	0.5	0.8
	standard deviation	0.1	0.1
Bassanite	% wt.	2.4	-
	standard deviation	0.1	-
Gypsum	% wt.	2.1	0.3
	standard deviation	0.1	0.0
Quartz	% wt.	0.3	-
	standard deviation	0.0	-

Syngenite	% wt.	0.9	-
	standard deviation	0.1	-

The manufacturing of samples took place in the premises of Experimental centre, Faculty of Civil Engineering, Czech Technical University in Prague. Two sets of samples were successively prepared for two irradiation experiments differing in conditions. All the prepared samples were prisms with dimensions 40×40×160 mm in order to perform both non-destructive and destructive tests. In both cases the preparation of samples followed the same procedure and curing times. After mixing, the samples were cast into moulds and covered with foil to avoid drying for one or two days. Then they were demoulded and placed into a box with 100 % RH to hydrate for 14 days due to restricted time. After that period, they were carefully packed within a box with high relative humidity (RH 99 %) and send to CEA - Saclay, France, the LABRA laboratory for the irradiation experiment, where it continued to cure before the start of experiment, which started at the age of 42 days. The used source of irradiation was gamma source Co-60. At the beginning of the experiment, the gamma dose was measured on the bottom and on the top of three samples evenly distributed to the source, the measured dose was in the range 1.52 – 3.31 kGy/h (Figure 2-1). All the samples were in the middle of the experiments turned over 180° along their longitudinal axis to be irradiated evenly from both sides.

For the first experiment, there were three samples for each kind of cement paste to be irradiated, three to be held in the same conditions outside the irradiation chamber and three samples to be stored in controlled conditions of 80 % RH and 21°C. The samples to be irradiated were placed in the irradiation chamber without any cover to be freely exposed to radiation. The samples which were left outside the irradiation chamber were left on air. The relative humidity of the two sets of samples was similar and both were exposed to the drying effect. Due to the outcomes of the first experiment (see chapters below), the second experiment was performed on samples placed into glass boxes to avoid the effect of drying while simulating closed conditions within the repository. During the preparation of the experiment the shielding effect of the glass box was omitted. It is possible to calculate the shielding effect of the glass box ex-post using thickness and composition of the glass or perform shielding measurements on the boxes used. This problem will be addressed in future experiments. Due to restricted space the second irradiation was performed on two and two samples of pastes NP and NP_C while reference samples were kept in high RH conditions. The first experiment lasted 80 days and the cumulated dose was in average 4.6 MGy. The achieved accumulated dose in the second experiment was in average 2 MGy, which represents accumulated dose to be absorbed in waste packages immobilizing waste containing the radionuclide Cs-137 with the initial activity 1 Ci/kg (3.7×10^{10} Bq/kg) (Bykov et al., 2008). Based on previous research (Koťátková, 2018) with similar conditions (source Co-60, dose rate between 0.5 to 4.5 kGy/h, same dimensions of samples), temperature changes inside the samples during irradiation were not measured, as these were found to be insignificant (within 2°C).

For both experiments, before the start and after the end of the irradiation experiment all the samples were measured, weighted and tested non-destructively in terms of ultrasonic impulse technique and impact-echo method with the use of a device Grindosonic ("ČSN 73 1371: Non-destructive testing of concrete – Method of ultrasonic pulse testing of concrete," 2012). After the end of experiments the samples were tested destructively to obtain flexural strength and compressive strength following the procedure of EN standards ("ČSN EN 1015-11: Testing methods for mortar for masonry - part 11: Determination of compressive and flexural strength of hardened mortars," 2000). Compressive strength was performed on 40×40×40 mm cubes sampled at the both ends of the 40×40×160 mm prism used for flexural strength.

Table 2-3: Simulated evaporator concentrate

Formula		[g/l]
NaOH	Sodium hydroxide	72.9
KOH	Potassium hydroxide	14.9
H_3BO_3	Boric Acid	76
Na_2SO_4	Sodium sulfate	3.5
$NaNO_2$	Sodium nitrite	14.5
$NaNO_3$	Sodium nitrite	27.1
NaCl	Sodium chloride	2
$C_6H_8O_7$	Citric Acid	1.6
$C_2H_2O_4 \cdot 2H_2O$	Oxalic acid dihydrate	2.8

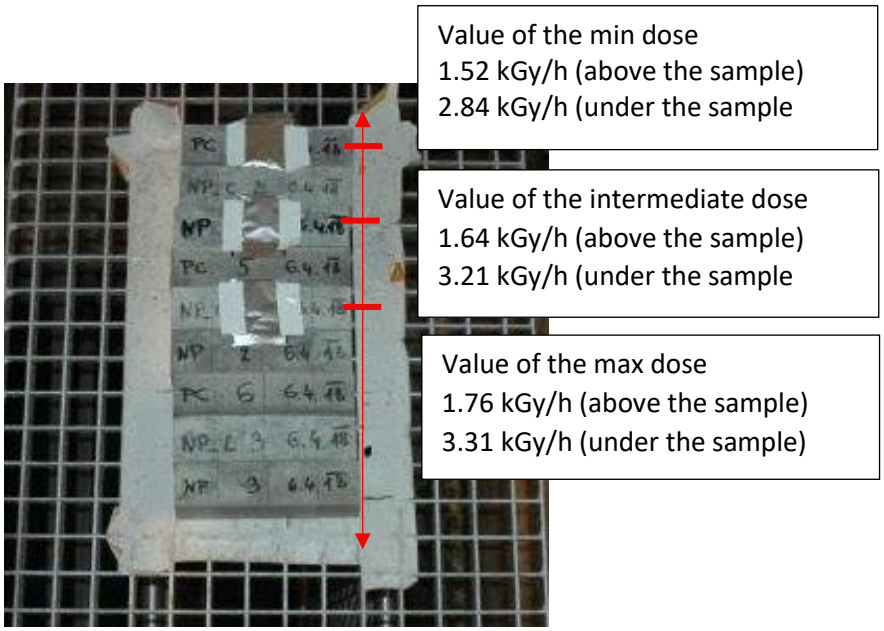

Figure 2-1: Samples prepared for irradiation with six dosimeters to measure gamma dose (Three dosimeters were installed above and three under the samples)

2.3. Results

2.3.1. Irradiation in an open environment (on air)

Results of the first experiment, i.e. on air conditions, are presented in Figures 2-3 – 2-8. Figure 2-2 displays the photo of irradiated samples. There are visible cracks on the samples marked as NP_C, however these cracks appeared also in the non-irradiated samples. This indicates that cracking was not caused by irradiation, but by the drying effect (see Figure 2-3), possibly coupled with the migration and expansion of salts present in the simulated evaporator concentrate, such as sodium sulphate, which is known as the most common efflorescent (Thaulow and Sahu, 2004). This finding is consistent with almost all observations, as summarized in (Reches, 2019). This is confirmed by the results of performed testing as follows.

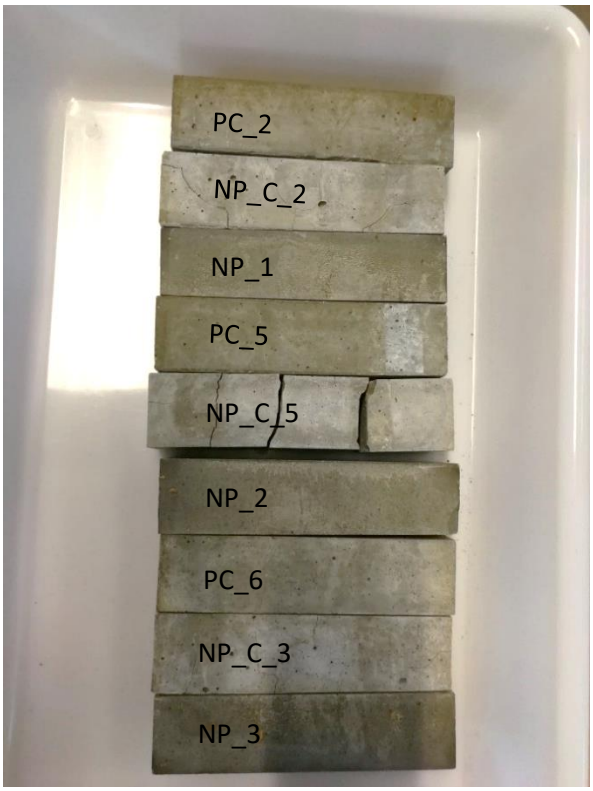

Figure 2-2: Irradiated samples – NP_C samples show cracks

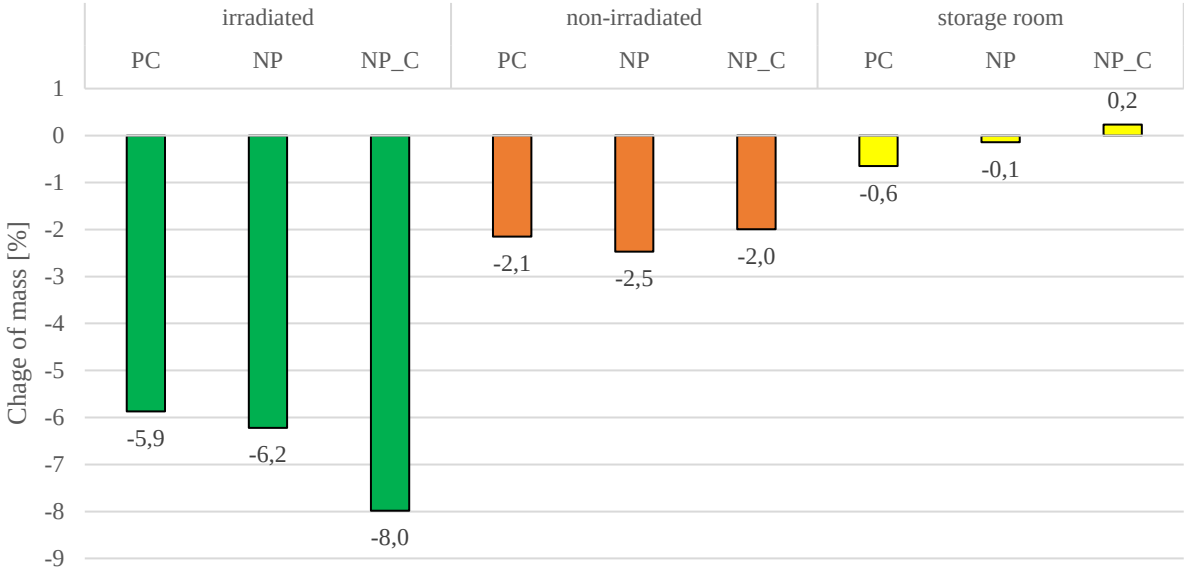

Figure 2-3: Mass difference ratio before and after irradiation experiment

Figure 2-4 gives the values of P-wave velocity measured by ultrasound impulse technique. There is a clear drop of values in case of irradiated NP_C samples – approximately by ¾ of the reference values (before the irradiation experiment), while for PC and NP samples there is a lower decrease – within 18 %. The drop of NP_C values was recorded also for non-irradiated samples - circa by one third of the reference values, while the decrease of NP and PC values were negligible, within 4 %. The changes in the values of all the samples stored in the storage room were also insignificant – within 5 %.

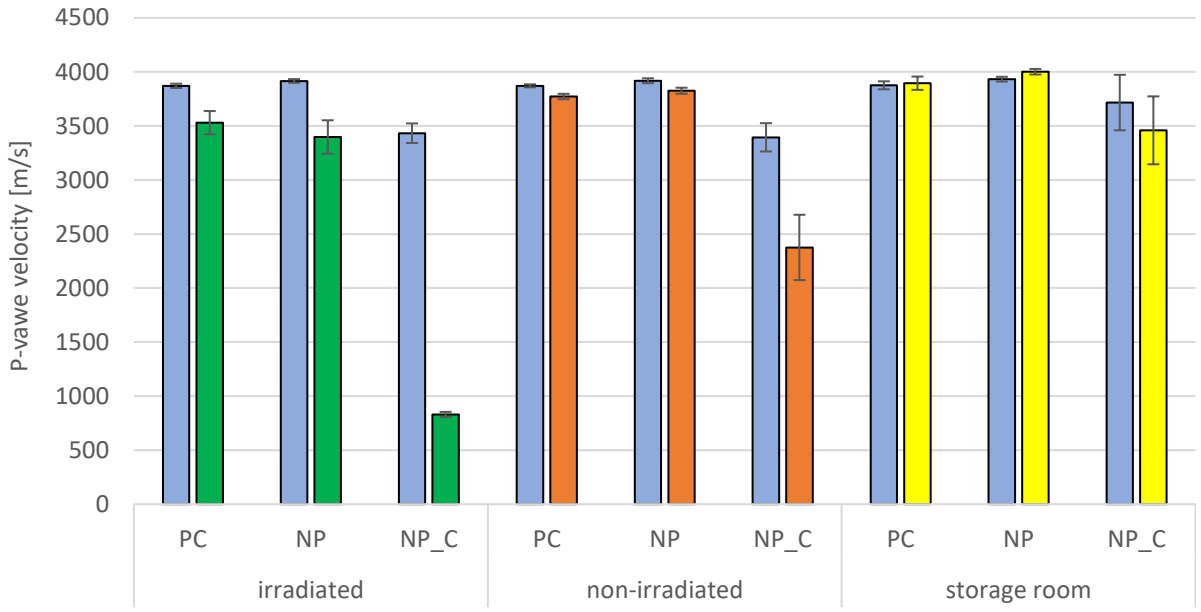

Figure 2-4: P-wave velocity of samples measured by ultrasound impulse technique before irradiation (in blue) and after the irradiation experiment: irradiated samples are given in green, non-irradiated in orange and samples placed in storage room in yellow (the given values are average of three samples and uncertainty bars were calculated as standard deviation)

The results of impact echo method are displayed in Figure 2-5 and Figure 2-6. The changes in both E and G moduli were marked for both irradiated and non-irradiated samples. For NP_C samples there was again the highest drop of values in case of irradiated samples but also in a similar scale for non-irradiated samples. It is worth to note, that also for PC and NP samples there was a significant drop of values, especially in the case of E-modulus where the decrease was found similar for irradiated and non-irradiated samples, while in the case of G-modulus, the drop was marked for irradiated samples, but in lesser scale for non-irradiated samples. This could be caused by the different water content in the samples before and after the irradiation experiment for both irradiated and non-irradiated samples. Both group of samples experienced water removal due to drying in case of non-irradiated and radiolysis in case of irradiated sample. Again, values of samples from the storage room were very similar before and after the experiment. A little increase of the moduli appears on these samples probably due to the long-time curing of the material.

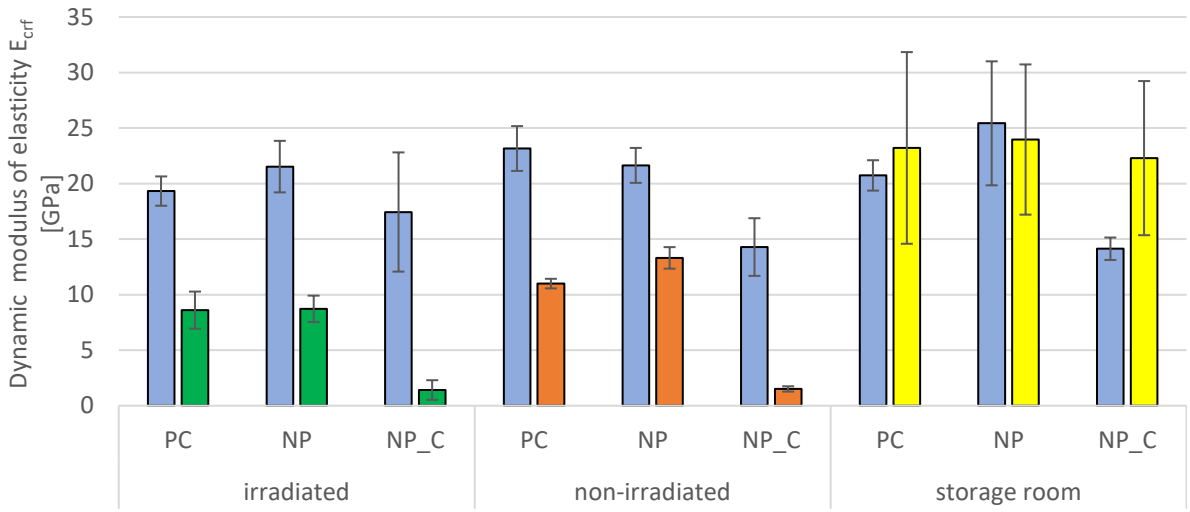

Figure 2-5: E-modulus of samples measured by impact echo method before the irradiation (in blue) and after irradiation experiment: irradiated samples are given in green, non-irradiated in orange and samples placed in storage room in yellow (the given values are average of three samples and uncertainty bars were calculated as standard deviation)

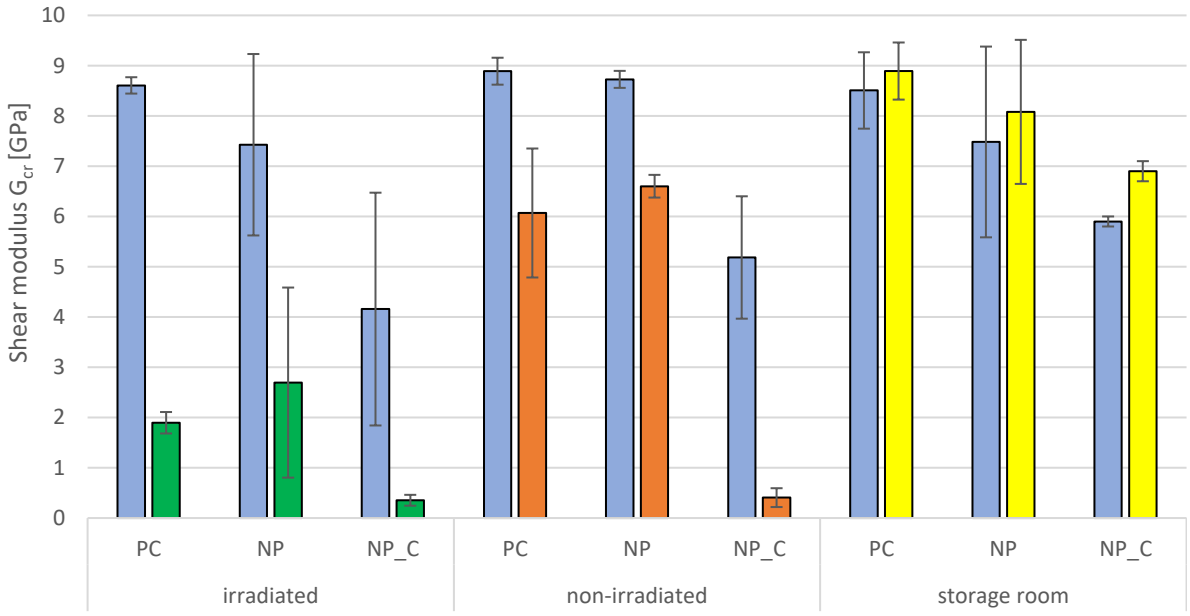

Figure 2-6: G-modulus of samples measured by impact echo method before the irradiation (in blue) and after irradiation experiment: irradiated samples are given in green, non-irradiated in orange and samples placed in storage room in yellow (the given values are average of three samples and uncertainty bars were calculated as standard deviation)

Figure 2-7 andFigure 2-8 display the results of destructive tests performed after the irradiation experiment. Flexural strength of NP_C irradiated samples could not be assessed due to the severe cracks in the samples (Figure 2-6). The values of non-irradiated NP_C samples were also very low due to the cracks and also for samples stored in the storage room with high RH, there were lower values for NP_C specimens when compared to the PC and NP samples. The values of PC and NP were comparable for all cases, even slightly higher for the irradiated samples when compared to the non-

irradiated ones. Compressive strength was performed on 40×40×40 mm cubes sampled at the both ends of the 40×40×160 mm prism used for flexural strength. Considering the complex mechanism of hydration process of NP_C samples due to the presence of the model concentrate compared to PC and NP samples, differences in strength were expected. Compressive strength of all the NP_C samples were approximately half the values recorded for PC and NP samples, with slightly less difference when compared to NP samples However, there were not any significant differences between irradiated, non-irradiated and storage room samples, even slightly higher values were recorded for the irradiated ones.

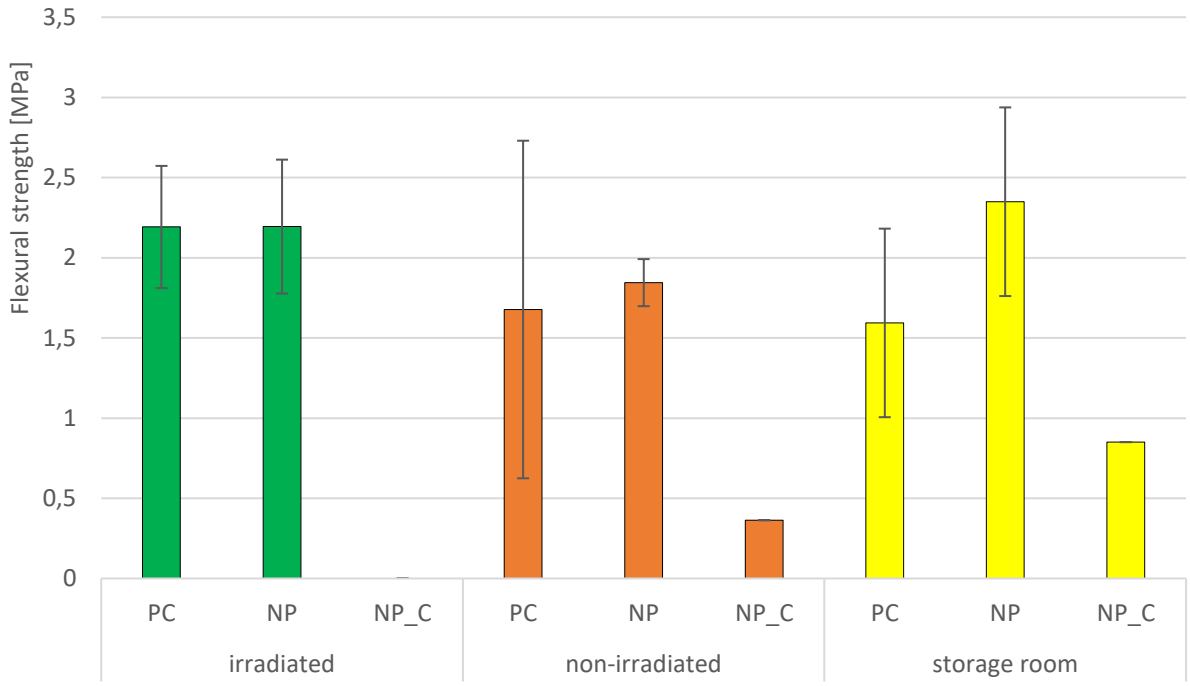

Figure 2-7: Flexural strength of samples after the irradiation experiment: irradiated samples are given in green, non-irradiated in orange and samples placed in storage room in yellow (the given values are average of three samples and uncertainty bars were calculated as standard deviation)

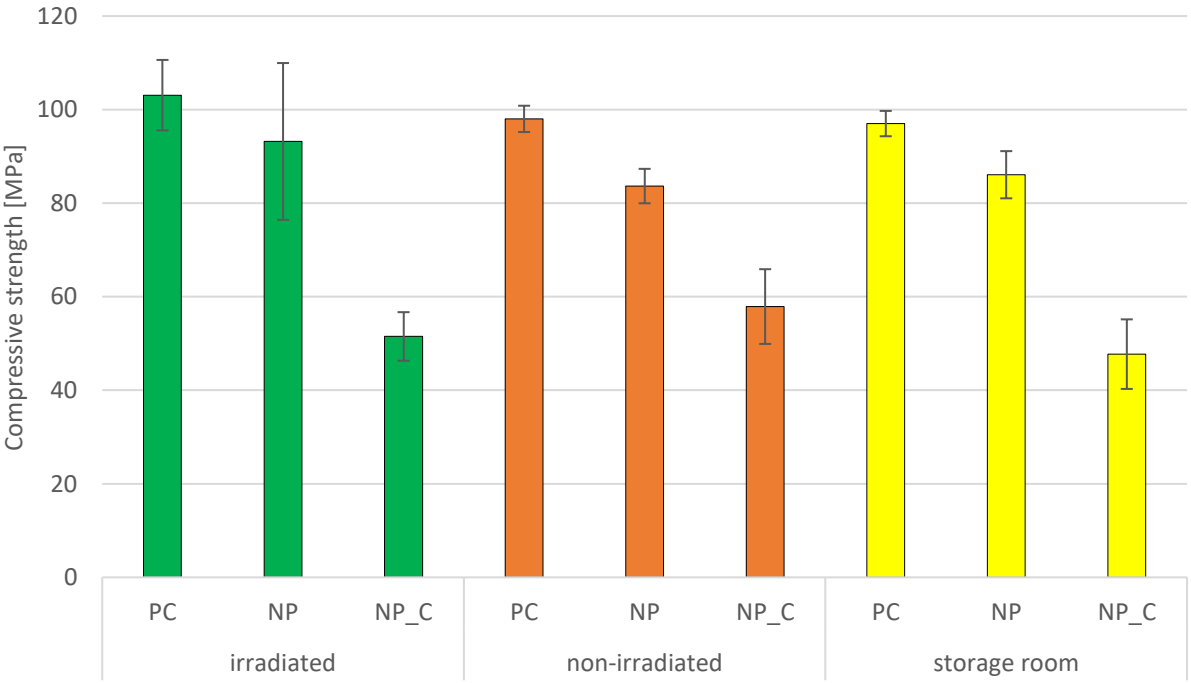

Figure 2-8: Compressive strength of samples after the irradiation experiment: irradiated samples are given in green, non-irradiated in orange and samples placed in storage room in yellow (the given values are average of six samples and uncertainty bars were calculated as standard deviation)

2.3.2. Irradiation in a closed environment

Figures 2-11 – 2-15 present the results of the second irradiation experiment, i.e. in the glass boxes to avoid drying driven by ventilation. Only four samples, two samples of formulation NP and two of NP_C, were irradiated due to space restrictions in the irradiation chamber. Figure 2-10 shows photographs of irradiated samples. Some cracks can be seen on samples of formulation NP_C (right hand-side), which were, however, found to be only surface cracks proven by the results below. The cracks were probably caused by shrinkage resulting from water loss in which radiolysis is only minor contributor compared to environmental conditions. Before non-destructive measurements, all the samples were left to dry on air, as the presence of water would significantly affect the measured values. It should be noted, that reference samples of NP_C after drying on air also exhibited surface cracks.

Figure 2-9: Photo of samples closed in glass boxes prepared for irradiation

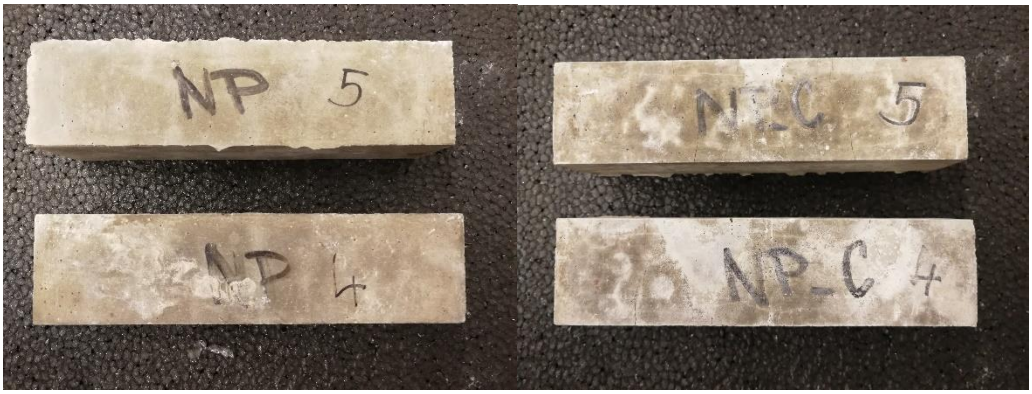

Figure 2-10: Photos of samples after irradiation: NP samples (left hand-side) and NP_C samples (right hand-side)

Figure 2-11 gives the values of P-wave velocity measured by ultrasound impulse technique. The differences in values before and after irradiation were within 10 % for all formulations. This means that the observed cracks on NP_C samples did not influence the internal integrity of the samples. Dynamic modulus of elasticity (Figure 2-12) and shear modulus (Figure 2-13) measured by impact echo method were found to be slightly higher after irradiation in case of NP_C, while values of non-irradiated PC and irradiated NP went down. Again, that does not indicate any internal defects inside the NP_C samples due to irradiation. Flexural strength (Figure 2-14) of NP_C samples was affected by the surface cracks, however in similar degree as non-irradiated NP_C samples which were dried on air before testing. Contrary, NP samples showed increase in flexural strength by 45 % after irradiation. Values of compressive strength (Figure 2-15) were positively affected by irradiation in both cases, only the scale

of increase was much higher for NP than for NP_C samples. However, the low value of NP sample was probably caused by a low number of testing specimens and should not be considered statistically significant.

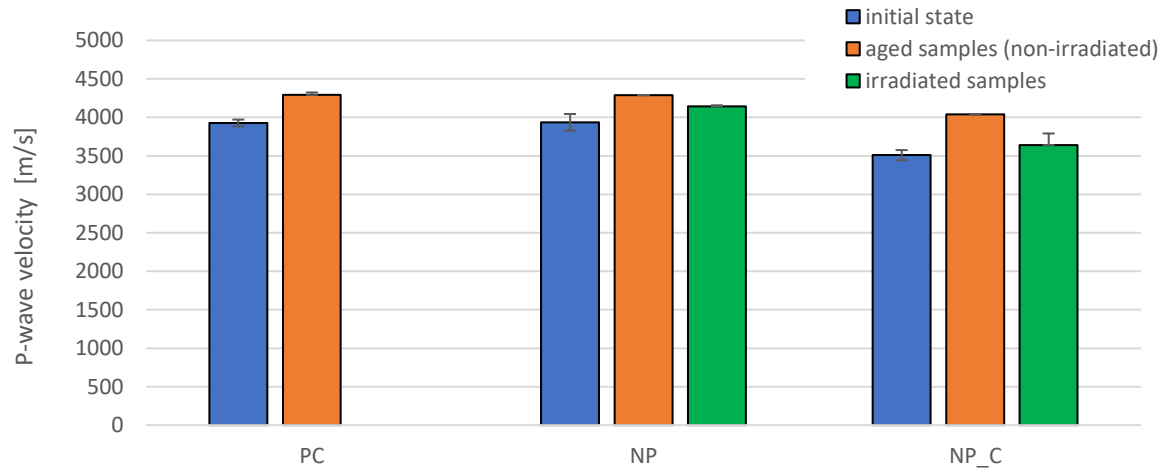

Figure 2-11: P-wave velocity of samples measured by ultrasound impulse technique in the initial state (in blue) and after the irradiation experiment (non-irradiated samples in orange and irradiated samples in grey). (note: PC samples were not irradiated due to space restrictions)

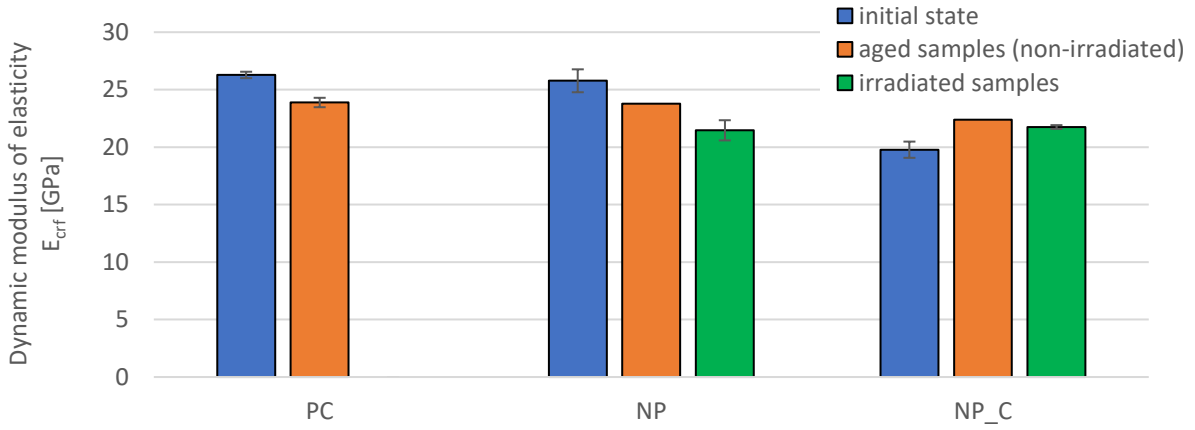

Figure 2-12: Dynamic modulus of elasticity of samples measured by impact echo method in the initial state (in blue) and after the irradiation experiment (non-irradiated samples in orange and irradiated samples in grey). (note: PC samples were not irradiated due to space restrictions)

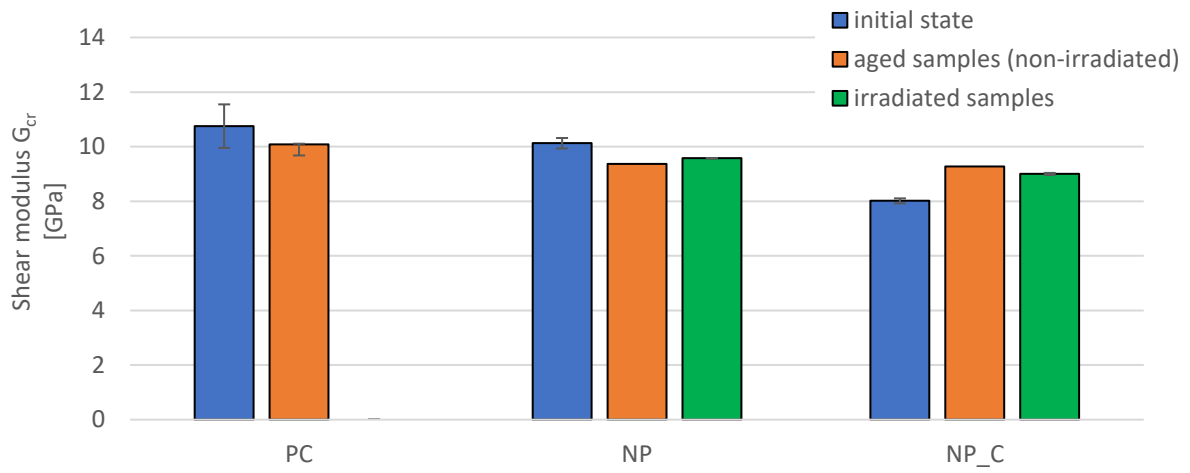

Figure 2-13: Shear modulus of samples measured by impact echo method in the initial state (in blue) and after the irradiation experiment (non-irradiated samples in orange and irradiated samples in grey). (note: PC samples were not irradiated due to space restrictions)

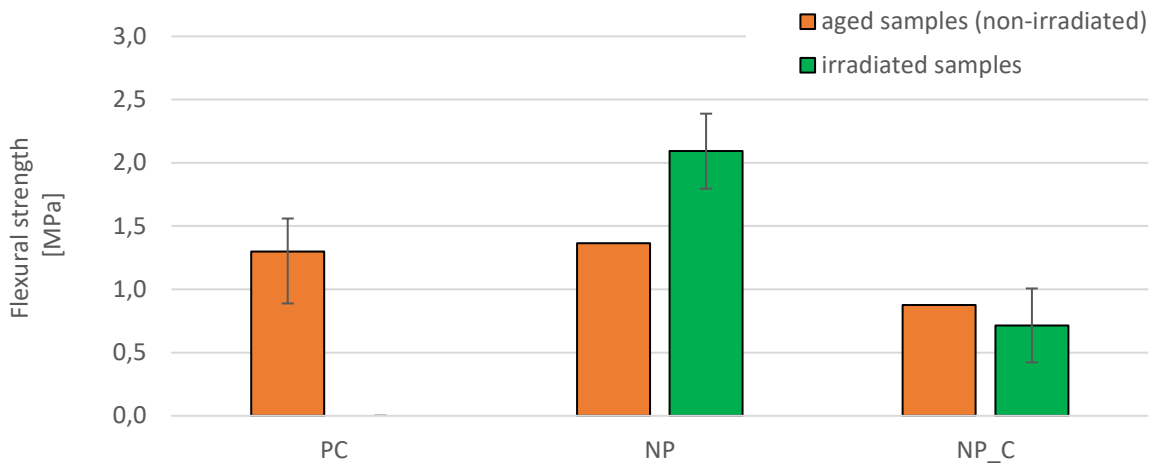

Figure 2-14: Flexural strength of non-irradiated samples (in orange) and irradiated samples (in grey). (note: PC samples were not irradiated due to space restrictions and were kept as reference)

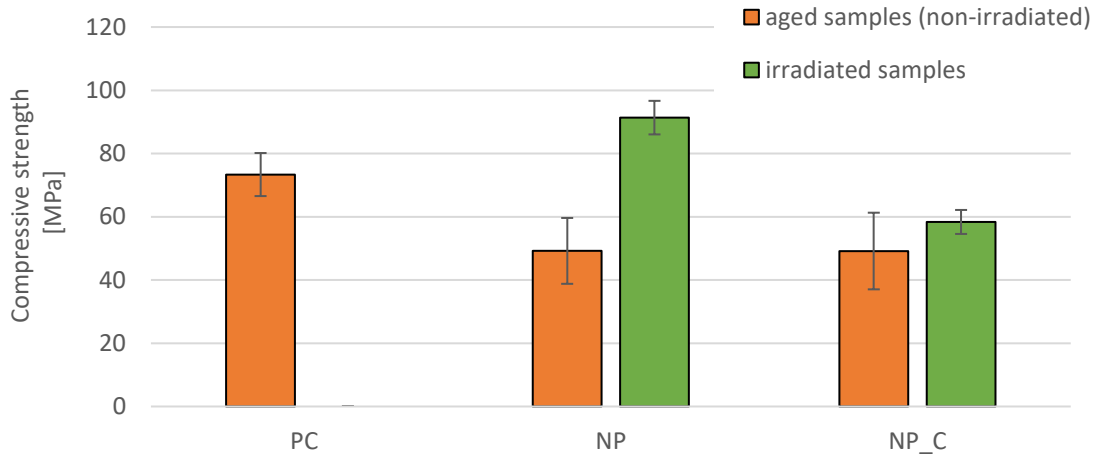

Figure 2-15: Compressive strength of non-irradiated samples (in orange) and irradiated samples (in grey). (note: PC samples were not irradiated due to space restrictions and were kept as reference)

Table 2-4: Summarization of the results – mean values

Compressive strength [MPa]						
	storage room	non-irradiated	irradiated	storage room	non-irradiated	irradiated
	batch 1			batch 2		
PC	97	98	103	-	73	-
NP	86	84	93	-	49	91
NP-C	48	58	52	-	50	58

Flexural strength [MPa]

	storage room	non-irradiated	irradiated	storage room	non-irradiated	irradiated
	batch 1			batch 2		
PC	1.6	1.7	2.2	-	1.3	-
NP	2.3	1.8	2.2	-	1.4	2.1
NP-C	0.9	0.4	-	-	0.9	0.7

P wave [m/s]								
	batch 1				batch 2			
	initial state	storage room	non-irradiated	irradiated	initial state	storage room	non-irradiated	irradiated
PC	3870	3900	3770	3530	3930	-	4300	-
NP	3920	4000	3830	3400	3940	-	4300	4140
NP-C	3430	3460	2380	830	3510	-	4040	3640

E_{crf} [GPa]								
	batch 1				batch 2			
	initial state	storage room	non-irradiated	irradiated	initial state	storage room	non-irradiated	irradiated
PC	21	23	11	9	26	-	24	-
NP	23	24	13	9	26	-	24	22
NP-C	15	22	2	2	20	-	23	22

G_{cr} [GPa]								
	batch 1				batch 2			
	initial state	storage room	non-irradiated	irradiated	initial state	storage room	non-irradiated	irradiated
PC	8.5	8.9	6.1	1.9	11	-	10	-
NP	8.0	8.1	6.6	2.7	10	-	9.4	9.6
NP-C	5.0	6.9	0.4	0.4	8.0	-	9.6	9.3

2.4. Conclusion

The effects of gamma irradiation on the mechanical properties of cement pastes designed to be used as a binder for composites immobilizing evaporator concentrates were investigated. The first experiment was conducted on air with high ventilation in the irradiation chamber which resulted in cracking of the NP and NP_C samples due to drying shrinkage having a negative effect on flexural strength and values obtained by non-destructive testing. Second experiment was therefore conducted in glass boxes to avoid severe drying shrinkage. Even though drying of the material by water evaporation and transport was prevented by confinement in sealed glass boxes, cracks similar to drying cracks observed in the first case were detected. Water loss due to gamma induced radiolysis is possible explanation of such phenomena. Described cracking was only observed on samples containing the model concentrate (NP_C), which displayed significantly lower flexural strength compared to samples mixed with pure water even without irradiation effect. However, the cracks did not affect the results from non-destructive testing and compressive strength, only flexural strength was slightly lowered.

This indicates that the internal structure of irradiated samples was without defects. Moreover, compressive strength was enhanced in both cases (i.e. for NP and NP_C). Therefore, future development of the composite will be targeted on limiting any drying-related volume changes of the investigated materials.

Chapter 3: Microstructure

This paper was published in Journal of Nuclear Materials (Journal Impact Factor 3.3), volume 540, article number 152346, DOI 10.1016/j.jnucmat.2020.152346. As of may 2025, the paper has been cited 3 times in WoS collection.

This paper investigates changes of micromechanical properties of cementious composites used for solidification of liquid intermediate level waste induced by irradiation by gamma rays. The experimental part of this work was performed at CEA Saclay, using ^{60}Co gamma source and material specimens prepared at Czech Technical University.

3. Microstructural and micro-mechanical property changes of cement pastes for ILW immobilization due to irradiation

By Jaroslava Zatloukalová, Véronique Dewynter-Marty, Jan Zatloukal, Karel Kolář, Fabien Bernachy-Barbe, Petr Bezdička and Petr Konvalinka

Abstract

While degradation of concrete due to irradiation is a widely studied subject, the deterioration and changes in microstructure of cement pastes immobilizing evaporator concentrates due to gamma radiation is a very specific subject because of the nature of the solidified radioactive waste. The cement paste proposed as possibly suitable binder for cementitious composites immobilizing evaporator concentrates (marked as NP in further text), a paste with the same composition but mixed with simulated evaporator concentrates (NP_C) and a reference paste (PC) were subjected to gamma irradiation from Co-60 source at doses of 2 MGy and studied in terms of microstructure changes using Scanning Electron Microscopy (SEM) with Energy Dispersive X ray Spectroscopy (EDX), X-ray diffraction (XRD) and nanoindentation. SEM-EDX revealed rise of new phases on the NP_C samples rich in Na^+ compounds due to the irradiation. Results from nanoindentation indicated a formation of carbonates in the irradiated samples, but XRD analysis did not find a significant rise in $CaCO_3$ minerals. The possible explanation is a rise of alkali carbonates in their amorphous form.

3.1. Introduction

Considering the importance of nuclear safety, the effects of irradiation (neutron, γ, α) has been widely studied (Elleuch et al., 1972; Fujiwara et al., 2009; Hilsdorf et al., 1978; ICHIKAWA and KOIZUMI, 2002; Kaplan, 1989; Kontani et al., 2012; Maruyama et al., 2017; McNearney et al., 1971; Pape, 2015; Pape et al., 2016; Soo and Milian, 2001; Vodák et al., 2011) and reviewed recently (Rosseel et al., 2016). However, in relation to radioactive waste disposal and thus specifically gamma irradiation of concrete or cementitious materials, there is inconsistency among research studies in terms of the threshold gamma dose causing deterioration of concrete mechanical properties. The historically proposed level of $2 \cdot 108$ Gy (Hilsdorf et al., 1978) was disputed by a few research studies, which showed a decrease in mechanical properties when irradiated to much lower doses - several hundreds of kGy (Soo and Milian, 2001; Vodák et al., 2011). It is believed that the main degradation of concrete due to gamma irradiation is caused by radiolysis of water present in the cement paste, shrinkage of cement paste due to the accompanying heat release and eventually changes in hydration products due to heating or generation of H_2 and radicals through radiolysis (Maruyama et al., 2017). The effects of radiation on micromechanical properties or microstructural changes has been reported little in literature (Ferreira et al., 2018; Hilloulin et al., 2018; Łowińska-Kluge and Piszora, 2008; Maruyama et al., 2018, 2017), however the knowledge of alterations in microstructure and micromechanical properties leads to better understanding of the degradation mechanisms and tools as nanoindentation offers large datasets for numerical modelling.

Evaporator concentrates come from the coolant of primary circuit of nuclear power plants as intermediate level radioactive waste (I Plecas et al., 2006). Thanks to their liquid state, the favourable solution for their handling and disposal is to immobilize them in a cementitious matrix, as they can be easily used instead of mixing water. Cementitious materials are in comparison to other materials such as bitumen supposed to be sufficiently stable and radiation resistant at low gamma doses (I Plecas et al., 2009). However, the complex chemistry of evaporator concentrates alters the environment of the hydrated cement paste and thus different degradation mechanisms may be engaged. Next to this, high amounts of boron constituents present in the evaporator concentrates cause retardation of Portland cement hydration(Champenois et al., 2015; Rakhimova et al., 2017). Therefore, the cementitious matrix has to be modified to gain a well hydrated cement paste. This leads to the design of new

materials with unique properties and thus their response to gamma irradiation is also specific and difficult to predict. The need to verify their properties when exposed to gamma radiation is obvious.

This study investigates the changes in microstructure and micro-mechanical properties of cement pastes proposed to be used as the main binder components in cement composites intended for evaporator concentrates immobilization. Scanning Electron Microscopy with Energy Dispersive X ray Spectroscopy (EDX), nanoindentation and X-ray diffraction are employed.

3.2. Materials and methods

3.2.1. Materials

Based on our previous research (Koťátková et al., 2018), cement paste composed of a mixture of cements was selected as possibly suitable binder for composites immobilizing evaporator concentrate as it displayed convenient setting and hardening times as well as good rheology of the fresh mixture. The paste is labelled "NP" and consists of Portland cement CEM I 52.5 R and non-gypsum cement in the ratio 1:1. The water/binder ratio was 0.3 and a melamine-formaldehyde resin Melment F10 was used as superplasticizer (supplied by Stachema spol. s.r.o., Czech Republic). As it is intended to immobilize evaporator concentrates, a dilution of chemicals simulating the composition of evaporator concentrate was prepared (Table 3-1) (Szalo and Žatkulák, 2000a) and mixed instead of mixing water with the same components as in case of "NP", the paste was labelled "NP-C". To maintain the same water/binder ratio, the dilution was prepared from the same amount of water as in case of NP, resulting in higher total weight of the prepared dilution. To have another reference, a third paste was prepared from Portland cement CEM I 42.5 R using the same w/b ratio and superplasticizer.

Table 3-1: Simulated evaporator concentrate

	g/l
NaOH	72.9
KOH	14.9
H_3BO_3	76.0
Na_2SO_4	3.5
$NaNO_2$	14.5
$NaNO_3$	27.1
NaCl	2.0
$C_6H_8O_7$	1.6
$C_2H_2O_4$. $2H_2O$	2.8

Table 3-2: Mineralogical composition of the used cements

Sample		**Portland cement CEM I 42.5 R**	**Non-gypsum cement**
C_3S	% wt.	59.0	67.3
	standard deviation	0.3	0.3
C_2S	% wt.	9.2	9.5
	standard deviation	0.3	0.2

C_4AF	% wt.	11.5	9.6
	standard deviation	0.2	0.1
Calcite	% wt.	5.9	-
	standard deviation	0.1	-
Portlandite	% wt.	2.1	1.9
	standard deviation	0.1	0.1
Periclase	% wt.	0.5	1.5
	standard deviation	0.0	0.1
Arcanite	% wt.	0.6	0.6
	standard deviation	0.1	0.1
Aphthitalite	% wt.	0.5	0.8
	standard deviation	0.1	0.1
Bassanite	% wt.	2.4	-
	standard deviation	0.1	-
Gypsum	% wt.	2.1	0.3
	standard deviation	0.1	0.0
Quartz	% wt.	0.3	-
	standard deviation	0.0	-
Syngenite	% wt.	0.9	-
	standard deviation	0.1	-

Samples of dimensions 40x40x160 mm were manufactured and cured in the premises of Experimental centre, Faculty of Civil Engineering, Czech Technical University in Prague. Then they were sent to CEA – Saclay, France where the irradiation experiments took place. Samples were cured for 40 days: first they were stored for 14 days in a chamber with 100% relative humidity and laboratory temperature, then they were sealed in boxes with high RH for the transport to France, where the samples, after unpacking, were placed again in a storage chamber with 100% RH. Small fragments were cut from the 40x40x160 mm prisms to manufacture samples for SEM, XRD and nanoindentation. After cutting, they were dried and cast in epoxy resin and left to set. Then, circle samples of diameter 50 mm were ground and polished in several subsequent steps in order to achieve good surface quality. The irradiation started at the samples´ age of 42 days. Atmospheric carbonation could not be avoided during the preparation and transport, but eventual radiation induced carbonation could be detected by comparison of irradiated samples with reference.

Six prepared samples were prepared for nanoindentation and SEM analysis. Three samples (one of each cement paste formulation) were intended for irradiation and three were kept as reference in a vacuum chamber. All samples together were studied before the start of the experiment and after its end. Reference samples are marked with letter “N” as non-irradiated in this paper, while samples for irradiation were marked with letters “IRR” as irradiated. Irradiation was executed by gamma source Co-60 with dose rate 3 kGy/h to achieve accumulated dose of 2 MGy. Firstly, on the prepared samples, nanoindentation analysis was conducted and the same samples were then also analysed by SEM. The exact location of SEM analysis was chosen to avoid the deformed surface parts by nanoindentation.

3.2.2. Nanoindentation

A grid of 25x25 indents with spacing 150 µm was obtained with the use of Nanoindenter Zwick-Roell ZHN/SEM® (Ulm, Germany) for each sample, used on air in a specific vibration dampening chamber. The device was equipped with 10 µm radius spherical diamond tip and the procedure was performed in standard laboratory conditions. The maximum applied force was 50 mN. The datasets were then analysed using hierarchical clustering algorithm (Bernachy-Barbe, 2019).

3.2.3. SEM

Scanning electron microscopy (SEM) using backscattered electron images and energy dispersive X-ray spectroscopy (EDS) were used to investigate the microstructure of the samples. Microscope Zeiss EVO LS15 and EDS detector Bruker X flash 6I30 were employed for analyses. Library of standards for spectrum analysis was provided by Esprit software. Samples were coated in thin layer of carbon to avoid surface charging. The used accelerating voltage was 15 kV.

3.2.4. XRD

X-ray diffraction was applied on the powder samples gained from grinding of cement pastes to obtain the mineralogical composition of studied samples. The measurement was performed by Institute of Inorganic Chemistry of the Czech Academy of Sciences, Czech Republic.

Diffraction patterns were collected with a PANalytical X´Pert PRO diffractometer equipped with a conventional X-ray tube (Cu K radiation, 40 kV, 30 mA, line focus) and a linear position sensitive detector PIXCel with an anti-scatter shield. X-ray patterns were measured in the range of 5 to 90° 2 Θ with step of 0.013° and 600 s counting per step, which produced a scan of about 4h 20 min. In this case conventional Bragg-Brentano geometry with 0.04 rad Soller slit, 0.25° divergence slit, and 15 mm mask in the incident beam, 0.5 anti-scatter slit, 0.04 rad Soller slit and Ni beta-filter in the diffracted beam was used. XRD patterns were not pre-treated before interpretation as no background correction was needed.

For estimating the amorphous content, the addition of an internal standard was used. Zinc oxide (Sigma Aldrich, fired to 700°C for 5 h) in the amount of 20 weight percent was mixed with the sample under acetone for about 10 min in an agate mortar. Such procedure was used to prevent the decomposition of fragile phases (ettringite, portlandite, hydrocalumite…) during the sample preparation. Then the prepared samples were analysed in the same way as the “as received” samples.

Qualitative analysis was performed with the HighScorePlus software package (PANalytical, The Netherlands, version 4.8.0) and JCPDS PDF-4 database (International Centre for Diffraction Data, 2019).

For quantitative analysis of XRD patterns Profex/BGMN software package with structural models based on ICSD database (“ICSD database FIZ Karlsruhe,” 2018) was used. This program permits to estimate the weight fractions of crystalline phases by means of Rietveld refinement procedure (Döbelin et al., 2015).

3.3. Results

3.3.1. SEM

Scanning Electron Microscopy using backscattered electron imaging (BSE) was used to study the changes in microstructure of the prepared samples before and after irradiation (Figures 3-1 – 3-4). Unfortunately, there were several cracks evenly distributed on all the studied pastes in both states (non-irradiated and irradiated), which arose during the preparation of samples for microstructural analysis and were not caused by irradiation or other conditioning of the samples. The reference paste (PC) exhibited no significant changes in microstructure, see Figure 3-1. On the contrary, in case of NP paste areas with lots of indistinct light spots appeared sporadically in the specimen, an example of the areas is depicted in Figure 3-2. There were also few dark spots with a "stripy" texture. Also, in case of the NP_C phase, these objects appeared, however, there was much more "dark" spots and less "light" ones, which is manifested in Figure 3-3. Due to the unfamiliar nature of the appearance of the new phases they were subjected to EDX analysis to obtain their chemical composition.

Figure 3-4 presents results of EDX analysis of NP_C paste at the sodium map (violet) and carbon map (green). There is brighter violet colour at the places of the "darker stripy" spots at the Na-map and brighter green colour at the C-map. These results of chemical analysis indicate the creation of sodium carbonates due to the irradiation of NP-C paste rather than calcium carbonates, as NP-C paste contains high amounts of free alkali coming from the evaporator concentrate.

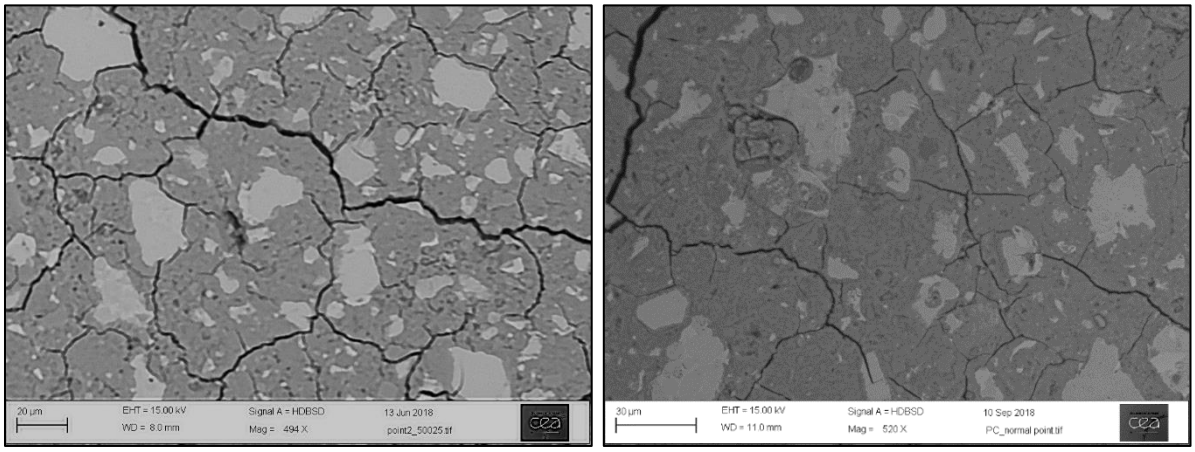

Figure 3-1: a) Microstructure of the paste PC before and b) after irradiation

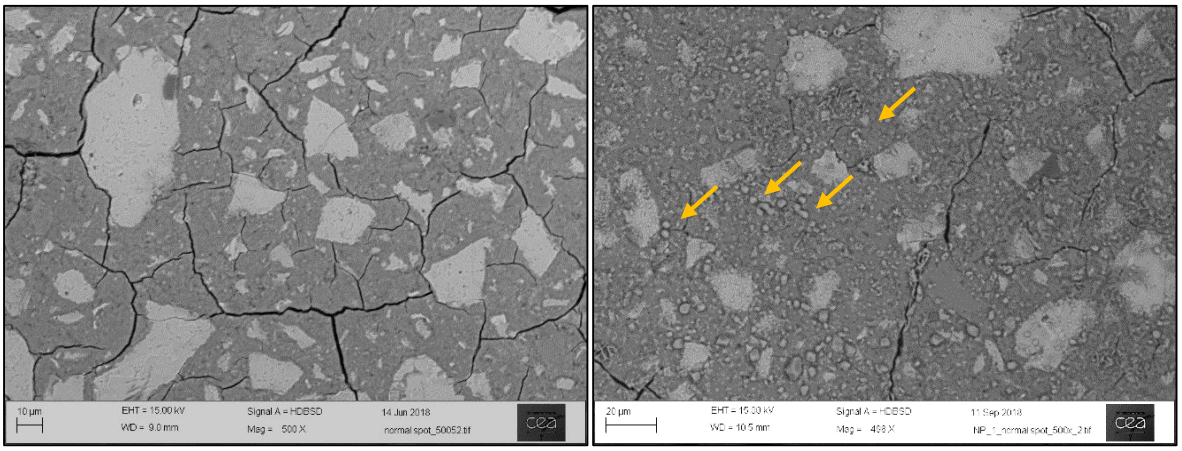

Figure 3-2: a) Microstructure of the paste NP before and b) after irradiation with arrows depicting the unfamiliar "light spots"

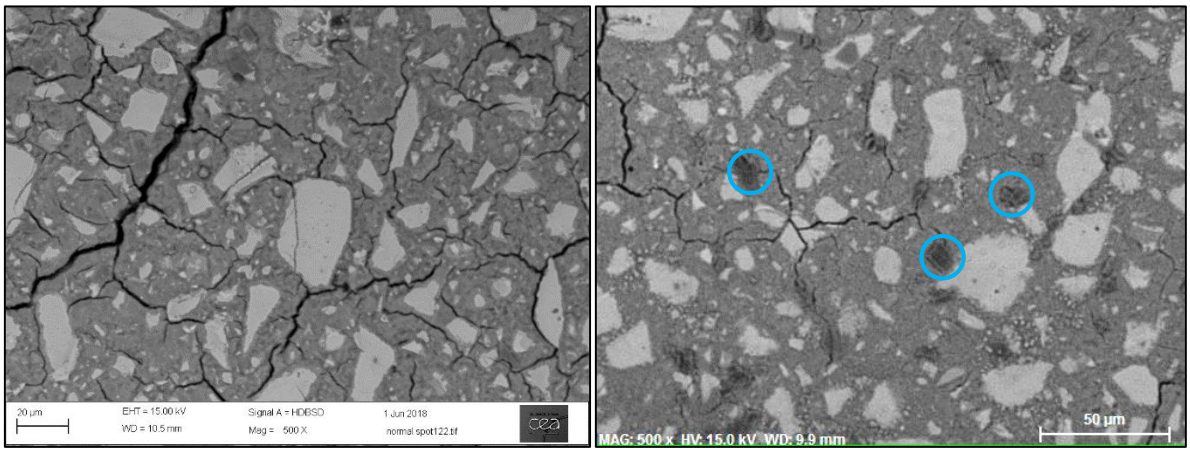

Figure 3-3: a) Microstructure of the paste NP_C before and b) after irradiation with circles depicting the unfamiliar "dark spots"

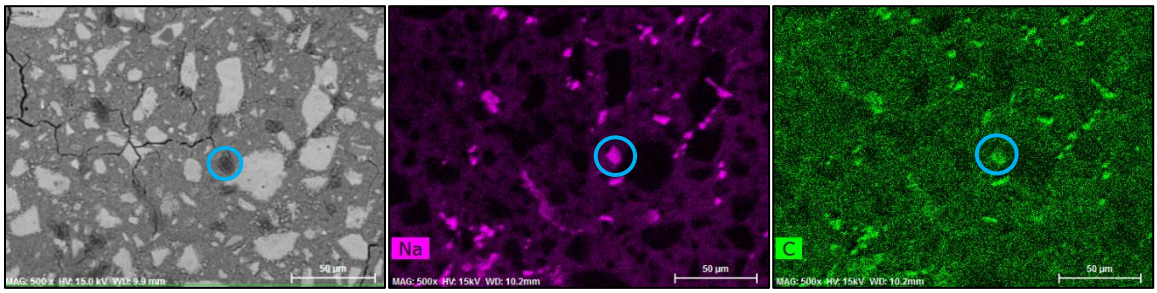

Figure 3-4: Microstructure of the NP_C paste after irradiation with EDX maps of Na (violet) and C (green)

3.3.2. XRD

X-ray diffraction was used to determine the mineralogical composition of the studied materials – non-irradiated samples (N) and irradiated specimens (IRR), which is summarized in Table 3-3. There was 15 – 25% by mass of un-hydrated particles (C_3S; C_2S; C_4AF) in each cement paste and 42 – 52% of amorphous phase, the rest was composed of crystalline minerals naturally present in hydrated cement pastes – Calcite $CaCO_3$; Portlandite $Ca(OH)_2$; Ettringite $Ca_6Al_2(SO_4)_3(OH)_{12}{\cdot}26H_2O$; Hemi-carbonate $Ca_4Al_2(OH)_{12}(OH)(CO_3)_{0.5}(H_2O)_5$; Mono-carbonate $Ca_4Al_2(OH)_{12}(CO_3)(H_2O)_5$; C-S-H; Katoite $Ca_3Al_2(OH)_{12}$. For cement pastes containing evaporator concentrate, there was no ettringite present, however it was replaced by Charlesite ($Ca_6(Al,Si)_2(SO_4)_2B(OH_4)(O,OH)_{12}{\cdot}26H_2$) [29]. Borates, which were in high amounts present in the concentrate, were embedded into the structure of the ettringite aluminate crystals to form charlesite instead. For PC samples, there were higher amounts of ettringite compared to NP and NP_C due to the content of gypsum in the Portland cement (used as a setting agent), while in NP and NP_C pastes, the sulphatic phases were reduced by blending of the cement with non-gypsum cement.

Irradiation caused reduction of the amounts of ettringite by 55% and 53% for PC and NP pastes in comparison to non-irradiated samples, while in case of NP_C charlesite content decreased by 72% due to irradiation. In case of PC and NP_C, there was also a decrease in the content of amorphous phases due to irradiation and apparent "increase" in the amount of C_3S and C_2S. As the increase of clinker

minerals is unlikely, it was probably the result of recalculation of the contents of all phases to give 100% in the sum after the loss of amorphous phase.

The presence of calcite in all specimens was the result of carbonation. However, there was no clear evidence of the enhanced carbonation due to irradiation as it was reported in some studies (Maruyama et al., 2017; Rosseel et al., 2016; Vodák et al., 2011), which may have been due to "quite low" gamma doses reached - 2 – 4 MGy. There were small variations in the remaining crystalline phases, i.e. Portlandite, Monocarbonate, Hemicarbonate and Katoite, but with no obvious trend.

Table 3-3: Proportional contents of individual mineralogical phases of studied pastes (PC, NP, and NP_C) for samples exposed to irradiation (IRR) and non-irradiated samples (N) obtained by X-ray diffraction

Sample	PC N	PC IRR	NP N	NP IRR	NP_C N	NP_C IRR
C_3S (Nishi)	7.8 ±1.4	14.4 ±0.3	17.0 ±0.2	12.8 ±0.3	9.2 ±0.4	11.9 ±0.3
C_2S (beta, Mumme)	0.0 ±0.2	3.1 ±0.3	1.9 ±0.1	4.1 ±0.2	3.7 ±0.2	4.2 ±0.2
C_4AF	5.0 ±0.2	5.9 ±0.2	4.3 ±0.2	5.1 ±0.2	3.6 ±0.1	4.6 ±0.1
Calcite	5.9 ±0.1	5.4 ±0.1	1.4 ±0.1	2.9 ±0.1	3.7 ±0.1	5.1 ±0.1
Portlandite	9.7 ±0.2	9.6 ±0.2	11.2 ±0.2	10.1 ±0.2	10.3 ±0.1	10.3 ±0.2
Ettringite	5.6 ±0.2	2.4 ±0.2	1.9 ±0.1	0.7 ±0.1	0	0
Charlesite	0	0	0	0	3.6 ±0.1	1.2 ±0.1
Hemicarbonate	0.6 ±0.1	0.5 ±0.1	1.9 ±0.1	2.0 ±0.1	1.5 ±0.1	0.9 ±0.1
Monocarbonate	2.9 ±0.3	1.9 ±0.3	3.0 ±0.2	3.8 ±0.2	4.0 ±0.2	5.0 ±0.2
Katoite	1.8 ±0.1	1.6 ±0.1	3.0 ±0.1	2.0 ±0.1	2.7 ±0.1	2.3 ±0.1
Amorph	60.6 ±1.5	55.2 ±0.5	54.5 ±0.5	56.5 ±0.5	57.8 ±0.6	54.4 ±0.5

3.3.3. Nanoindentation

For nanoindentation, six samples were prepared – three were exposed to irradiation and three were kept in a desiccator with low RH. Nanoindentation procedure was executed on each sample before and after the irradiation experiment. The standard Oliver & Pharr method was used to analyse the force – depth of indentation curves (Oliver and Pharr, 1992). The obtained data were then processed by hierarchical clustering algorithm, which groups the data with similar parameters (E, H, etc.) together in clusters. These clusters correspond to real mineralogical and amorphous phases in the microstructure of the studied material. The output data were then plotted into histograms of Young modulus. The respective percentage of individual phases, their mean values and standard deviations are summarized in Table 3-4.

The aim of this experiment was not to name and localize each phase, as it would need to be directly coupled with SEM, but to investigate changes in the phase distribution and changes in the phases´

micromechanical parameters in general. However, based on literature, the recorded phases correspond to LD-CSH + HD-CSH and $Ca(OH)_2$/$CaCO_3$ with typical values of Young modulus of elasticity according to Constantinides and Ulm (Ulm and Constantinides, 2014): 21.7 ± 2 GPa; 29.4 ± 2.4 GPa and 38 ± 5 GPa respectively. The remaining phases correspond to porosity or represent clusters with very low statistical value. Histograms of modulus of elasticity values are given in Figures 3-5 – 3-7 for samples PC, NP and NP-C respectively. For all irradiated specimens there is a significant rise of phases with mean values around 35 – 38 GPa which correspond to phases of $Ca(OH)_2$ or carbonates. Assuming that $Ca(OH)_2$ is likely to be rather depleted due to irradiation, this phase probably stands for carbonates. As some authors reported enhanced carbonation due to irradiation (Maruyama et al., 2017; Rosseel et al., 2016; Vodák et al., 2011), it is tempting to assume $CaCO_3$ to be the arisen phase, however, results from XRD did not show a marked rise in the amounts of crystalline $CaCO_3$. However, as in (Goto et al., 1995) an amorphous form of carbonates may be present. Considering also the results from SEM, the possible explanation is the rise of alkali carbonates in their amorphous state. Table 3-4 summarizes observation frequency of individual phases, the mean values and standard deviations of dynamic moduli before irradiation and the change due to irradiation (calculated as obtained values after irradiation minus values before irradiation). For all samples there is a decrease in the amount of phase 2 which corresponds to CSH and a rise in the amount of phase 3 corresponding to carbonates in range of 20 – 50 %. This shows that irradiation has a hardening effect on the investigated pastes.

Pastes immobilizing evaporator concentrates do not have a load bearing function, but their ability to keep structural integrity is critical. Cracking or binder disintegration may induce release of radionuclides into the surrounding environment. Nanoindentation showed that irradiation of studied pastes did not have adverse effects of the phase composition, but rather a slight hardening effect on the material.

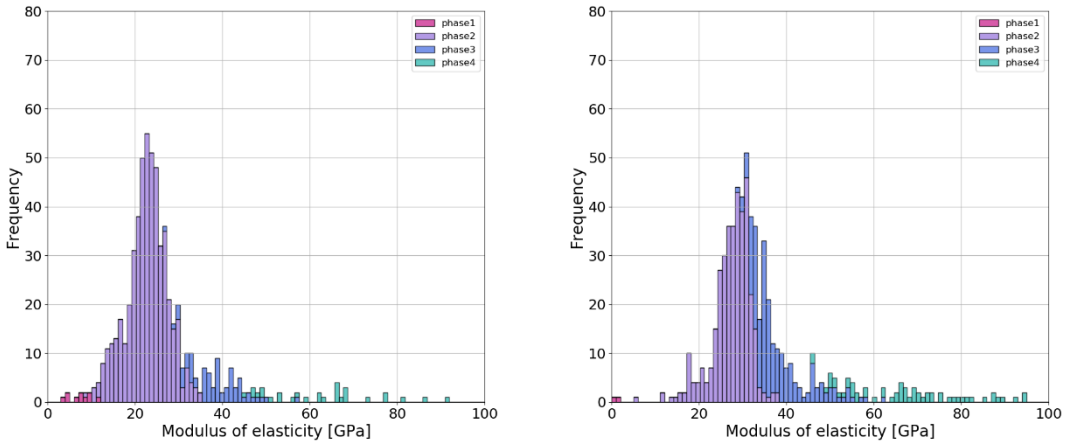

Figure 3-5: Histograms of modulus of elasticity values measured on the sample PC before (left-hand side) and after irradiation (right-hand side); phase 2 correspond to CSH phases, phase 3 to carbonates, phase 1 and 4 are statistically insignificant and may correspond to porosity and other phases

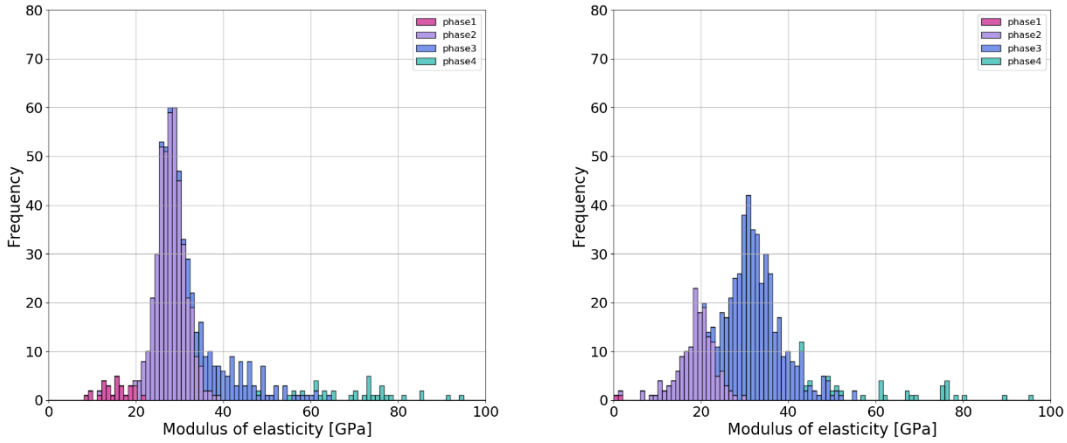

Figure 3-6: Histograms of modulus of elasticity values measured on the sample NP before (left-hand side) and after irradiation (right-hand side); phase 2 correspond to CSH phases, phase 3 to carbonates, phase 1 and 4 are statistically insignificant and may correspond to porosity and other phases

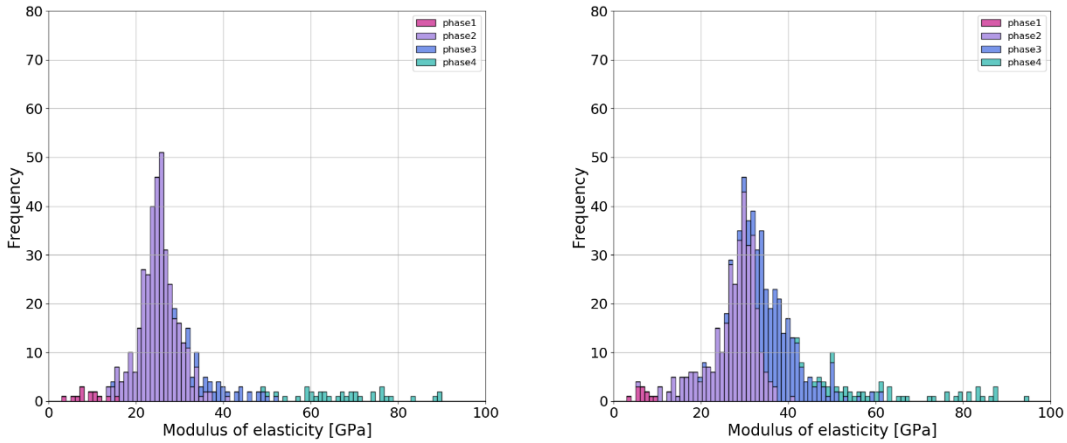

Figure 3-7: Histograms of modulus of elasticity values measured on the sample NP_C before (left-hand side) and after irradiation (right-hand side); phase 2 correspond to CSH phases, phase 3 to carbonates, phase 1 and 4 are statistically insignificant and may correspond to porosity and other phases

Table 3-4. Summarization of values of Modulus of elasticity E [GPa] of all specimens before irradiation and its change due to irradiation (increase is marked with +, decrease marked with -). Individual phases were identified using the hierarchical clustering algorithm

	values before irradiation			**increase (+) / decrease (-) in values after irradiation**		
	E			E		
phase	%	mean value	standard deviation	%	Mean value	standard deviation

			PC_1			
1	2	7	2	-2	-6	-1.6
2	82	23	5	**-24**	+4	-1
3	12	38	6	**+20**	0	0
4	5	63	12	+5	+5	+2
			NP_1			
1	4	15	3	-4	-14	-2.4
2	70	28	3	**-45**	-9	+1
3	20	41	8	**+49**	-8	-2
4	5	76	25	0	-6	-5
			NP_C_1			
1	3	9	3	-1	-2	-1.4
2	80	25	4	**-26**	+2	+1.4
3	9	38	7	**+28**	0	-0.8
4	8	69	12	0	-4	+2.3

3.4. Conclusion

A cement paste made of mixture of cements (NP), cement paste mixed with simulated evaporator concentrate (NP_C) and a reference paste (PC) were studied in terms of microstructural changes due to gamma irradiation to accumulated dose of 2 MGy using Co-60 source. Employed methods were Scanning Electron Microscopy with Energy Dispersive X ray Spectroscopy (EDX), X-ray diffraction (XRD) and nanoindentation. Conclusions derived from the results can be summarized as follows:

- SEM revealed a creation of new phases on NP_C paste due to irradiation; EDX showed these phases to be rich in sodium carbonates, thanks to high amounts of free alkali present in the evaporator concentrates;

- Shown from X-ray diffraction results, there is no ettringite phase in the paste NP_C as in case of PC and NP pastes, but thanks to boron incorporation into the structure, charlesite was found instead;

- XRD recorded decrease in ettringite content in the PC and NP pastes and decrease in charlesite content in the NP_C, decrease in the amorphous phase for PC and NP_C and no significant rise in $CaCO_3$ contents for any of the pastes due to irradiation;

- Nanoindentation indicated a creation of a new phases in the pastes thanks to irradiation with mean values of Young modulus of elasticity around 35 – 38 GPa, which probably corresponds to carbonates.

From the above mentioned it can be concluded that there was a rise of amorphous alkali carbonates on the irradiated pastes, mainly on the NP_C paste as there was a high content of free alkali in the simulated evaporator concentrate. Increase in carbonates caused slight hardening of the cement paste, and no disintegration or harmful effects on the material microstructure was observed. This indicates the ability of the material to preserve its function as a solid and safe encapsulation matrix during the lifetime of the immobilized waste in terms of radiation stability.

Chapter 4: Radiolysis

This paper was published in Annals of Nuclear Energy (Journal Impact Factor 1.9), volume 151, article number 107901, DOI 10.1016/j.anucene.2020.107901. As of may 2025, the paper has been cited 3 times in WoS collection.

The paper investigats the effect of radiolysis of water molecules occurring in hydrated cement pastes and hydrogen release on mechanical properties of the irradiated composite. The experimental part of this work was performed at CEA Saclay, using ^{60}Co gamma source and material specimens prepared at Czech Technical University.

4. Investigation of Radiolysis in Cement Pastes Immobilizing Simulated Evaporator Concentrates

Abstract

The waste management of radioactive evaporator concentrates (EC) in deep geological repositories requires safe immobilization in a solid matrix, such as cement composites. Radiolysis occurs inside the hydrated cement paste due to irradiation of either free or bonded water. As a result, the generation of hydrogen and the consequent pressure build-up within the material may pose safety risks within the geological repository. Three kinds of cement pastes sealed in steel containers were irradiated by gamma source ^{60}Co to achieve absorbed dose of 1.75 MGy simulating the conditions inside a repository. Specific binder matrix suitable for cement composites immobilizing EC marked as "NP" was studied, as well as the actual simulated immobilized waste (model concentrate) in the binder marked as "NP_C" and a reference paste "PC". Results showed an increase in pressure of generated gas from the irradiated samples up to 100 kPa. After 120 days of irradiation the reference paste reached steady state, while NP and NP_C continued in the rising trend. However, the absolute values of NP_C were lower than the values of the reference paste, probably due to the presence of dissolved salts in the model concentrates, especially nitrates. The maximum value reached does not present safety risks within the repository, moreover the presence of certain salts in the concentrate has a positive effect on the decrease of the rate and the final values of the pressure build-up.

Keywords: *evaporator concentrates, gamma irradiation, radiolysis*

4.1. Introduction

Considering the rising amounts of radioactive waste and the need of its´ safe disposal in an underground repository, there is obvious urgency to develop techniques for safe disposal and investigate possible scenarios and risks. Evaporator concentrates (EC) are intermediate-level radioactive waste generated from the cooling system in the primary circuit of nuclear power plants (NPPs) after its treatment by evaporation. There are high concentrations of boric acid in the concentrates, several salts and many radionuclides, e.g. ^{137}Cs, ^{134}Cs, ^{60}Co, ^{90}Sr, ^{54}Mn. In the Czech Republic these are currently being immobilized in bitumen within metallic drums and stored in temporary repositories. However, bitumen as an organic material is not allowed to be stored within an underground repository for long-term storage. For medium lived radioisotopes, typical storage period is in the range of 100 – 300 years, as about 7 half-lives of decay of these isotopes is required to lower the activity under 1% of the original waste activity. For most prolific component of the waste mixture, ^{137}Cs, this period is about 200 years. Possible and cost-effective alternative with perspective durability in the range of couple of centuries is the immobilization of EC in cementitious materials. The advantages of such a solution are the radiation stability and sufficient temperature stability of cement composites, durability and vast experience with these materials from civil engineering which gives us the knowledge of their degradation mechanisms and ways how to mitigate them. On the other hand, there are specifics of radioactive waste which may cause problems and thus research in these areas is necessary. One of them is the radiolysis phenomenon, which can take place in any kind of water molecules present in the composite. The decomposition of water molecule due to irradiation gives rise to H_2 and other gases generation accompanied with pressure increase inside the closed system of a waste package and possible risk of explosion or other hazards (Bobrowski et al., 2016; Buxton, 2008). Besides, the pressure build-up may induce internal stress within the composite leading to micro-cracks and loss of integrity, changing the gas and liquid transport properties or even affecting the hydration process of cement.

The prediction of radiolysis progress in the cement composite is not an easy task, as there is a variety of factors influencing the mechanisms, such as the type of radiation source, the radiation dose rate

and cumulated dose, chemical composition of the cementitious material and of the waste, porosity of the cement composite etc. The radiolysis progress in the cement environment is controlled by the precipitation of calcium peroxide octahydrate ($CaO_2 \cdot 8H_2O$) which precipitates in case of sufficient accumulation of peroxide ions in the pore solution as follows (Bouniol and Bjergbakke, 2008; Bouniol and Lapuerta-Cochet, 2012):

$$Ca(OH)_{2aq} + H_2O_2 + 6H_2O \rightarrow CaO_2 \cdot 8H_2O\downarrow \quad (2)$$

This process leads to a significant reduction in O_2 production and indirectly in the decline of H_2 production. However, the process is dependent on several factors such as the gamma dose rate and temperature. Also the composition of the waste may influence the radiolysis mechanisms. It has been reported in literature that the presence of nitrates in the waste significantly decreases the dihydrogen generation (Bykov et al., 2008), while ferrous substances slow down the H_2 recycling effect and thus result in higher dihydrogen accumulation. The presence of organic compounds, such as superplasticizers or other additives, can lead to generation of gas compounds such as CH_4, C_2H_6, CO_2, H_2CO. Specific codes for simulation of the radiolysis phenomenon are being developed (Bouniol, 2010; Bouniol et al., 2018; Bouniol and Bjergbakke, 2008; Bykov et al., 2008; Foct et al., 2013; Kirkegaard et al., 2014), however the complexity of such a problem needs verification and sufficient amount of input data for the simulations needs to be generated (Bouniol et al., 2013; Dewynter et al., 2017).

This article presents a study of the H_2 generation due to radiolysis in terms of pressure increase and gas analysis for different formulations of cement pastes which were selected as suitable binder for a composite immobilizing evaporator concentrates and a reference binder. A model evaporator concentrate was prepared and mixed with the binder to simulate real conditions as close as possible.

4.2. Materials and experimental setup

Three kinds of formulations were prepared for this experiment. Based on our previous research (Koťátková et al., 2018), a binder suitable for future cement composite immobilizing radioactive evaporator concentrates was developed. The binder is composed of two kinds of cement – Portland cement CEM I 52.5 R and non-gypsum cement in mutual ratio 50:50. Cement paste is made with water/binder ratio (w/b) 0.3 and superplasticizer based on melamine-formaldehyde resin Melment F10 (supplied by Stachema spol. s.r.o., Czech Republic) at the dose of 2% of cement weight. This formulation was marked as NP. Second formulation was made with a simulated evaporator concentrate (without radionuclides) instead of mixing water and was marked as NP_C. The composition of the simulated concentrate is given in Table 4-11 (Szalo and Žatkulák, 2000a). A reference mixture marked as PC was made by Portland cement CEM I 42.5 R with the same w/b ratio and plasticizer.

Twelve cylinders with dimensions 45 mm in diameter and 120 mm in height were prepared and stored in relative humidity 100% for 14 days. After that period, they were transported to CEA - Saclay, France, the LABRA laboratory where the experiment took place. The samples were unpacked, measured, weighed and six of them were placed in steel cylinder containers of dimensions 50 mm in diameter and 165 mm in height, the rest were left as spare samples. The containers were sealed and tested for gas-tightness using helium mass spectrometer leak detector (Figure 4-1). Then three of the samples were installed in the irradiation chamber according to the layout in the Figure 4-3 and three were placed outside the irradiator. Thin tubes from the containers were connected to the measuring system and both the containers and tubes were evacuated and then filled with inert argon gas. Before the start of the experiment the absolute argon pressure in the containers was introduced to be about 0.1 Bar, i.e. 10 kPa. The scheme of the experimental system is illustrated in Figure 4-3. The source of radiation was gamma source ^{60}Co.

The irradiation started at the samples´ age of 73 days and the experiment lasted for 140 days. Before the start of the experiment the actual dose rate inside the container was measured to be 528 Gy/h. Therefore, the reached cumulated dose was 1.75 MGy. This value was assessed based on the study of Bykov et al. (Bykov et al., 2008). Assuming a waste containing 137Cs with specific activity 1 Ci/l (3.7 1010 Bq/l), the absorbed dose over one half-life of ^{137}Cs (30.17 years) reaches 1 MGy. To reach a reduction in the activity by a factor 100, which corresponds to c. 6.5 half-lives, the absorbed dose is about 2 MGy. A slightly lower value of 1.75 MGy was reached due to time limitations of the experiment. Actual specific activities measured on real evaporator concentrates from VVER type nuclear plants in Czech Republic and Slovakia never exceeded 1 MBq/l of ^{137}Cs, ^{134}Cs and ^{60}Co activity, comprising usually more than 90% of total activity of the concentrate. Other radionuclides detected in the concentrates were ^{14}C, ^{41}Ca, ^{54}Mn, ^{58}Co, ^{59}Ni, ^{63}Ni, ^{79}Se, ^{90}Sr, ^{93}Zr, ^{93}Mo, ^{99}Tc, ^{107}Pd, ^{129}I, ^{110m}Ag, ^{151}Sm, ^{238}Pu, ^{239}Pu, ^{240}Pu and ^{241}Am in measurable amounts. The above mentioned assumption of maximum permitted activity of the concentrate 37 GBq/l still contains four orders of magnitude safety margin.

Gas pressure development induced by radiolysis during irradiation was continuously measured during the whole duration of the experiment and at the end, gas samples from all the containers were collected and analysed for their chemical composition. Using the classical ideal gas law, the obtained data of gas pressure were corrected in terms of temperature influence on the pressure changes and actual measured atmospheric pressure fluctuations as the used pressure sensors measured differential pressure relative to the atmospheric pressure.

Table 4-1: Simulated evaporator concentrate

	g/l
NaOH	72.9
KOH	14.9
H_3BO_3	76
Na_2SO_4	3.5
$NaNO_2$	14.5
$NaNO_3$	27.1
NaCl	2
$C_6H_8O_7$	1.6
$C_2H_2O_4 \cdot 2H_2O$	2.8

Figure 4-1: Samples inserted in containers prepared for the experiment

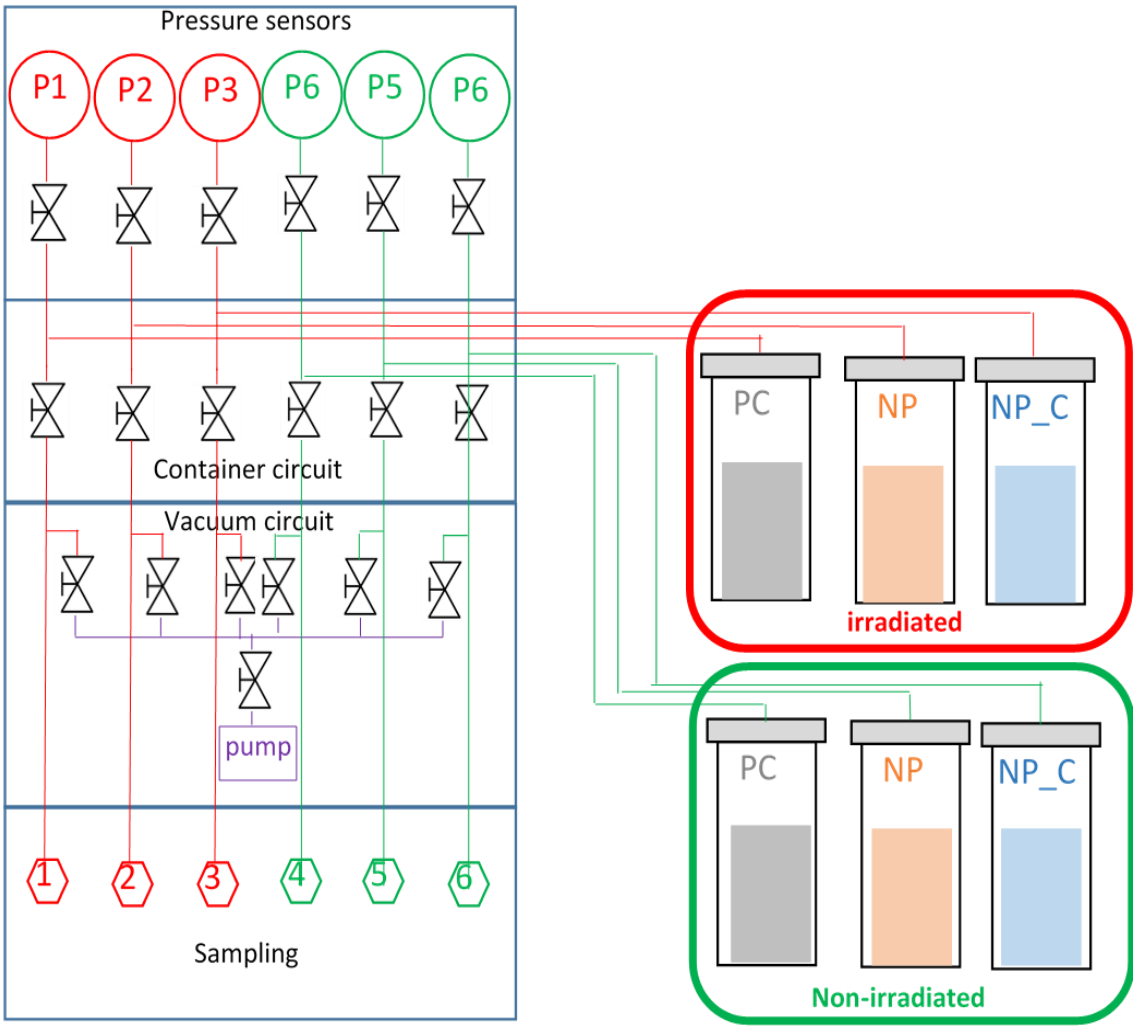

Figure 4-2: Layout of the experiment

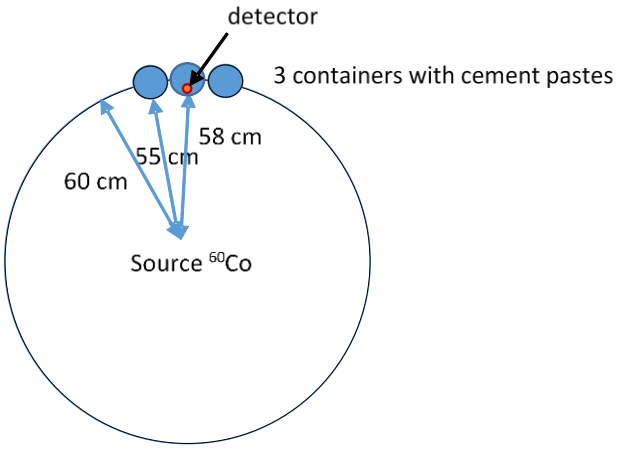

Figure 4-3: Position of the samples inside irradiation chamber

4.3. Results

Results of the experiment are summarized in Figure 4-4 and Table 4-2 (irradiated specimens are marked with No. 1, non-irradiated samples with No. 2). Figure 4-4 presents the change of values relative to the beginning of the experiment. The pressure in the containers before the start of the experiment was set to be 10 kPa and the flat horizontal parts in the curves are due to electricity shutdown or technical problems, which however did not have any influence on the overall picture of the experiment results. The black curve in the graphs represents the temperature changes inside the irradiation chamber very close to the installed containers with samples. Curves of non-irradiated (reference) samples show only small fluctuations in the pressure values which may be within the sensors´ measurement error or due to vapour pressure fluctuations to achieve equilibrium between pore water and the surrounding gas phase according to temperature fluctuations. Contrary, for the irradiated samples, there is a marked increase in the gas pressure induced by radiolysis of the water molecules contained in the pastes, either in the form of pore water, physically or chemically bound water. During the first c. 110 days of the experiment, the highest increase of pressure was recorded for reference sample PC_1, while NP_1 showed lower slope of the curve and NP_C the lowest. The reason for lower values recorded for NP_C may be the presence of many dissolved salt substances present in the model concentrate which was immobilized in the mixture. Especially nitrates, which are present in quite significant amounts in the concentrate (see Table 4-1), were reported in literature to be the suppressors of H_2 generation during radiolysis in cement pastes (Bykov et al., 2008). However, from the time point of 120 days the sample PC_1 exhibit the tendency to reach a steady state in the pressure build-up due to H_2 release, while NP_1 and NP_C_1 show rather continuing increase and moreover, the paste NP_1 achieves even higher values than the reference, but contrary the absolute values of NP_C_1 are lower than values of the other two irradiated specimens. The maximum values of pressure increase reached due to radiolysis for irradiated samples were about 100 kPa, which does not indicate the risk of explosion or other hazards within the radioactive waste repository as the pressure in the container with reference sample has already reached a steady state and which may be soon expected also for the other two formulations. But of course, further experiments are needed to confirm this hypothesis.

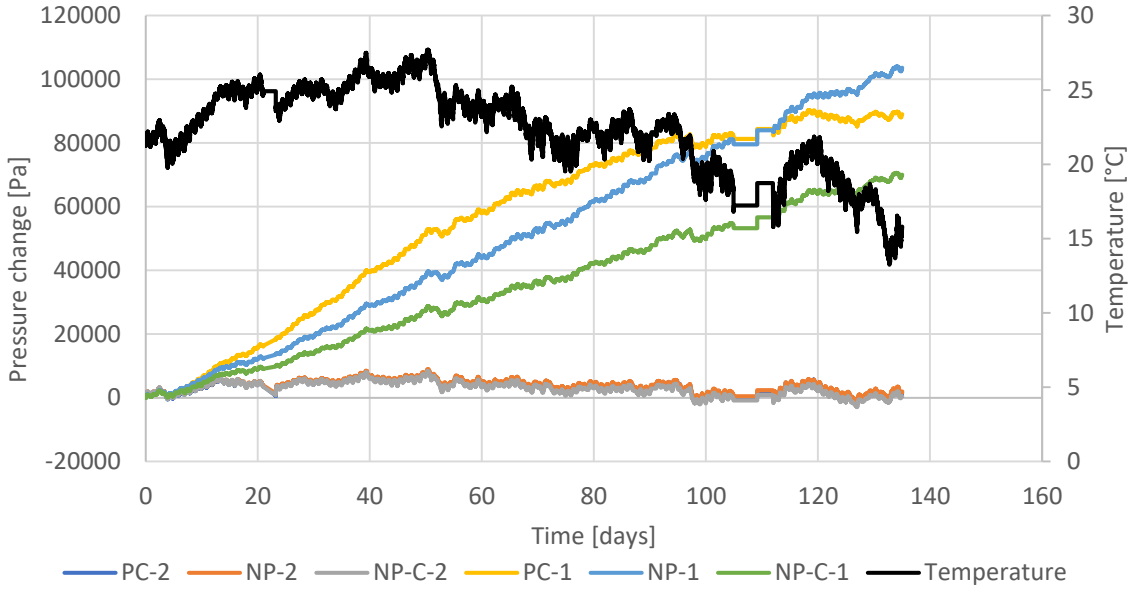

Figure 4-4: Values evolution of gas pressure inside the containers during the irradiation experiment (samples marked with No. 1 were irradiated; samples No. 2 were reference)

Table 4-2 presents the results of gas analysis sampled from all the containers at the end of the experiment. The composition of the gas is quantified as the amounts of individual species in volume percent. The high amounts of argon are obvious as the gas was used as an inert filler of the containers gas phase before the start of the experiment and the traces of helium are due to the testing of gas-tightness of the containers after their closure. Important are the values of dihydrogen, which is the main product of water radiolysis and is responsible for the pressure increase. There are also significant values of N_2 and N_2O (in bold). Possible explanation of rise of these gases is the interaction between melamine-formaldehyde resins used as plasticizers and released hydrogen particles. Decomposition of superplasticizers can also explain occurrence of hydrocarbon gases in the mixture. It can be seen that for the irradiated samples there are high values of dihydrogen compared to the non-irradiated samples, which was expected. An interesting fact is, however, that for PC_1 there are also higher amounts of N_2 and N_2O in comparison to NP_1 and NP_C_1 which showed similar values as non-irradiated samples (marked with No. 2). As mentioned above, these nitrogenous gases may be generated from the decomposition of the superplasticizer and may be the effect of reaching the steady state, while the curves of NP_1 and NP_C_1 still exhibited rising tendency. However, these are just assumptions and need to be studied further.

Table 4-2: Composition of gas inside the containers after the irradiation experiment – per cent volume (samples marked with No. 1 were irradiated; samples No. 2 were reference)

Vol. %	**PC-1**	**PC-2**	**NP-1**	**NP-2**	**NP-C-1**	**NP-C-2**
H_2	**14.810**	12.244	**36.131**	14.204	**30.036**	14.943
He	1.114	1.508	1.125	1.507	0.914	1.278
CH_4	0.024	0.019	0.056	0.025	0.044	0.027
CO	0.000	0.000	0.038	0.018	0.000	0.062
N_2	**10.049**	3.784	**2.774**	3.616	**3.047**	3.685
C_2H_4	0.000	0.000	0.000	0.000	0.000	0.000

C_2H_6	0.000	0.003	0.006	0.007	0.006	0.000
O_2	0.054	0.042	0.061	0.047	0.050	0.074
≥ C3	0.000	0.014	0.010	0.018	0.019	0.000
CO_2	0.000	0.000	0.000	0.000	0.000	0.006
N_2O	**12.407**	3.552	**2.396**	3.305	**2.800**	3.683
Ar	61.542	78.825	57.401	77.236	63.055	76.214
other species	0.000	0.008	0.004	0.017	0.029	0.028
Sum	100.000	100.000	100.000	100.000	100.000	100.000

Values in Table 4-2 represent volume fraction of analysed gas samples. Due to change in pressure in the irradiated containers (samples marked No. 1), these values do not represent absolute amount of the gasses, which can be more clearly understood by their mass in unit volume. The adjusted values of mass of gasses in the mix, adjusted to actual pressure in the container is in

Table 4-3.

Table 4-3: Composition of gas inside the containers after the irradiation experiment – mass per unit volume (samples marked with No. 1 were irradiated; samples No. 2 were reference)

Mass per unit volume [g/m^3]	**PC-1**	**PC-2**	**NP-1**	**NP-2**	**NP-C-1**	**NP-C-2**
Absolute Pressure [atm]	1.9504	1.0868	2.0951	1.0918	1.7693	1.0771
H_2	25,997	11,976	68,128	13,957	47,828	14,485
He	3,883	2,929	4,212	2,940	2,890	2,460
CH_4	0,335	0,148	0,840	0,195	0,558	0,208
CO	0,000	0,000	0,996	0,246	0,000	0,835
N_2	245,12	51,429	72,684	49,372	67,421	49,637
C_2H_4	0,000	0,000	0,000	0,000	0,000	0,000
C_2H_6	0,000	0,044	0,169	0,103	0,143	0,000
O_2	1,505	0,652	1,826	0,733	1,264	1,139
≥ C3	0,000	0,000	0,000	0,000	0,000	0,000
CO_2	0,000	0,000	0,000	0,000	0,000	0,127
N_2O	475,48	75,847	98,633	70,898	97,339	77,942
Ar	2140,8	1527,8	2144,8	1503,9	1989,7	1464,0

Table 4-3 shows the trends in gas generation in the containers. Generation of dihydrogen is clearly visible, as in the irradiated samples the proportion of dihydrogen gas increases significantly in all cases. Very notable is the increase in nitrogenous gases (N_2 and N_2O) in the PC samples, where is about 5-fold increase compared to the non-irradiated sample. These gases probably emerge from superplasticiser decomposition.

4.4. Conclusion

Radiolysis of water present in cement composites may be influenced by several factors, especially in the case of composites immobilizing waste with complex composition such as evaporator concentrates (EC). The article studied the radiolysis phenomenon in cement binders which may be suitable for a composite immobilizing EC. Gas analysis at the end of the experiment proved gas pressure increase in the sealed container, caused by generation of higher amounts of H_2 in vol. % for irradiated samples compared to non-irradiated ones. However, interesting fact was exhibited for the reference mixture PC showing similar amounts of H_2 as for non-irradiated samples, but higher amounts of N_2 and N_2O. These may be generated from the decomposition of melamine-formaldehyde resin superplasticizer occurring at higher rate than in samples using NP cement. These assumptions, however, need additional research to be proved. The pressure increase after achieving 1.75 MGy, which was selected to simulate the real conditions in a repository, was about 100 kPa which does not present potential safety hazards if taken into consideration when designing the container.

Chapter 5: Leaching

This paper was published in Progress in Nuclear Energy (Journal Impact Factor 2.7), volume 140, article number 103919, DOI 10.1016/j.pnucene.2021.103919. As of may 2025, the paper has been cited 4 times in WoS collection.

The paper summarizes results of research done on six different composite samples in order to investigate the retention ability of caesium ions under leaching conditions, which may occur in the underground repository od radioactive waste of the integrity of the waste package is compromised. The retentnion capacity of the material is evaluated according to standard ANSI/ANS-16.1-2003: Measurement Of The Leachability Of Solidified Low-Level Radioactive Wastes By A Short-Term Test Procedure.

5. Study on the properties of cement composites for immobilization of evaporator concentrates

Abstract

The disposal of evaporator concentrates (EC) as an intermediate-level radioactive waste requires reliable immobilization in a solid matrix, such as cement. Six types of cement composites were studied in terms of drying and saturation cycling, water absorption, mechanical properties and leaching to assess their suitability to EC immobilization. Composites differed in the binder composition – five of them were based on a mixture of non-gypsum cement with Ordinary Portland cement (NP)/metakaolin (NM) and admixtures of natural zeolite and metakaolin (NP_M, NP_Z, NM_Z). Sulpho-aluminate cement (SAC) was chosen for comparison. SAC composite exhibited superior parameters of compressive strength and water absorption in the reference state, however after cycling severe cracks and disintegration appeared causing this matrix inappropriate for EC immobilization. NM-based mixtures showed highest Cs^+ retention capacity, however less resistance to cycling and lower mechanical parameters than NP based composites. In terms of leachability, all mixtures met the requirements according to ANSI/ANS-16.1-2003.

Keywords: *radioactive waste, evaporator concentrates, leaching, immobilization, resistance to drying and saturation cycling*

5.1. Introduction

Evaporator concentrates (EC) are classified as liquid intermediate-level radioactive waste (ILW). The concentrate used in this study is generated during operation of VVER-type nuclear power plants (NPPs) with pressurized water reactors which use light water cooling system with addition of boric acid as a neutron absorber. The coolant is usually treated by filtration, ion exchange and evaporation. Filtration is used as a physical pre-treatment to exclude fine particulates from the waste stream, while ion exchange is chemical processing to remove soluble radionuclides. Evaporation is used mainly for large volume reduction of the effluent and high decontamination factor (up to 10^4 in a single stage evaporator) (International Atomic Energy Agency, 2001; Rahman et al., 2011). The process is in principle quite simple - based on distilling the solvent from the liquid waste, however it is quite expensive in comparison to other treatment processes (e.g. chemical precipitation) due to high energy consumption. The scale of volume reduction is limited by the solubility of dissolved salts and their content reaching a saturated solution. Therefore, the final product of evaporation is in this case a salt concentrate of total salt concentration up to 400 g/l, see Table 5-1 (Szalo and Žatkulák, 2000a).

As an intermediate-level waste, evaporator concentrates have to be immobilized and isolated from human environment for the majority of their lifetime in an interim storage facility or underground repository for final deposition. EC contain short (^{134}Cs, ^{60}Co, ^{54}Mn) and medium lived radioisotopes (^{137}Cs, ^{1} ^{90}Sr,). To lower the activity of medium-lived e radioisotopes under 1%, it takes about 7 half-lives of decay, or using 10 half-lives rule to lower activity under 0,1%, requires waste storage period in the range of 100 – 300 years.

Table 5-1: An example of evaporator concentrates´ composition typical for NPP Jaslovské Bohunice (Szalo and Žatkulák, 2000a)

Parameter	Unit	Value
pH	[-]	11.3- 13.3
Conductivity	[mS·cm^{-1}]	76.5 - 105.2
Boric Acid	**[g·l^{-1}]**	**73 - 160**
Salt content	[g·l^{-1}]	150 - 397

Na^+	[$g \cdot l^{-1}$]	42 - 100
K^+	[$g \cdot l^{-1}$]	9.4 - 21.5
Cl^-	[$g \cdot l^{-1}$]	0.9 - 1.8
NO_3^-	[$g \cdot l^{-1}$]	5 - 29.6
SO_4^{2-}	[$g \cdot l^{-1}$]	1.9 - 3.4
Organic substances	[g $O_2 \cdot l^{-1}$]	14.5 - 34.8
^{110m}Ag	[$Bq.l^{-1}$]	$1.0x10^4$ - $3.1x10^5$
^{60}Co	[$Bq.l^{-1}$]	$3.0x10^4$ - $1.1x10^6$
^{134}Cs	[$Bq.l^{-1}$]	$8.2x10^4$ - $2.0x10^6$
^{137}Cs	[$Bq.l^{-1}$]	$1.3x10^6$ - $8.4x10^6$
^{54}Mn	[$Bq.l^{-1}$]	$1.3x10^3$ - $5.0x10^5$

There are several possibilities of EC immobilization such as bituminization, cementation, vitrification and encapsulation in geopolymers (Ojovan et al., 2004). Geopolymers have high potential for good retention properties, but there is not enough data regarding their long-term durability, radiation stability etc. (Ojovan, 2011). Bitumen has usually higher waste loading ratio compared to cement and lower initial leaching rates, however it is flammable, melts under elevated temperatures, its radiation resistance is lower than in case of cement based composites and moreover under irradiation it releases H_2 from radiolysis of hydrocarbons causing the matrix to be inapplicable to underground repositories (Choppin et al., 2013).

Cement based materials are thermal and radiation stable, cost effective and easily handled. However, the high content of boric acid in EC result in postponed or improper hydration of Ordinary Portland cement, which needs to be dealt with by the design of alternative binders. High attention amongst a number of researchers has been paid to sulpho-aluminate cements (SAC) for their enhanced performance in immobilization of evaporator concentrates (Cau-dit-Coumes, 2013; Champenois et al., 2015; Coumes et al., 2017; Sun and Wang, 2010). The rate of hydration of sulpho-aluminate cements was reported to be less retarded in comparison with Ordinary Portland cement, the rise of early strength is higher and the hydration products are mainly AFm and AFt phases which are believed to provide high sorption capacity to radionuclides (Bothe and Brown, 1998; Champenois et al., 2012; Sun et al., 2011a, 2011b; Sun and Wang, 2010). However, the log-term properties of such a system have not been anywhere addressed yet.

The presented work studies the design possibilities of novel cement-based matrices and their efficiency for immobilization of evaporator concentrates and provides a comparison with properties of matrix based on SAC cement. The criterion of matrix suitability for EC immobilization was leaching analysis based on ANSI/ANS-16.1-2003. Durability of studied composites was studied in terms of resistance to drying and saturation cycling and subsequent changes in water absorption and mechanical properties. Materials and experimental plan

In order to be able to work in common laboratory conditions, i.e. outside a Controlled Radiation Area, a model evaporator concentrate without radionuclides but with a representative composition and properties was prepared. The composition of a model concentrate was taken from the study of Szalo and Žatkulák (Szalo and Žatkulák, 2000a) and is presented in Table 5-2. The individual compounds were sequentially mixed with distilled water. Prepared concentrate was used later as mixing water in the cement composites.

Table 5-2: Composition of a model evaporator concentrate (Szalo and Žatkulák, 2000a)

	g/l
NaOH	72.9
KOH	14.9
H_3BO_3	76.0
Na_2SO_4	3.5
$NaNO_2$	14.5
$NaNO_3$	27.1
NaCl	2.0
$C_6H_8O_7$	1.6
$C_2H_2O_4 \cdot 2H_2O$	2.8

Based on literature review (Koťátková et al., 2017a) and our previous experiments (Koťátková et al., 2020; Zatloukalová et al., 2021, 2020a, 2020b) six types of cement composites were designed. Five of them are based on the utilization of non-gypsum cement and for the sake of comparison a calcium-sulpho-aluminate (SAC) cement was also chosen as one of the binders. Calcium-sulpho-aluminate cement was supplied by Caltra Nederland B.V. and it is composed of ye'elimite (calcium sulfoauminate $Ca_4(AlO_2)_6SO_3$), α-belite and calcium-suplhate which hydrate into ettringite mainly. The next five mixtures contain 50% of non-gypsum cement to achieve proper hydration of the composites and 50% of binding agents: Portland cement, metakaolin and natural zeolite. The composition of the proposed **binders** is as follows:

- SAC: 100 % calcium-sulpho-aluminate cement
- NP: 50 % non-gypsum cement + 50 % Portland cement 42.5 R
- NM: 50 % non-gypsum cement + 50 % metakaolin
- NP_M: 50 % non-gypsum cement + 45 % Portland cement 42.5 R + 5% of metakaolin
- NP_Z: 50 % non-gypsum cement + 45 % Portland cement 42.5 R + 5% of natural zeolite
- NM_Z: 50 % non-gypsum cement + 45 % metakaolin + 5% of natural zeolite

In order to avoid volume changes of the materials, pure fine silica aggregate was added at dose of 40 wt%. The aggregate was supplied by Sklopísek Střeleč, Czech Republic, and was proved to be inactive to alkali-silica reaction according to ČSN EN ISO/IEC 17025 ("ČSN EN ISO/IEC 17025: Všeobecné požadavky na kompetenci zkušebních a kalibračních laboratoří," 2005).

The mixtures were prepared using two water/binder ratios:

- 0.4
- 0.5

Binder and filler materials were mixed with evaporator concentrate due to its liquid state instead of mixing water. As there is a requirement to achieve high volume fraction of solidified waste, water/binder ratio has to be quite high (0.4; 0.5), which is in contradiction with the pursuit of achieving good physical and mechanical properties of the final composite. It is widely known, that high water content results in high porosity, especially in terms of capillary pores which favor the transport of liquid media, possibly leading to radionuclide release. Therefore, leaching analysis of the studied composites was performed on samples with higher w/b ratio.

Table 5-3: Chemical and physical characteristics of used binder materials, as % of mass

[%m]	Portland cement 42.5 R	Zeolite	Metakaolin	Non-gypsum cement	Sulpho-aluminate cement
SiO_2	19.5	74.5	54.10	19.84	≤ 12.0
Al_2O_3	4.7	15.4	40.1	5.4	≥ 20.0
Fe_2O_3	3.3	1.6	1.1	3.10	≤ 2.0
CaO	63.2	3.3	0.13	63.5	≥ 45.0
MgO	1.5	0.7	0.18	2.39	-
K_2O	0.78	3.5	0.8	0.70	-
Na_2O	0.15	0.6	-	0.40	-
TiO_2	-	0.2	1.8	0.33	≤ 2.5
SO_3	3.07	4.9	-	0.25	≤ 20.0
P_2O_5	-	0.2	-	0.14	-
LOI	3.38	5.32	2.2	3.1	≤ 3.0
IR	0.8	-	-	0.35	-
Bulk density [kg/m^3]	3130	2210	2420	3150	~ 2970
Blaine´ s surface area [m^2/kg]	338	~620	~550	~320	~450

Six prismatic samples of dimensions 40 x 40 x 160 mm were manufactured for each mixture type and cured for 28 days at laboratory conditions (T = 20±1°C, RH = 50±5%). After this period, they were subjected to testing of drying and saturation cycles. Three samples of each mixture were periodically heated to 80°C for two weeks and then saturated with water over next two weeks' period and three samples were left as reference samples in laboratory conditions. Between the heating and saturation cycles all the samples were weighed and measured by ultrasound impulse technique following ČSN 73 1371 ("ČSN 73 1371: Non-destructive testing of concrete – Method of ultrasonic pulse testing of concrete," 2012) to assess its changes in microstructure expressed as changes in dynamic modulus of elasticity. Three cycles of heating and saturation were performed in order to compare the performance of the mixtures in circumstances simulating the harsh conditions in case of failure of other barriers in an underground repository.

Afterwards, the samples were subjected to water absorption testing following the procedure of Vejmelková et al. (Vejmelková et al., 2009). All samples (including reference samples) were dried at 60°C, the lower parts of their lateral sides were sealed in order to achieve one-directional water passage through the material and then subsequently subjected to the absorption experiment. Each sample was immersed in water in depth of 10 mm under the water level so that the base of the prism of dimensions 40x40 mm was under water. The sample immersed in water was hung on to the balance and automatically weighed in periods of 30 s until the steady state on the sample's weight was reached. The measured cumulative mass of the samples was then plotted against square root of time. The absorption coefficient was then calculated as the slope of the rising linear part of the obtained curve. After the experiment, the samples were left in laboratory conditions to evaporate the majority of water and reach hygric equilibrium with the environment. At the end, after half a year from manufacturing, all the samples were tested destructively to determine their compressive and flexural strength according to ČSN EN 1015-11 ("ČSN EN 1015-11: Testing methods for mortar for masonry - part 11: Determination of compressive and flexural strength of hardened mortars," 2000). Open porosities and

sorptivities were calculated using ČSN EN ISO 12570 ("ČSN EN ISO 12570 (730573) Tepelně vlhkostní chování stavebních materiálů a výrobků - Stanovení vlhkosti sušením při zvýšené teplotě," 2001).

Due to the lack of Czech standard regarding leaching of liquid ILW from a solid matrix, the leaching test followed American ANSI/ANS-16.1-2003 method ("ANSI/ANS-16.1-2003 American National Standard Measurement of the Leachability of Solidified Low-Level Radioactive Wastes by a Short-Term Test Procedure," 2003), however instead of radioactivity of the leachate (source ^{137}Cs), the concentration of stable Cs^+ was measured. CsCl at concentration of Cs 8.9 g/l was added in the simulated evaporator concentrate before the preparation of the samples. Samples of dimensions 20 x 20 x 100 mm were kept in 75% RH to simulate a closed environment and were subjected to testing at the age of year and a half.

Each sample was immersed in 880 ml deionized water, which was replaced at cumulative times of 2 h, 7 h, 1 d, 2 d, 3 d, 4 d, 5 d, 19 d, 47 d and 90 days. The concentration of Cs^+ in leachates was analyzed by an atomic absorption spectrometer GBC 933 AA (GBC Scientific Equipment, Australia). Cesium hollow cathode lamp was operated at 852.1 nm with 1.0 nm slit width. Atomization was performed with an air-acetylene flame. To suppress partial ionization of cesium during its determination, potassium chloride was added to all the samples to get a final concentration of 2 500 µg/mL of K^+. Blank samples and reference materials were also measured to verify the accuracy of the cesium determination.

The leached fraction Φ_n [-] of Cs^+ was determined from the expression:

$$\Phi_n = \frac{c_n V}{M_0} \quad (1)$$

where c_n *[g/l]* is the concentration of Cs^+ in the leachate at the *n*th interval, *V [l]* is the leaching solution volume and M_0 is the mass of Cs^+ in the sample at the beginning of the experiment.

The leached fraction corresponds to $\frac{a_n}{A_0}$ in the standard leaching test, where a_n is the radioactivity of the leachate at the leaching interval *n* and A_0 is the initial radioactivity of the wasteform.

The apparent diffusion coefficient D_e *[cm²/s]* is calculated as follows:

$$D_e = \frac{\pi\, m^2\, {V_s}^2}{4\, S^2} \quad (2)$$

where *m* is the slope of $\frac{\Sigma a_n}{A_0}$ vs $t^{1/2}$ *[s$^{1/2}$]*, V_s *[cm³]* is the volume of the sample and *S [cm²]* is the surface area of the sample.

Finally, the leachability index is calculated using:

$$L = \log \frac{\beta}{D_e} \quad (3)$$

where β is a constant, β = 1 cm²/s.

5.2. Results

5.2.1. Drying and saturation cycles

Figures 5-1 – 5-4 present the results obtained from tests of durability based on drying and saturation cycling. Figure 5-1 gives bulk densities of the mixtures and their changes after each cycle. There are only minor changes between both the individual mixtures and the cycles of drying and saturation (within 5%), although the differences in open porosities are considerable, see Figure 5-2. Sulpho-aluminate cement based composites exhibited the highest values of open porosities at all stages of cycling.

For w/b=0.4 mixtures based on NP binder showed open porosities around 24 %, while mixtures based on NM binder showed open porosities around 28 % and SAC mixture is the most porous with open porosity of 31 % after the first cycle. Also, variations between individual cycles were recorded. The smallest differences were found to be in case of NP mixture, within 3 %, but with the addition of admixtures (NP_M and NP_Z) and for mixtures based on NM binder there were higher variations between individual cycles. Generally, the open porosities decreased after the second cycle and slightly rose again after the third cycle. The decrease after the second cycle may have been caused by the continuing hydration of the binder, while the further cycle had a rather adverse effect causing microcracks due to crystallization of concentrate constituents in pores and thus slight rise of the open porosity. This rise was very significant in case of SAC mixture – by 19 %, as the sample suffered with a lot of widely open cracks, see Figure 5-5 (similarly for samples with w/b =0.5, see Figure 5-6). The cause of SAC cracking is the dissolution and rehydration of the main hydration product of the binder – ettringite. Ettringite is known for its highly expansive character which is destructive when hydrating in an already hardened matrix. Figure 5-3 gives values of sorptivities, which follow roughly the same trend as open porosities ranging from 10 to 19 %.

Changes in dynamic modulus elasticity E_{bu}, which were measured by ultrasound impulse technique, between individual cycles are presented in Figure 5-4. Due to the fact, that ultrasound passes through different media with different velocity, this method is sensitive to the presence of any microcracks and cracks. Therefore, it is clearly visible, what mixture types suffered from deterioration due to cycling. The initial values of individual mixtures showed superior values for SAC mixture, while the lowest values were found for mixtures based on NM binder. However, with cycling the values of SAC rapidly decreased and after the last cycle, the measurement could not be performed due to the presence of severe cracks (Figure 5-5 and Figure 5-6). There was also a big drop in values with NP_Z and a decreasing trend was also found for both NM-based mixtures. The lowest decreasing trends were found for mixtures NP and NP_M. Overall, the best behavior in terms of resistance to cycles of drought and saturation for was shown in cases of NP and NP_M and NP_Z. Contrary, the integrity of SAC samples was visibly disturbed, which was not the case of any other mixtures.

Results gained from samples with w/b = 0.5 showed very similar trends as for w/b=0.4, only as expected, the absolute values were generally slightly worse thanks to higher total porosity resulting by higher amount of mixing water. The absolute values of open porosities for samples with w/b=0.5 were from 2 to 14 % higher in comparison to those with w/b=0.4, similarly values of sorptivity were 0.5 to 4.5 % higher. This is in agreement with values of dynamic modulus of elasticity, which showed 10 to 20 % lower values for w/b=0.5 compared to w/b=0.4.

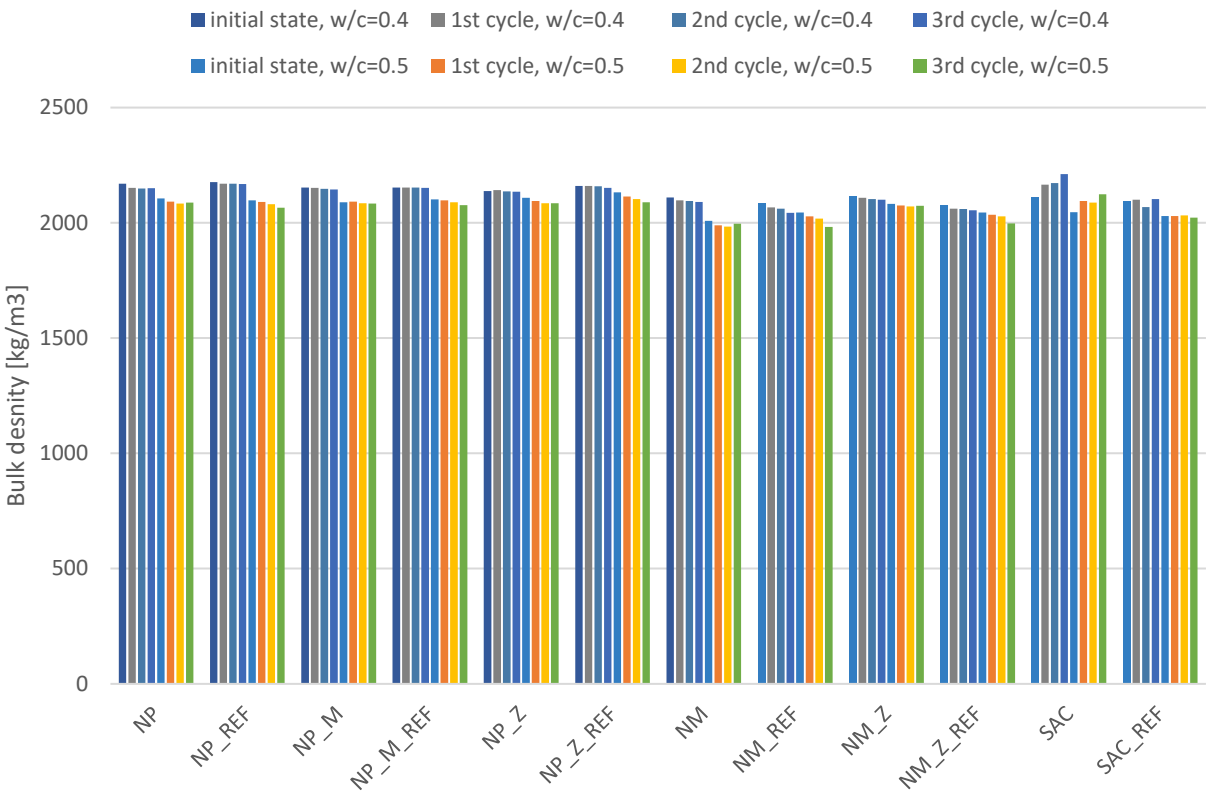

Figure 5-1: Bulk density of studied mixtures

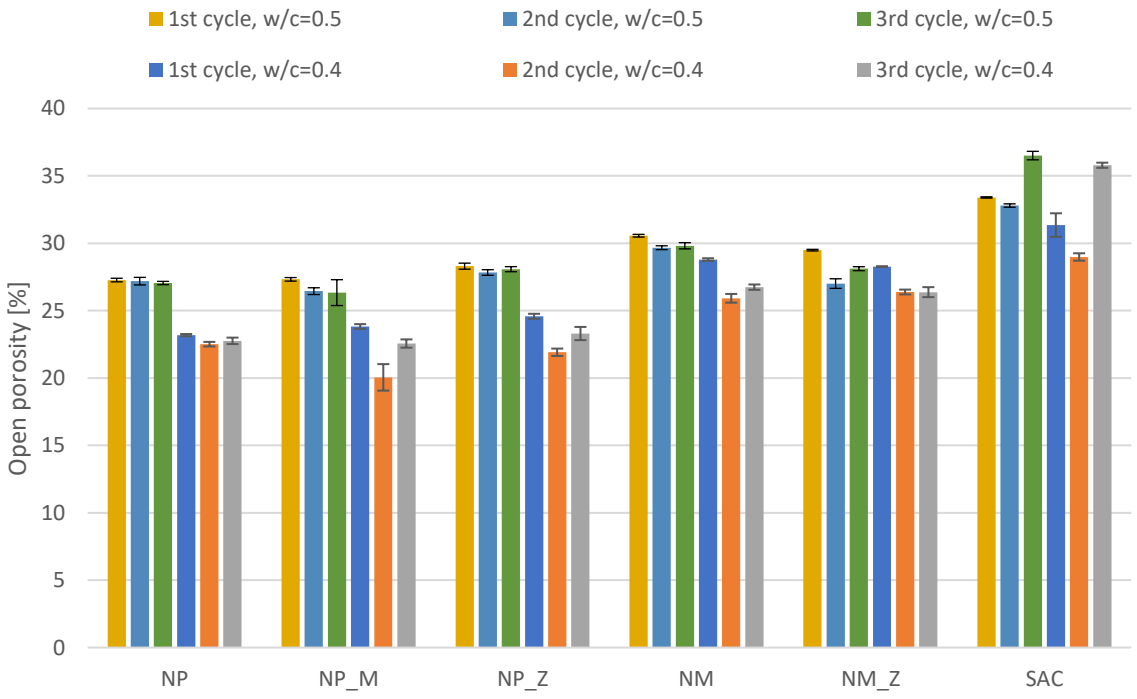

Figure 5-2: Open porosity of studied mixtures

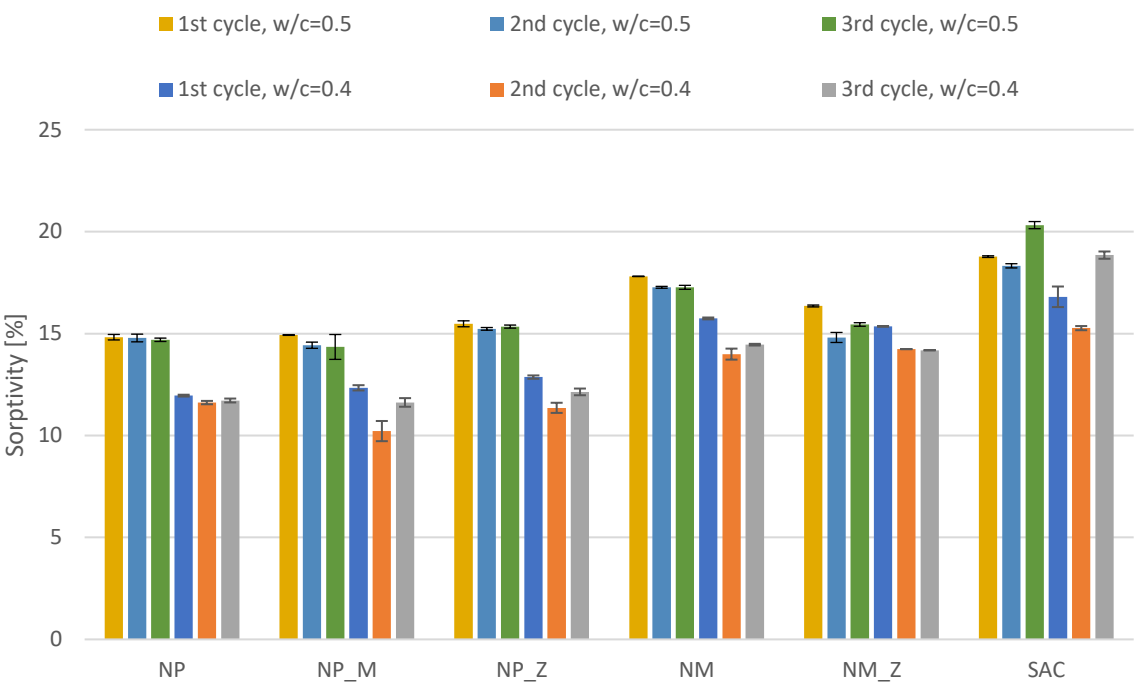

Figure 5-3: Sorptivity of studied mixtures

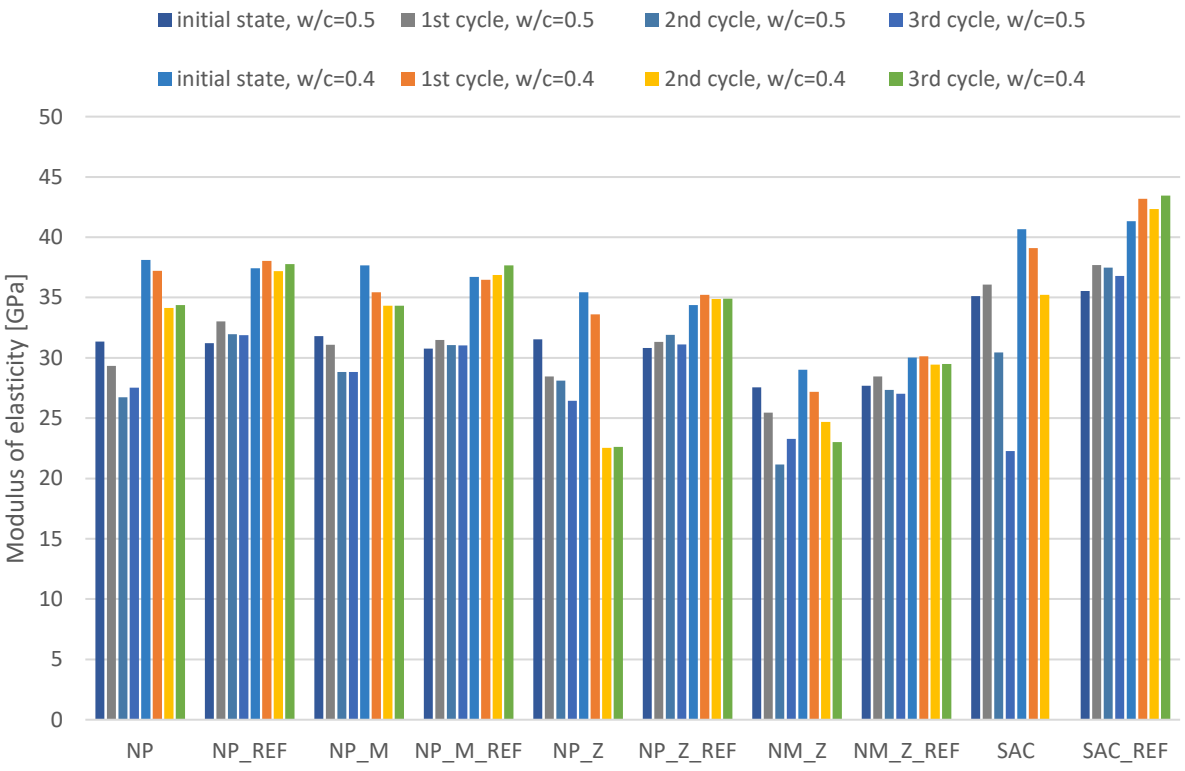

Figure 5-4: Dynamic modulus of elasticity of studied mixtures

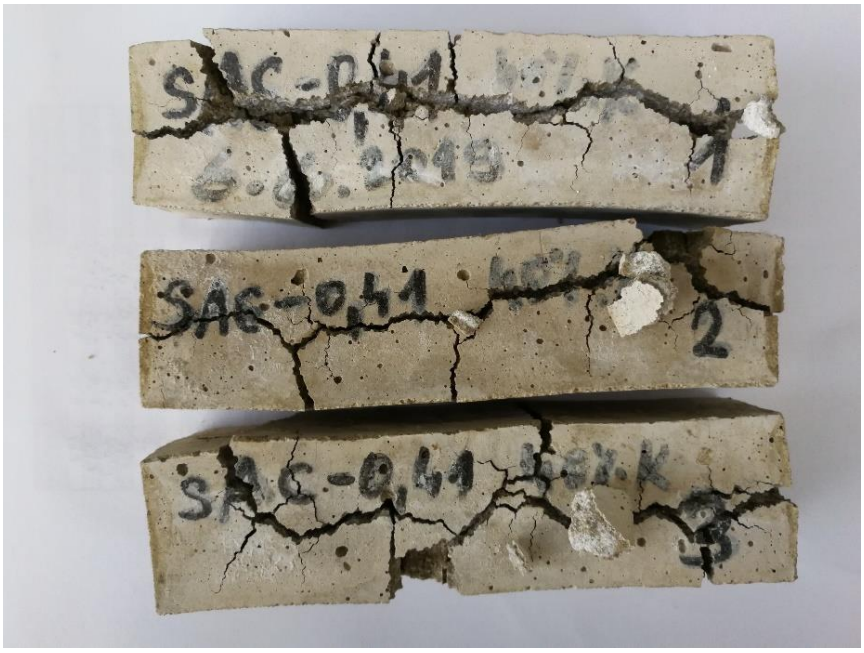

Figure 5-5: Samples of SAC mixtures manufactured with w/b=0.4 after the three cycles of drying and saturation

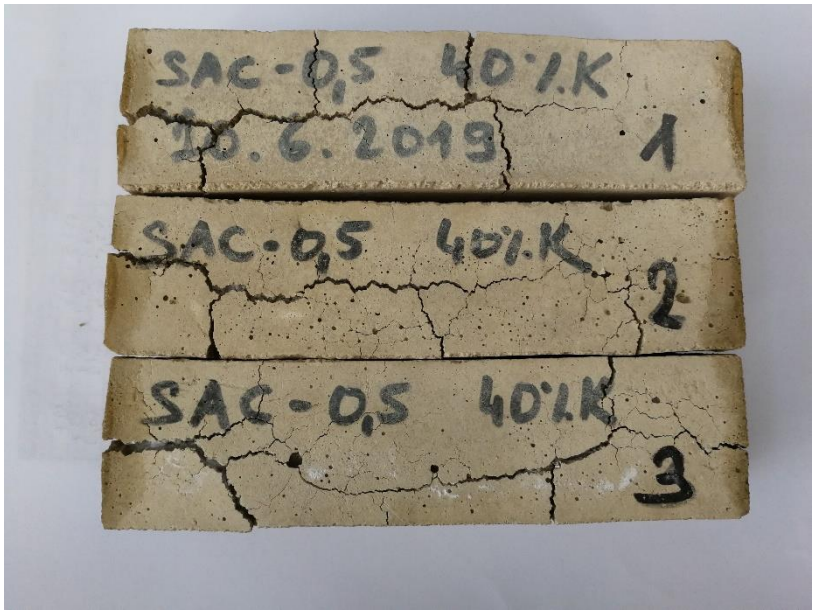

Figure 5-6: Samples of SAC mixtures manufactured with w/b=0.5 after three cycles of drying and saturation

5.2.2. Water absorption

After cycling, the absorption experiment was performed in order to evaluate the ability of samples to maintain its sealing function. Values of water absorption coefficient are given in Figure 5-7. Apart from SAC mixtures, for all mixtures based on NP and NM binders, values of absorption coefficient decreased after cycling, which is in agreement with the results of open porosities (see Figure 5-2) and sorptivities (see Figure 5-3). There was higher scatter in the scale of decrease in values for mixtures with water/binder ratio 0.5, ranging from 9 to 45 %, while in case of w/b = 0.4, the reduction in values ranged between 20 to 40 %. The reason of reduction of the water absorption ability is the rehydration

of cement grains due to cycling resulting in alternation of the porous system. The effect of saturation and drying at elevated temperature can affect hydration process of cement paste in similar way as curing at elevated temperature. Previous study by Ma, Hu and Ye (Ma et al., 2013) has shown significant effect of curing cement pastes at elevated temperature to pore system permeability by reduction of volume of capillary pores and the effect to tortuosity and connectivity of the pore network. Their cement specimens, cured at elevated temperatures (40°C vs. 20°C) showed decrease in water permeability exceeding an order of magnitude. The effect lays in the decrease of radii of individual pores mitigating the capillary elevation phenomenon and general densification of the material's microstructure, as a result of transition from capillary pores to gel pores during hydration. Contrary, the cracking of SAC samples caused a considerable rise in values, having higher impact on the mixture with lower water/binder ratio (w/b= 0.4), which reached 10 times higher value after cycling compared to the reference value.

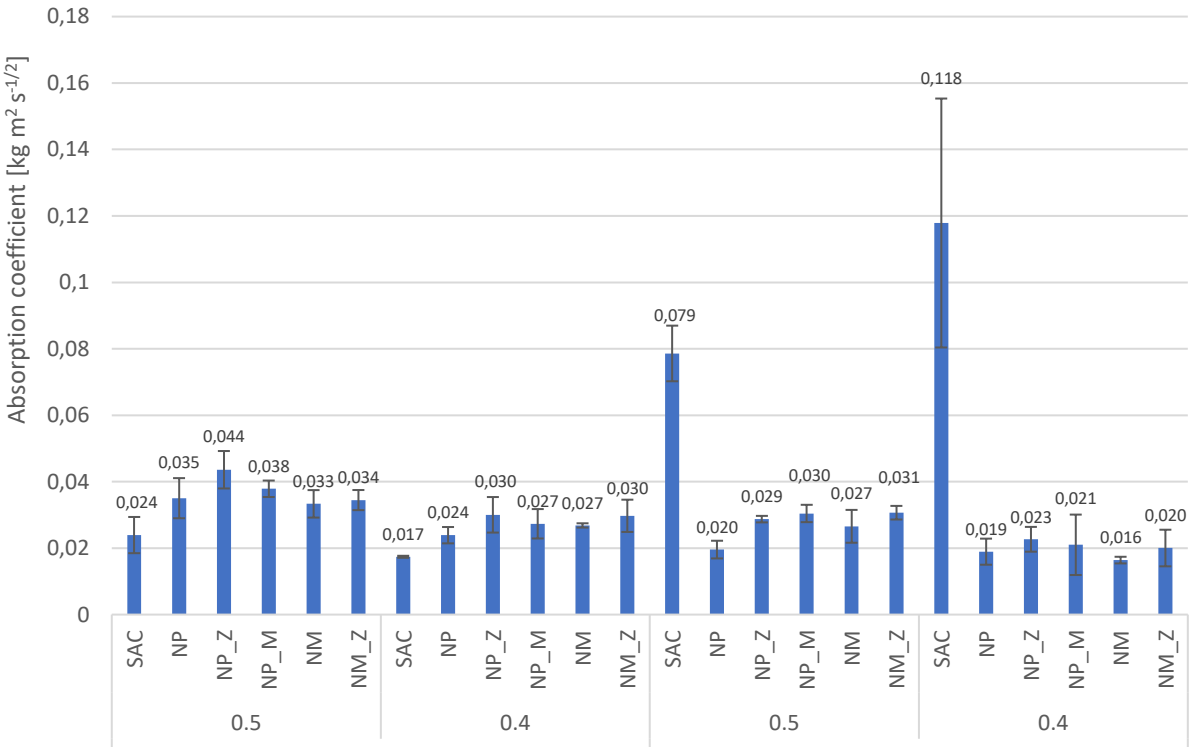

Figure 5-7: Absorption coefficient of studied samples after three cycles of drying and saturation compared to values of reference samples

5.2.3.Mechanical properties

Figures 5-8 – 5-9 give testing results of mechanical properties. Flexural strength of reference mixtures with w/b ratio 0.4 ranged in values from 3 to 4.5 MPa without any significant differences (see Figure 5-8), while in case of w/b=0.5 there was notably higher value of SAC mixture reaching 4.2 MPa, which exceeded its equivalent mixture with w/b = 0.4.On the other hand, NP_M with w/b = 0.5 showed significantly lower value than in case of w/b 0.4 by almost 50 %. Generally, values after cycling for all mixtures notably increased for both w/b ratios by 6 – 50 %, except from SAC mixtures which could not be assessed due to its severe damage. Values of flexural strength after cycling were in range of 4.5 – 6 MPa for w/b = 0.4 and 3.3 – 4.5 MPa for w/b = 0.5, which is more than sufficient in order to maintain their integrity during underground storage.

Compressive strength of reference samples ranged from 41 – 67 MPa for w/b = 0.4 and 34 – 47 MPa for w/b = 0.5 (Figure 5-9). Again, cycling had a positive effect on the compressive strength of all

mixtures (except from the damaged SAC samples), the rise in values ranged from 15 to 45 %. Absolute values of compressive strength after cycling did not differ significantly in case of w/b = 0.5, ranging from 50 – 60 MPa, while in case of w/b = 0.4 there was higher scatter in values, ranging from 60 – 90 MPa in favor of NP mixtures.

The decrease of mechanical properties with increasing w/c ratio is consistent with previous research (Rahman and Zaki, 2020). The unusually high w/c ratios are desirable due to the need to decrease the volume of final package while including maximum amount of waste in the matrix. While the solidified matrix keeps sufficient mechanical properties, even with such high w/c ratios, the pore structure of the matrix is suspected to cause loss of retention capacity and increase in leachability (Ma et al., 2013).

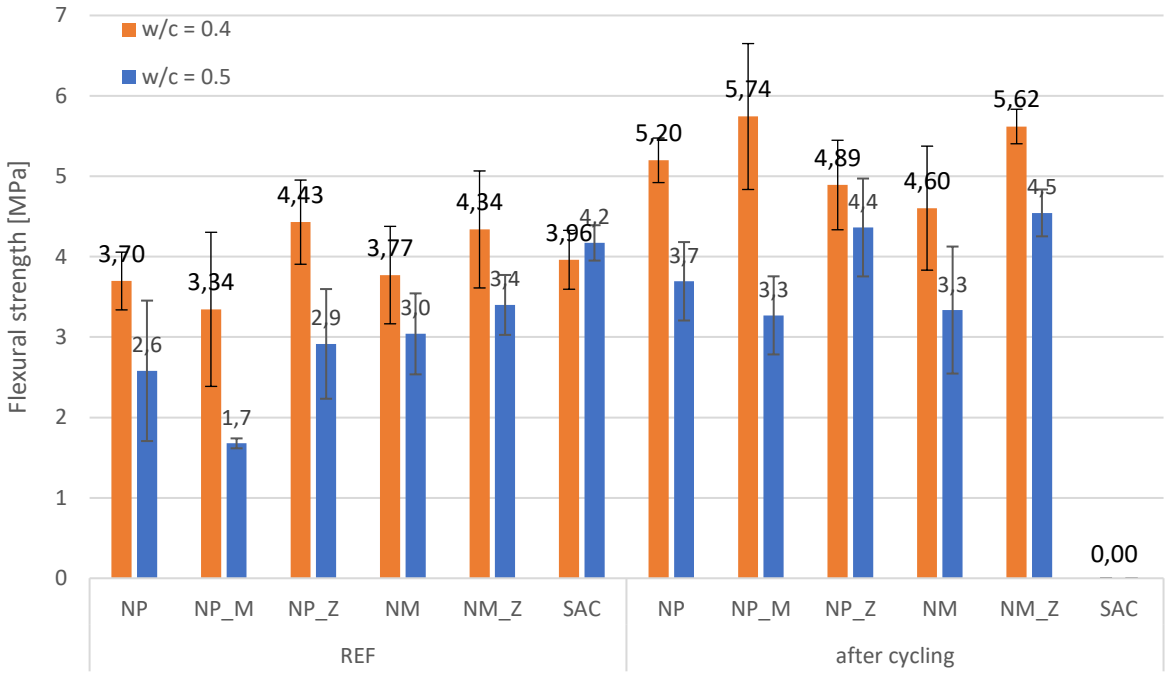

Figure 5-8: Flexural strength of samples manufactured after three cycles of drying and saturation, note: SAC disintegrated after cycling

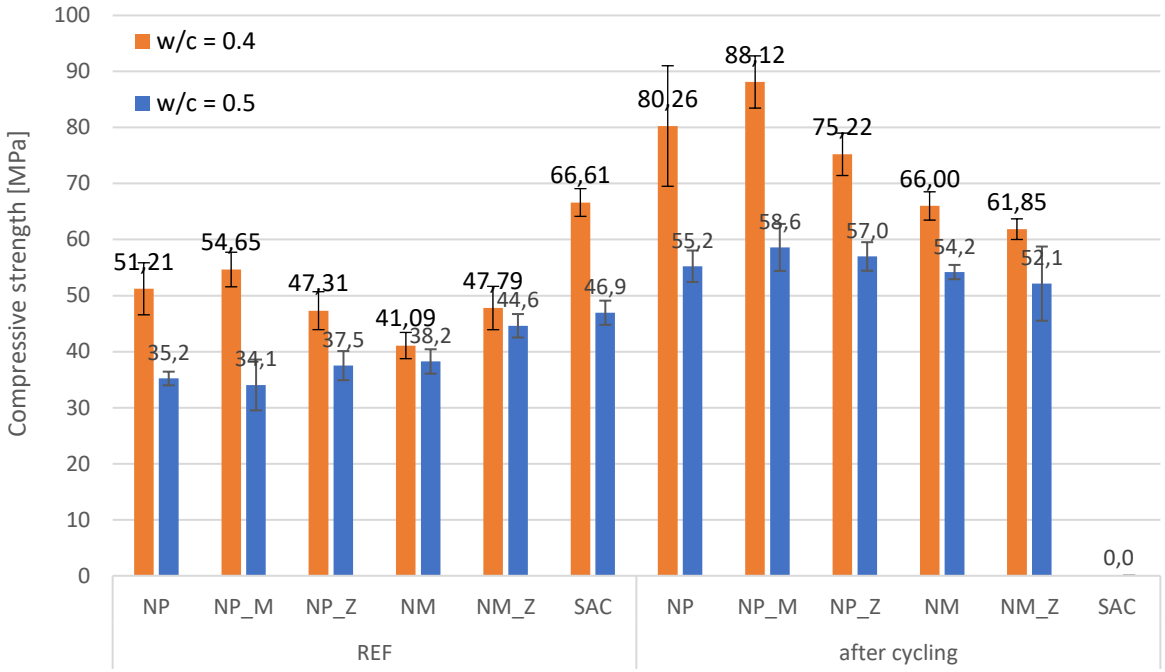

Figure 5-9: Compressive strength of samples manufactured after three cycles of drying and saturation, note: SAC disintegrated after cycling

5.2.4.Leaching

For evaluation of the capability of a matrix to encapsulate radioactive waste (RW) in regard to radionuclide release into the environment, the leachability index is used. According to ANSI/ANS-16.1-2003 ("ANSI/ANS-16.1-2003 American National Standard Measurement of the Leachability of Solidified Low-Level Radioactive Wastes by a Short-Term Test Procedure," 2003) the threshold level for a material to be classified as satisfactory for rad-waste immobilization is at least 6. As Table 5-4 shows, all studied cement composites have met the threshold value. However direct comparison with results published by other authors is difficult, as the vast majority of studies has been conducted with the actual radionuclide ^{137}Cs measuring its activity, while in this study the concentration of a stable nuclide was measured. In order to the ensure feasible mixing of the model evaporator concentrate and to reach detectable and reliable measurements by the atomic absorption spectrometer, the input concentration of the Cs^{+} in the model EC was much higher (c. by 6-7 orders of magnitude) than the real concentration of the radionuclide in evaporator concentrates are. With regard to the time-consuming procedure, the test was only performed on samples with water/binder ratio 0.5.

The highest leaching index was recorded for mixture NM_Z, followed by NM, which means that metakaolin acts as good sorption material. As well, natural zeolite has good retention capacity, however it is present only in 5 % of the binder weight (in mixtures NP_Z and NM_Z) due to its negative effects on the mechanical properties on cement composites when added in higher amounts, and therefore the effect on the retention capacity of the composite is not so pronounced as in case of metakaolin being present in 50 %, resp. 45 % of binder weight in mixtures NM and NM_Z. As the value of leachability index of NM_Z exceeds value of NM, it is obvious that natural zeolite acts better on retention than metakaolin. As the requirements on mechanical properties of the waste form are not high (it depends on the regulations of different countries, e.g. compressive strength usually in the order of single MPa (Coumes et al., 2009)), it is possible to further increase the amount of natural zeolite to achieve higher retention capacity while paying attention to other significant parameters, such as setting of fresh mixture. Sulpho-aluminate cement (SAC) reached higher leachability index than mixtures based on NP binder, however lower than NM mixtures. SAC mixture therefore does not

present superior retention capacity to counterbalance the severe disadvantage of cracking and disintegration during drying and saturation, see section *drying and saturation cycles*.

Table 5-4: Leachability index of samples manufactured with w/b=0.5. Minimal value L = 6

mixture	Leachability index L [-]
NP	8.2
NP_M	7.6
NP_Z	8.2
NM	9.1
NM_Z	9.3
SAC	8.6

The dominant leaching mechanism was identified by plotting the release as function of time, as described in (de Groot and van der Sloot, 1992). Possible distinguishable modes of leaching are surface wash-off, diffusion and dissolution. In the surface wash-off mode the material specimen is covered by layer of soluble substance, usually as a result of preparation process of the sample and this layer is dissolved in the initial phase of leaching, giving near zero slope of the release curve, as function of cumulative release of the substance in time, plotted in log-log scale. Diffusion controlled are most common leaching processes in cement-based materials, the release rate of the substance decreases with time, as surface layers of the specimen are depleted of the leached substance and the transport is retarded, e.g. by tortuosity of the pore system. The slope of the release curve in diffusion controlled leaching test is supposed to be around the value of 0.5, indicating the gradually decreasing release rate of the leached substance. During dissolution the release rate of the leached substance is nearly constant, as the dissolution of the surface of the specimen proceeds faster than diffusion of material through pore system of the matrix. The slope of the release curve in case of dissolution has theoretical value of +1.

Calculated slopes of measured release curves were for all types of used binders around +0.4, indicating the diffusion as dominant leaching mechanism. For SAC the slope of release curve was the highest observed, with value 0.43, this might be the result of microcrack formation in the SAC matrix, as observed in previous experiments, and thus slightly higher diffusion coefficient of this material.

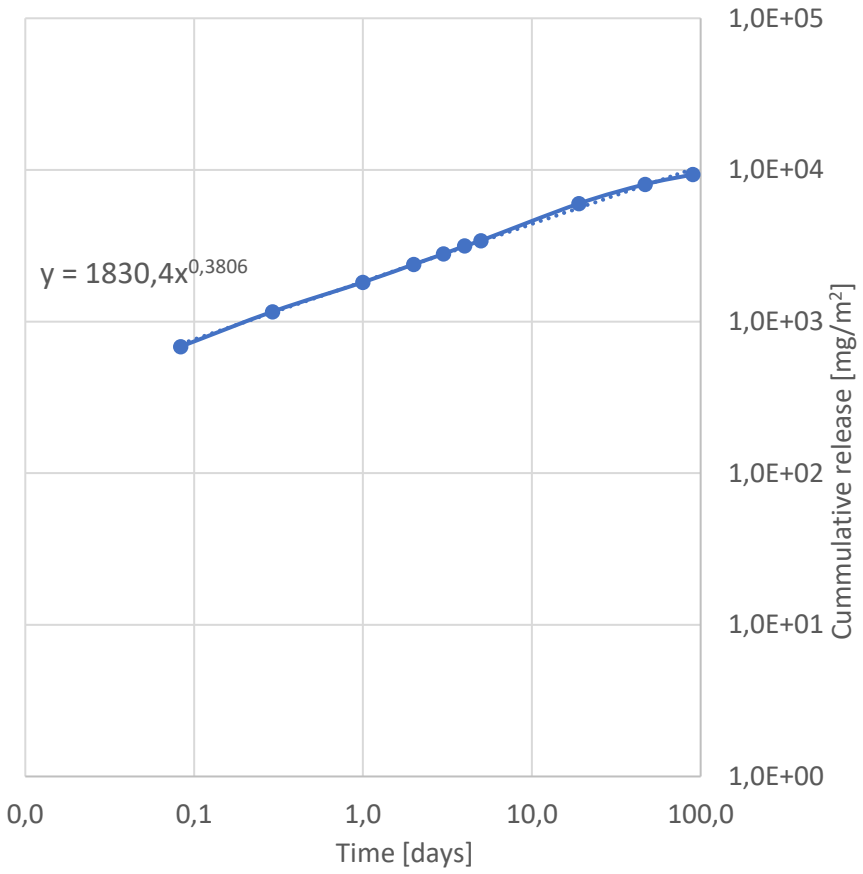

Figure 5-10: Example of a source plot used for identification of the leaching mechanism: Cumulative release vs time for sample NP_2

Table 5-5: Identification of the controlling leaching mechanism by plotting the cumulative release as a function of contact time; for slopes close to 0 the controlling mechanism is surface wash-off, for slopes close to 0.50 the controlling mechanism is diffusion and for slopes close to 1 the controlling mechanism is dissolution

mixture	slope [-]	Leaching mechanism
NP	0.389	diffusion
NP_M	0.383	diffusion
NP_Z	0.376	diffusion
NM	0.361	diffusion
NM_Z	0.399	diffusion
SAC	0.430	diffusion

5.3. Conclusion

Cement composites based on the mixture of non-gypsum cement with Ordinary Portland cement or metakaolin with admixtures of natural zeolite or metakolin were studied in terms of their suitability as an immobilization matrix for evaporator concentrates, liquid intermediate-level

radioactive waste. Investigated parameters were resistance to drying and saturation cycles, water absorption, mechanical properties and leaching of Cs^+. The obtained results can be summarized as:

- Drying and saturation cycles caused decrease in open porosities and sorptivities for all NP and NM based mixtures. SAC mixture showed severe cracking and disintegration.
- Changes in dynamic modulus of elasticity as indicators of internal defects showed decrease for all mixtures after cycling. The most pronounced drop was the one of SAC value, contrary NP and NP_M showed the lowest changes.
- Water absorption of samples in the reference state (not exposed to cycling) is the lowest for SAC mixture, however after cycling cracks in SAC samples caused rapid rise of water absorption coefficient, up to ten times the reference value. Results of the remaining samples were in agreement with open porosities and sorptivities as water absorption coefficient decreased after cycling. The probable explanation is the alternation of the porous system due to rehydration of unhydrated cement grains.
- Values of flexural strength and compressive strength in the reference state were in ranges of 3 – 4 MPa, resp. 40 – 55 MPa, which is more than satisfactory for an immobilization matrix.
- After cycling, there was a rise in both flexural and compressive strength again as a result of their microstructure densification due to rehydration of cements grains.
- Leaching index exceeded the threshold value of 6 for all investigated cement composites. The best Cs^+ retention was found for NM_Z mixture followed by NM mixture, showing that natural zeolite followed by metakaolin have good sorption abilities.

To conclude, SAC composite did not show any superior retention capacity of Cs^+ to other mixtures, as it was expected based on literature review, and due to its instability to drying and saturation cycles it is not appropriate for evaporator concentrates immobilization. NM and NP based composites exhibited promising potential, NM mixtures showing higher radionuclide retention capacity but being less resistant to environmental changes than NP mixtures.

Chapter 6: Thaumasite sulfate attack

This paper was published in Progress in Nuclear Energy (Journal Impact Factor 2.7), volume 176, article number 105356, DOI 10.1016/j.pnucene.2024.105356. As of may 2025, the paper has been cited 1 time in WoS collection.

Future outlook in the field of cement compsites for radioactive waste deposition are further investigated in this paper. There is still not thoroughly enough investigated field of degradation mode, specific to cement composites in subsurface repository. Sulfate attack is well known problem for cement composites, with ettrigite being the most famous of all sulfates, but in conditions often present in near-surface underground repository (temperature under 15°C, presence of water and carbonates), suitable for intermediate-level waste reposition, sulfate thaumasite can form in the structure of the material, resulting in material degradation.

Presented paper reviews published work in the field of thaumasite sulfate attack (TSA) research, identifying possible future points of interest for further investigation.

6. Thaumasite formation in cementitious composites used in underground repositories – conditions and impact on composite´s properties: A review

Abstract

Cement-based materials (CBM) are used for several applications in radioactive waste underground repositories as engineered barriers. Thaumasite sulfate attack (TSA) is a type of cement-based materials' corrosion, which has been investigated in regard to civil engineering structures, but very little research has been made on TSA in the environment of rad-waste repositories. The paper introduces types of rad-waste repositories and thaumasite characterization; summarizes mechanisms of TSA corrosion and its impact on CBM properties and durability; and defines the specifics of underground repositories in relation to TSA. High relative humidity is typical for underground disposal sites, cold temperatures (below 15°C) are characteristic for near-surface repositories, while in deep geological repositories the temperatures may reach 80-100°C which allows the decomposition and recrystallization of ettringite and eventually thaumasite. Sites located in clay rock, salt rock, limestone, dolomite etc., but also some waste forms itself may be rich in sulfates and carbonates. All these are conditions favoring TSA on CBM and thus research in this area should not be underestimated.

Keywords: *thaumasite sulfate attack, underground radioactive waste repositories, cementitious materials*

6.1. Introduction

Underground repositories are used for long-term storage of a variety of radioactive waste types. Low- and intermediate-level waste generated from medicine, nuclear power plants, industry or agriculture needs to be safety disposed and isolated from our environment. Some of these types of waste are solidified in cementitious materials and then stored in near-surface repositories. High-level waste, which presents much higher risk, is currently stored in temporary storage facilities, but it is planned, one day, to be stored in deep-geological repositories (DGR). Both types of repositories have to be comprised of a multi-barrier system of engineering barriers, each of them ensuring the inhibition of radionuclides' release into the environment. Cement materials can be used for both primary and secondary barrier of the system. Unfortunately, as all other materials known, cement-based materials are degraded by a variety of mechanisms in dependence on the external and/or internal conditions. One domain of these degradation mechanisms is the action of sulfates and other aggressive substances, collectively known as "sulfate-attack". Particularly, there can be suitable conditions for the formation of thaumasite in underground repositories. Recently, there has been research investigating alternative cementitious materials for nuclear waste encapsulation, such as calcium aluminate, calcium sulfoaluminate, phosphate, magnesium silicate, and alkali-activated cements (Rakhimova, 2022). The degradation mechanisms of these matrices differ from Portland cement materials due to their different chemistry, however some of them may undergo sulfate attack as well.

Thaumasite is less known than his usual accompaniment, ettringite. Although they may seem similar in their composition, crystal structure or behavior under elevated temperatures, they have their own specifics. While both ettringite and thaumasite are corrosion products of cement-based materials, ettringite is also intentionally formed in fresh cement paste to prolong its' setting and hardening process and avoid "flash setting", which is referred to as "primary ettringite". However, when ettringite is formed in an already hardened cement paste ("secondary ettringite"), it causes cracking of the cement composite or concrete due to its expansive behavior during crystallization. The action of thaumasite seems similar, but has its own specifics, which will be discussed further in this paper.

6.2. Types of underground repositories for radioactive waste disposal

Generally, there are two basic types of radioactive waste repositories: (i) near-surface repository and (ii) deep geological repository, but additional "categories" can be distinguished by the specifics of the repository. The convenient disposal option of a certain waste depends on the activity content and half-life of the radionuclide inventory in the waste. In dependence of these two parameters radioactive waste can be categorized, as classification scheme was established by International Atomic Energy Agency (IAEA) (International Atomic Energy Agency, 2009). There are short-lived radionuclides, whose half-life is shorter than the half-life of ^{137}Cs (30.17 years), and the rest are classified as long-lived radionuclides. According to the activity content, the waste can be categorized as: (i) exempt waste; (ii) very short-lived waste (VSLW); (iii) very low-level waste (VLLW); (iv) low level waste (LLW); (v) intermediate level waste (ILW) and (vi) high level waste (HLW). The suitable repository type for each waste category is illustrated in Figure 6-1. Exempt waste, VSLW or VLLW present very low or no risk of radionuclide release into biosphere and thus after proper treatment it can be disposed at landfills. LLW and short-lived ILW is supposed to be disposed in near-surface repositories, while HLW or spent fuel (SF) require disposal in a deep-geological repository.

Several other options have been investigated for rad-waste disposal, such as long-term above ground disposal, disposal in outer space, rock-melting (melting of wastes in the adjacent rock), disposal at subduction zones, sea disposal, sub-seabed disposal, disposal in ice sheets (for wastes generating heat) or deep well injection (for liquid wastes). These are however either not planned to be implemented due to various reasons, such as high cost, risks (outer space disposal) etc. or are not permitted by international agreements (sea disposal, sub-seabed disposal, disposal at subduction zones) (World Nuclear Association, 2023).

Radioactive waste requires a reliable and safe disposal system. Both near-surface and deep geological repositories use a multi-barrier system, where each of the barriers has its specific role in dependence on the type of the encapsulated waste. There are natural barriers comprised of the host rock and overlying formations and engineered (man-made) barriers, consisting of waste forms, waste canisters, buffer, backfill and seal.

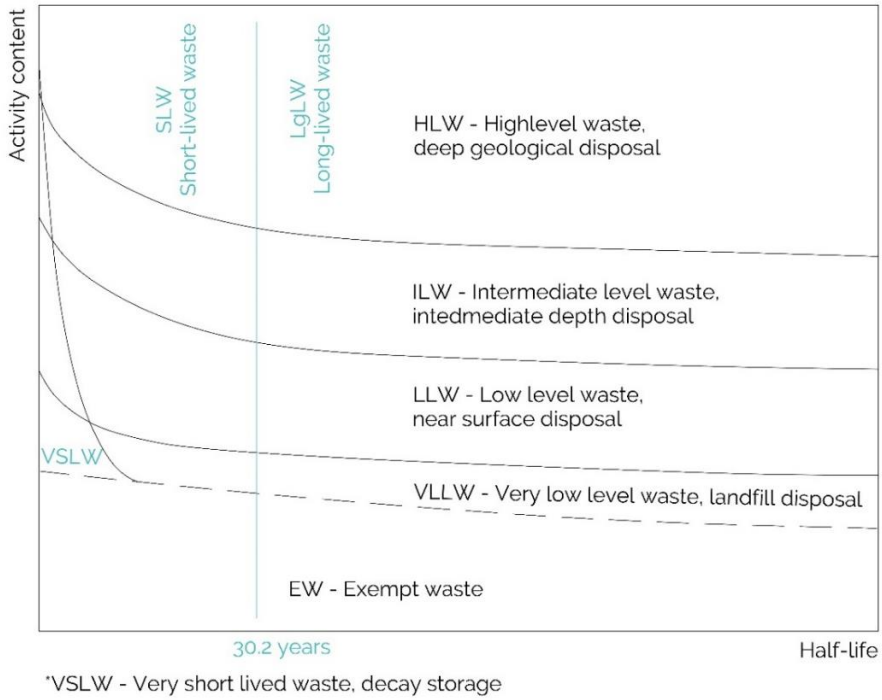

Figure 6-1: End points for each type of radioactive waste including options of storage, clearance, storage for decay and disposal – IAEA classification scheme ***(International Atomic Energy Agency, 2009)***

6.2.1.Near-surface repository

Low- and short-lived intermediate level waste can be disposed of in near-surface repositories. These are disposal sites built at the ground level or underground in depths up to 60 m, such as surface and (semi)buried vaults, near-surface silos, shallow drift or tunnels. Near-surface repositories are implemented in many countries, such as Czech Republic, Finland, France, Japan, Netherlands, Spain, Sweden, Finland, UK, and USA; and contain large amounts of institutional waste (waste generated from medicine, research facilities, agriculture, industry), some waste from nuclear power plants etc. Such facilities are suitable only for LLW or short-lived ILW due to the fact, that they can be affected by long-term climate changes, such as glaciation. Short-term safe protection of our biosphere from radionuclide release is ensured by engineered barriers, usually consisting of a primary matrix (e.g. cement paste), secondary casing (typically metal drums), concrete packages and eventually concrete grout (International Atomic Energy Agency, 2020).

In Czech Republic, the operational radioactive waste (of categories LLW or ILW) from Temelín and Dukovany power plants are stored at Dukovany disposal site. It consists of concrete reservoirs with volume of 55 000 m^3, where stainless steel drums filled with immobilized waste are stored. The waste stored at the site consists of contaminated protective equipment, rubble, packaging or waste produced in the process of water management, such as waste water, sludge, ion-exchangers etc. Institutional radioactive waste is being disposed at two disposal sites: *Richard* near Litoměřice and *Bratrství* near Jáchymov. The repository *Richard* was built in the location of former limestone mine and repository *Bratrství* is located in former mine for uranium ore. *Bratrství* serves only for disposal of wastes, which contain naturally occurring radionuclides (Czech Radioactive Waste Repository Authority (RAWRA), 2023).

6.2.2. Deep-geological repository

Deep-geological repository (DGR) is intended to store long-lived intermediate waste and high-level waste, spent fuel (SF) and sealed radioactive sources (SRS) in great depths from 500 to 2000 m under ground level. There are two concepts of deep-geological repositories: wet and dry. Dry geological repository concept presumes no ingress of underground water, while wet deep-geological repository is prepared to be saturated with water. Both repositories' types are supposed to be constructed in a stable geological formation, the considered rock types are evaporites (especially halite), mudrock (shale, mudstone etc.) or crystalline rocks.

Isolation of the waste from biosphere is ensured by a multi-barrier system, which differs in dependence on the location conditions, type of waste and other parameters, but essentially it comprises of natural barrier made by the host rock and engineered barriers which contain waste form (immobilized waste in a suitable matrix), casing and overpacks (e.g. metal), buffer, backfill (e.g. clay materials like bentonite), and seals/plugs. The idea of deep-geological repository is preferred in most countries: Argentina, Australia, Belgium, Canada, Czech Republic, Finland, France, Japan, the Netherlands, Republic of Korea, Russia, Spain, Sweden, Switzerland, the UK, and the USA. There is only one built deep geological repository in operation - Waste Isolation Pilot Plant (WIPP) in the USA, which is however not licensed for storage of HLW or spent fuel (SF). Advanced plans for HLW and SF disposal are in Finland, Sweden, France and USA.

Alternative to DGR is very deep geological repository (VDGR), which is supposed to be built in at least 3 km depths, which would extremely limit any transport of radionuclides trough geosphere and ideally the heat release from HLW would react with the surrounding granitic rock resulting in a sealing granite layer, encapsulating the waste permanently (Lee et al., 2013). This approach however needs extensive research, which can take many decades.

6.3. Cement-based materials used in radioactive-waste repositories

Cement-based materials are suitable for several of the barriers of the aforementioned multi-barrier system. There is vast experience with these materials from civil engineering industry providing

knowledge about their technology and durability; cement-based materials are easily manufactured, handled, transported, and are relatively cheap. Cement composites can be used as immobilization matrix for encapsulating ILW and LLW rad-waste (primary barrier), grout filling of the interspace between individual barriers, and concrete as secondary barriers, shaft and drift lining or plugs.

Direct immobilization of LLW and ILW radioactive waste into cement matrix or cement composite is used for institutional waste (generated from medicine, industry, research, agriculture) and nuclear waste, for both solid and liquid state. Solid waste includes spent radiation sources (SRS), ion exchange resins, protective clothing and tools, old measuring instruments, paper, filters, swarf, dross or chips etc. Waste generated from decommissioning of nuclear facilities such as bulk metallic waste, bulk concrete, rubble etc. are nuclear specific types of solid waste. Liquid wastes include waste water, , evaporator concentrates, sludges, lubricants, solvents, hydraulic fluids from reactor operation, scintillation liquids from radio-analytical laboratories etc. (Abdel Rahman and Ojovan, 2021; Pátzay et al., 2011; Varlakov and Zherebtsov, 2021). The design of cementitious waste form has to consider the chemistry of both radioactive and inactive compounds present in the waste, its physical characteristics and also site-specific conditions. Many types of matrices and composites have been investigated around the world for this purpose next to conventional Ordinary Portland cement (OPC). These include calcium aluminate cements (CAC), calcium sulfo-aluminate cements (CSAC), magnesium phosphate cements (MPC), alkali-activated cements (AAC), gypsum-free cement, and their blends with OPC(Rakhimova, 2022). Another approach is adding supplementary materials such as blast furnace slag, fly ash, clay minerals (bentonite, zeolite, diatomite, vermiculite, red clay), metakaolin or silica fume (Abdel Rahman and Ojovan, 2021; Koťátková et al., 2017b) to the matrix mixture.

Cement grouts and concrete are widely used as engineered barriers in both near-surface repository and deep geological repository. While grouts are used to fill up the space between other barriers, concrete is used as structural elements for either secondary packaging of waste forms or for lining of tunnels, shafts, drifts or plugs. The main function of secondary concrete barriers is therefore load-bearing and it has to provide its long-term stability, but also limit any negative interactions with the surrounding barriers. Concrete in deep geological repositories is in direct contact with buffer and/or backfill, which is likely to be made of bentonite. However, the high alkalinity of concrete pore water (pH 12.5-13) leaching through barriers can have adverse effects on bentonite's sealing function in terms of the potential reduction of its swelling ability. The mix design therefore needs to be oriented towards low-alkalinity concrete with pH ≤ 11 (Dhir et al., 2005; García Calvo et al., 2010; Ramírez et al., 2002).

6.4. Thaumasite characterization and its similarity to ettringite

Thaumasite belongs to the so-called ettringite group of minerals occurring in nature, along with other sulfates such as ettriginte or bentorite (Gougar et al., 1996). Ettringite and thaumasite can be also classified as AFt (Alumina, Ferric oxide, tri-sulfate) phases (Skalny et al., 2002), which is a group of calcium sulfo-aluminate hydrates used in concrete chemistry to distinguish from AFm (Alumina, Ferric oxide, mono-sulfate) phases. Both ettringite and thaumasite are as well corrosion products of cement-based materials, however controlled formation of ettringite in fresh cement paste is actually beneficial as it is intentionally formed (by adding calcium sulfate to cement) to control the setting time of the fresh mix and avoid flash setting.

Thaumasite is a calcium silicate carbonate sulfate hydrate ($[Ca_3Si(OH)_6{\cdot}12H_2O]{\cdot}(SO_4)(CO_3)$, abbr. $C_3S\bar{S}\bar{C}H_{15}$) and it is structurally very similar to ettringite ($[Ca_3Al(OH)_6\ {\cdot}12H_2O]_2{\cdot}(SO_4)_3{\cdot}2H_2O$, abbr. $C_6A\bar{S}_3H_{32}$). Both minerals have two distinct structural components: column and channel. The columnar component of ettringite consists of $[Ca_6Al_2(OH)_{12}{\cdot}24H_2O]^{6+}$ group with Al and Ca coordinated polyhedrons, which run parallel to the c-axis and channel is composed of $[(SO_4)_3{\cdot}2H_2O]^{6-}$ group - sulfate tetrahedral and water molecules. In thaumasite, Al^{3+} is substituted with Si^{4+} in its columns, i.e. $[Ca_3Si(OH)_6 \cdot 12H_2O]^{4+}$ group; and triangular channel consists of $2SO_4^{2-} \cdot 2CO_3^{2-}$ instead of $3SO_4^{2-} \cdot 2H_2O$ (Barnett et al., 2002; San et al., 2018). Both thaumasite and ettringite crystalize in acicular or prismatic

crystals, but thaumasite has hexagonal cell (space group $P6_3$, Z = 2) with lattice parameter a = b = 11.06 Å, c = 10.52 Å, α = β = 90°, and γ = 120°, while ettringite has trigonal cell (space group $P31c$, Z = 2) with lattice parameter a = b = 1.12 Å, c = 23.06 Å, α = β = 90.0°, and γ = 120° (San et al., 2018). Exemplary SEM images showing the similarity of thaumasite and ettringite needle-like crystals is given in Figure 6-2, taken from (Terzijski et al., 2021).

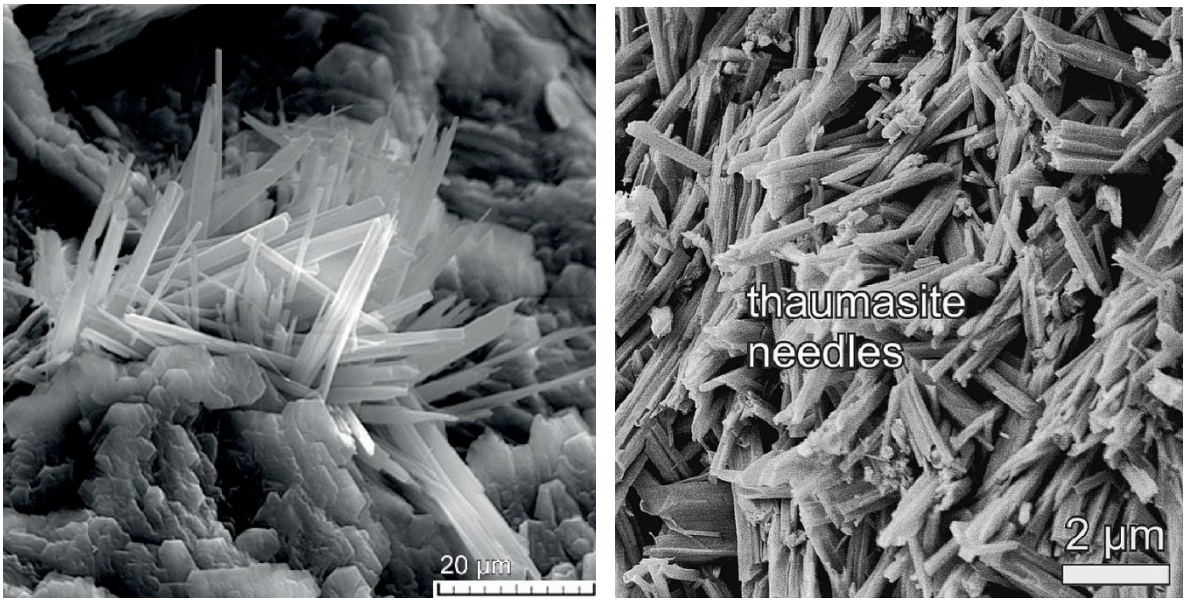

Figure 6-2: (a) Crystals of ettringite ***(Pospíšil et al., 2008)****; (b) crystals of thaumasite* ***(Galan et al., 2023)***

6.5. Sulfate attack types

Thaumasite formation is one of several degradation mechanisms of concrete induced by sulfuric compounds which are known as "sulfate attack". There are three types of sulfate attack on cement-based materials according to the products formed:

(i) Gypsum corrosion
(ii) Sulfo-aluminate corrosion → formation of ettringite
(iii) Sulfo-carbonate corrosion ("thaumasite sulfate attack" = TSA) → formation of thaumasite

The most common corrosion type is the formation of secondary ettringite. Sulfate ions penetrate into the porous system of concrete and react with calcium ions, while forming gypsum. Gypsum is likely to further react with calcium aluminate (C_4AH_{13}), monosulfate ($C_4A\bar{S}H_{12-18}$) or unhydrated tricalcium aluminate (C_3A) while producing secondary ettringite. Gypsum corrosion usually occurs after the depletion of suitable conditions for ettringite formation, usually at concentration of SO_4^{2-} higher than 5000 mg/l. The crystallization of ettringite and gypsum is highly expansive process inducing internal cracks within the material (Skalny et al., 2002; Tian and Cohen, 2000). If sodium or potassium compounds are the source of sulfates, then they react with C-S-H to form ettringite, which next to expansion induced cracking is also responsible for the decalcification of C-S-H (Dyer, 2014). The source of sulfate ions can be either external (e.g. from groundwater) or internal originating from the decomposition of primary ettringite during heating of concrete to 85-90°C.

6.6. Thaumasite sulfate attack (TSA)

The third type of sulfate attack forming thaumasite is moreover subjected to the presence of carbonates. Calcium carbonates are present in the cement paste due to its carbonation or in the form of aggregate (e.g. limestone, dolomite etc.). However, these sources are less soluble and therefore are usually not the cause of thaumasite formation. The probability of the carbonate filler reaction

increases with the fineness of the filler. The biggest external source of carbonates is the groundwater (Collett et al., 2004).

Next to the source of sulfate and carbonate ions, the conditions of thaumasite formation are: presence of calcium and silicate ions (from hydration products of cement paste), suitable temperature (below 15°C) and pH (above 10.5) and abundance of moisture or water.

There are two possible scenarios of thaumasite formation: (i) forming directly from C-S-H, which is called the "direct route" or (ii) indirectly from ettringite, called the "Woodfordite route" (Bensted, 2003; Rahman and Bassuoni, 2014; Schmidt et al., 2007).

(i) Direct route

The direct route of thaumasite formation is the reaction between C-S-H, gypsum, calcite and excess water. This reaction is very slow and may last several months before thaumasite is detectable.

$$Ca_3Si_2O_7{\cdot}3H_2O + 2CaSO_4{\cdot}2H_2O + 2CaCO_3 + 24H_2O \rightarrow Ca_6[Si(OH)_6]_2{\cdot}(CO_3)_2(SO_4)_2{\cdot}24H_2O + Ca(OH)_2 \quad (1)$$

or

$$Ca_3Si_2O_7{\cdot}3H_2O + 2CaSO_4{\cdot}2H_2O + CaCO_3 + CO_2 + 23H_2O \rightarrow Ca_6[Si(OH)_6]_2{\cdot}(CO_3)_2(SO_4)_2{\cdot}24H_2 \quad (2)$$

The calcium hydroxide formed in (1) would probably react with atmospheric CO_2 or CO_2 dissolved in water:

$$Ca(OH)_2 + CO_2 \rightarrow CaCO_3 + H_2O \quad (3)$$

(ii) Woodfordite (indirect) route

The woodfordite route was named after the partial solid solution, from which ettringite and thaumasite can arise (Bensted, 2006). At the beginning, this process is also very slow, but once thaumasite arises, the reaction rate increases notably. Next to ettringite and water, the reactants commonly are C-S-H and calcite:

$$Ca_6[Al_xFe_{(1-x)}(OH)_6]_2{\cdot}(SO_4)_3{\cdot}26H_2O + Ca_3Si_2O_7{\cdot}3H_2O + 2CaCO_3 + 4H_2O \rightarrow Ca_6[Si(OH)_6]_2{\cdot}(CO_3)_2(SO_4)_2{\cdot}24H_2O + CaSO_4{\cdot}2H_2O + (2x)Al(OH)_3 + 2(1-x)Fe(OH)_3 + 4Ca(OH)_2 \quad (4)$$

or

$$Ca_6[Al_xFe_{(1-x)}(OH)_6]_2{\cdot}(SO_4)_3{\cdot}26H_2O + Ca_3Si_2O_7{\cdot}3H_2O + CaCO_3 + CO_2 + 3H_2O \rightarrow Ca_6[Si(OH)_6]_2{\cdot}(CO_3)_2(SO_4)_2{\cdot}24H_2O + CaSO_4{\cdot}2H_2O + (2x)Al(OH)_3 + 2(1-x)Fe(OH)_3 + 3Ca(OH)_2 \quad (5)$$

Also, in this case, the formed portlandite would probably react with carbonate according to (3) to form calcite and water. The formed calcite may serve as reactant for further formation of thaumasite (Bensted, 2006, 2003). The process is not continuous – firstly (before thaumasite formation) an intermediate solid solution – "woodfordite" is formed.

Overview of suitable conditions for thaumasite formation:

- Source of calcium and silicate ions, supplied by the hydration products of cement paste (C-S-H, $Ca(OH)_2$) or unhydrated clinker minerals
- Source of sulfates: external (groundwater, soil, bacteria, oxidized sulfur compounds - gaseous SO_2, sulfides etc.) or internal (dissolved primary ettringite) (Blanco-Varela et al., 2003)
- Source of carbonates: external (aggressive atmospheric CO_2 or carbonates in groundwater etc.) or internal (carbonate aggregate or fine filler, calcium carbonate formed in the paste)
- Cold environment – temperatures below 15°C, ideally 0-5°C; at these temperatures, thaumasite is less soluble, while CO_2 and portlandite are more soluble (Sims and Huntley, 2004); moreover the thaumasite's coordinated $Si(OH)_6$ groups are more stable (Crammond,

2003), however thaumasite formation at higher temperatures is possible (Rahman and Bassuoni, 2014)
- Source of moisture or water
- pH of sulfate bearing solutions above 10.5 (Gaze and Crammond, 2000)

Figure 6-3 shows an example of thaumasite appearance in concrete, taken from (Leemann and Loser, 2011). The concrete lining of a ventilation shaft was exposed to sulfate-bearing groundwater for 45 years.

The rate of thaumasite corrosion is dependent on several factors. These are sulfate and carbonate concentration; the regime of underground water flow and its contact with concrete; temperature; presence of other compounds (chlorides, salts such as $MgSO_4$); the composition and amount of cement in the mix; permeability of concrete/cement composite. Standing water causes the formation of corrosion products only on the surface of the material until the source of sulfates and carbonates in the nearby environment is depleted and the reaction significantly slows down. Contrary, running water ensures constant supply of these compounds towards the concrete surface, which allows their diffusion deeper into the concrete mass. Also cycles of wetting and drying increase the sulfates concentration in the pore water (Mittermayr et al., 2013).

The presence of chloride ions may have a positive influence in terms of lowering the risk of thaumasite formation. Chloride ions have higher diffusion rate compared to sulfates and thus they readily react with aluminate phases to form Friedel's salt ($3CaO{\cdot}Al_2O_3{\cdot}CaCl_2{\cdot}10H_2O$) instead of ettringite (Benton, 1970; Ben-Yair, 1974). Moreover, both ettringite and thaumasite are more soluble in chloride-rich solution than in deionized water, therefore the likelihood sulfate attack is reduced (Sotiriadis et al., 2012). Chloride ions also react with portlandite ($Ca(OH)_2$) dissolved in the porous water to form $CaCl_2$ limiting gypsum, ettringite and eventually thaumasite crystallization (Guerrero et al., 2009). The decrease of $Ca(OH)_2$ concentration in the porous water causes reduction of pH which is unfavorable for thaumasite formation (Rahman and Bassuoni, 2014; Sotiriadis et al., 2012).

Contrary, the presence of magnesium sulfate causing "magnesium sulfate attack" reinforces formation of thaumasite either by direct route according to the following reaction (6) or by the woodfordite route (Bensted, 2003).

$$Ca_3Si_2O_7{\cdot}3H_2O + Ca(OH)_2 + 2CaCO_3 + 2MgSO_4 + 28H_2O \rightarrow Ca_6[Si(OH)_6]_2{\cdot}(CO_3)_2(SO_4)_2{\cdot}24H_2O + 2Mg(OH)_2 \quad (6)$$

In regard to cement composition, the main compound supporting corrosion due to gypsum and ettringite formation (and eventually thaumasite through woodfordite route) is the clinker mineral tri-calcium-aluminate (C_3A). There are low C_3A cements on the market which may help to decrease these types of corrosion, but it however does not inhibit thaumasite formation fully as in the case of the direct route it reacts with silicate phases instead of aluminates (Nobst and Stark, 2003). Permeability of concrete or cement-based materials can be lowered generally by low water/cement ratio, use of fine filler or supplementary cementitious materials (SCM) and proper compaction of the fresh mix. The pozzolanic admixtures added as partial cement replacement also lower the content of C_3A and portlandite reducing the risk of thaumasite formation through woodfordite route (Bellmann and Stark, 2008; Rahman and Bassuoni, 2014; Ramezanianpour and Hooton, 2013).

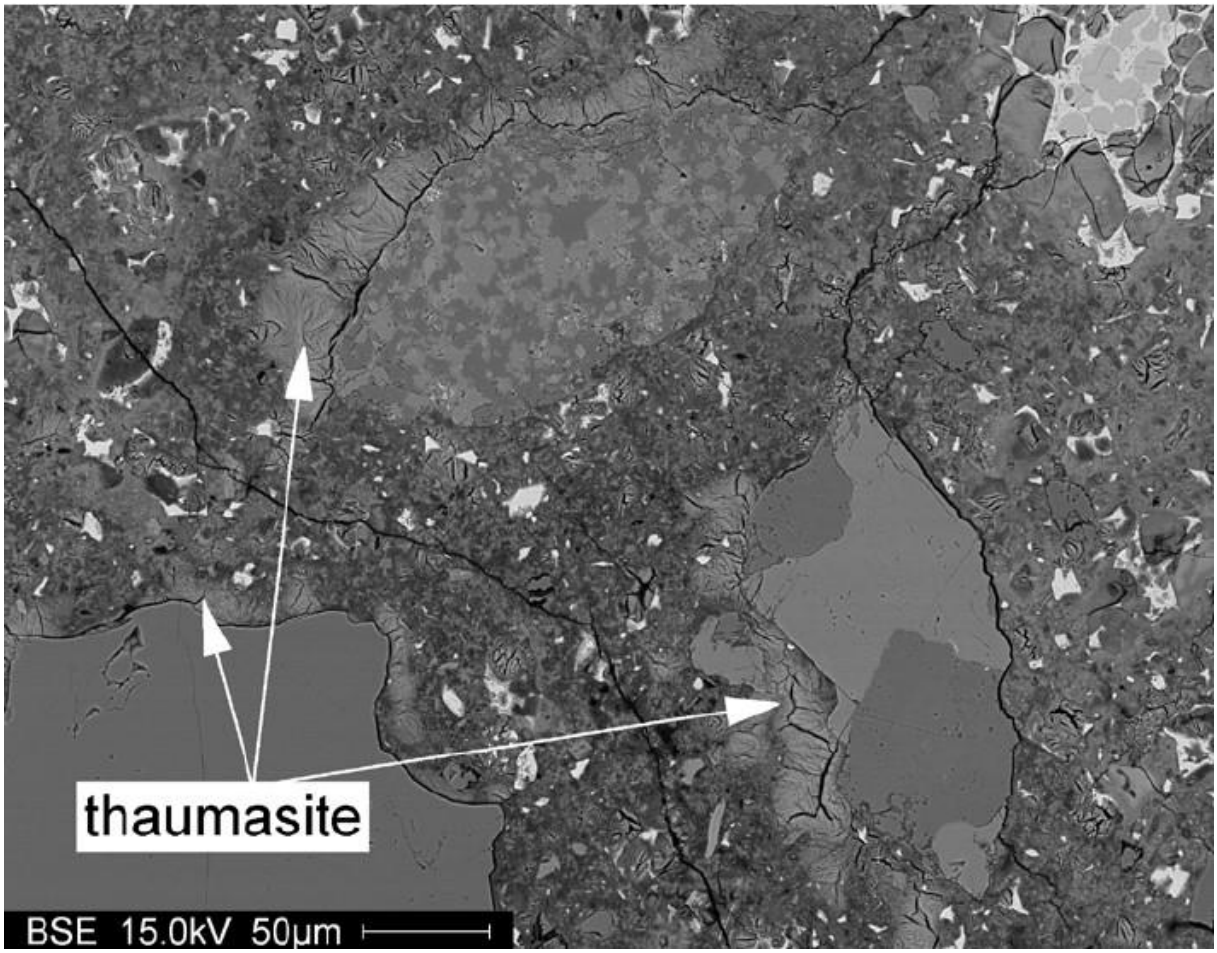

Figure 6-3:Thaumasite appearance around the aggregate grains found in concrete lining exposed to sulfate-bearing groundwater ***(Leemann and Loser, 2011)***

6.7. Degradation mechanisms of cement-based materials due to TSA

Many research studies have been made to investigate the degradation mechanisms of TSA (Abubaker et al., 2014a; Barnett et al., 2002; Collett et al., 2004; Romer et al., 2003; Schmidt et al., 2007; Sims and Huntley, 2004). In UK, there was "Thaumasite Expert Group" established by the government to study the mechanisms and deterioration effects of TSA on concrete (Crammond, 2003). The degradation mechanisms are different from other types of sulfate attack, as thaumasite forms by the conversion of C-S-H, which is the main binding phase of cement hydration products. Thaumasite begins to form at the surface layers of concrete and gradually progresses towards the core of the concrete mass. The result of TSA on concrete is a white mushy paste with no bond and strength, the aggregate grains can be separated easily. There are four steps of concrete degradation due to TSA according to Thaumasite Expert Group (Clark et al., 1999):

Table 6-1: Steps of concrete degradation induced by TSA ***(Clark et al., 1999)***

Step 1	occasional voids, pores lined with thaumasite
Step 2	thin cracks filled in with thaumasite
Step 3	wide cracks filled with thaumasite, thaumasite around aggregates
Step 4	complete transformation of cement paste matrix into thaumasite

It is not clear, whether TSA causes cracking due to expansion. It has been reported by several researchers, that expansion was observed (Clark and Thaumasite Expert Group., 2002; Ma et al., 2006; Slater et al., 2003), however the cracking can be induced by other degradation mechanisms and/or they could be present from earlier stages of sulfate attack (e.g. as a result of ettringite formation).

Thaumasite formation in concrete or cement composites does not necessarily have to cause damage to the host material. Thaumasite Expert Group distinguished two forms of observed thaumasite action on concrete: (i) Thaumasite formation (TF) and (ii) thaumasite sulfate attack (TSA). TF refers to cases where thaumasite was found in voids, pores or preexisting cracks of concrete structures, but it did not have significant deteriorating effects on the host cement paste; contrary TSA is used when thaumasite formation results in notable damage of the concrete through C-S-H disintegration (Clark et al., 1999).

6.8. Specifics of underground repositories in regard to potential risk due to thaumasite formation

The conditions of underground repositories differ significantly from site to site and naturally there is also huge difference between the conditions in near-surface repositories and deep-geological repositories.

Temperatures at sites situated at ground level vary with seasonal and weather changes, however from depths at about 15 m there is no effects of climate variations, the temperature is stable throughout the year but it is dependent on geothermal gradient. Therefore, sub-surface repositories located in depths of few dozens of meters are exposed to stable temperatures at around 10 – 15°C, e.g., in both Czech sub-surface repositories *Richard* (situated in depth of 70 m) and *Bratrství* there is constant temperature of 10°C. Deep-geological repositories are supposed to be built in higher depths from 500 m to 2 km, where the temperatures can reach up to 80°C. As written above, temperatures around 10 – 15 °C can favor the formation of thaumasite; at temperatures around 80°C thaumasite and ettringite decompose and can recrystallize within the material.

Due to the lack of air circulation underground, the air is naturally saturated with moisture, i.e. almost 100% RH. Therefore, except from times, when there is operating technical ventilation in order to ensure fresh air for the working staff, the high relative humidity in the repositories is also likely to promote thaumasite formation (Rahman and Bassuoni, 2014).

The chemical composition of the adjacent rock in the repository and consequently the composition of groundwater is critical factor in terms of the risk of thaumasite formation. The presence of carbonates and sulfates in the host environment or groundwater cannot be excluded at any site.. Although the intrusion of ground-water into the disposal site is considered an accident, the cement and concrete parts of the multibarrier system should also provide an endurance to the consequent degradation mechanisms in case of failure of the seal.

Near-surface repositories may be located at various sites and may be affected by the host rock and in some low-depth cases by the adjacent soil. Table 6-2 presents the overview of the most common sulfate- and sulfide-rich minerals in soil and their solubility (Trudinger, 1971). As shown in the table, sulfides such as pyrite, marcasite or pyrrhotite are insoluble minerals, hovewer sulfides may be converted into sulfates either by oxidization e.g. due to soil disruption during construction or by the action of sulfur-oxidising bacteria. Also sulfur present for example in peaty soils may oxidise into sulfates. The effects sulfates present in pyritic clay/mudrock on thaumasite formation were studied by Abubaker et. al. (Abubaker et al., 2014b, 2014a; Wilson et al., 2021). Sulfate occurrence and action may be moreover affected by microbial action (Nuclear Energy Agency (NEA), 2018, 2014). High supply of carbonates could be found at sites, where the adjacent rock is limestone, as in the Czech repository Richard or in DGR for LLW and ILW at Bruce in Canada, or any other carbonate-rich rock (Bergström et al., 2011).

The presence of carbonates and sulfates is likely also in geological formations of deep underground repositories. Evaporite rocks are usually composed of limestone or dolomites on the base, the majority of the rock is made of gypsum or halite and a thin complex of Mg-K sulphates and K-chloride at the top (Warren, 2006). Embedded lenses of sulfates spread throughout the rock are typical for evaporite formations in Eastern Alps (Upper Permian to Lower Triassic Haselgebirge Formation) (Leitner and Neubauer, 2011; Neubauer and Schorn, 2011). Gypsum-based rocks are unstable under elevated

temperatures of DGR (at 85°C) and therefore they are not suitable for any kind of radioactive waste storage. Anhydrite, however, is thermally stable and potentially, if naturally protected from water inflow, appropriate for LLW or ILW disposal. Halite formations are thermally stable, low-porosity and show a desirable creep behavior, however they are highly soluble, heat-conductive and gypsum or anhydrite lenses are often embedded in halite formations (Šoštarić and Neubauer, 2013). Significant amounts of sulphates and carbonates may be present also in mudrock (Abubaker et al., 2014a, 2014b; Xiang et al., 2020).

Table 6-2: Sulfate and sulfide minerals and their solubility

Mineral	Chemical Formula	Solubility at 25°C (mg/L)
Barite	$BaSO_4$	2
Anhydrite	$CaSO_4$	3 178
Gypsum	$CaSO_4 . 2H_2O$	2 692
Epsomite	$MgSO_4 . 7H_2O$	713 100
Jarosite	$KFe_3(OH)_6(SO_4)_2$	5
Mirabilite	$NaSO_4 . 10 H_2O$	435 900
Glauberite	$Na_2Ca(SO_4)_2$	118 500
Pyrite	FeS_2	0
Marcasite	FeS_2	0
Pyrrhotite	FeS	0

The source of sulfates and carbonates may be also the cementitious waste form itself. For example, evaporator concentrates, which is densified liquid waste from coolant of PWR, can contain both sulfates and carbonates (I. Plecas et al., 2009, 2006; Szalo and Žatkulák, 2000b). The regeneration of ion-exchange resins through the reaction of sulfuric acid and sodium hydroxide generates radioactive waste containing high amounts of sodium sulfate. Due to its organic nature, ion exchange resins may be damaged by radiolysis arising from the irradiation by the present radioisotopes ^{60}Co, ^{134}Cs, ^{137}Cs (Bayoumi and Tawfik, 2017) resulting in the release of sulfates directly into the cement matrix (Frizon and Cau-dit-Coumes, 2006).

Waste water from washing of protective clothes or other equipment from institutional facilities is also sulfate-rich. Another liquid sulfate-rich radioactive waste is produced during treatment of ^{90}Sr contaminated streams by coprecipitation of strontium with barium sulfate (Lenoir et al., 2009). Example of carbonate-rich radioactive waste, which is immobilized by cementation, is the lime waste produced by the neutralization of liquid wastes obtained from the ammonium uranyl carbonate (AUC) ($(NH_4)_4UO_2(CO_3)_3$) wet process, which is uranium reconversion process (Shon et al., 2022).

Gamma radiation is not supposed to have any direct impact on sulfate attack, however at higher doses it may lead to localized heating of the cement matrix induced by the absorption of radiation energy and radiolysis of the pore the material. Accompanying heat and radiolysis may interact with the radioactive waste changing the chemistry of the cement environment – i.e. the release of sulfates due to radiolysis damage of ion exchange resins as stated above (Frizon and Cau-dit-Coumes, 2006).

Apart from the well-known effects of ordinary sulfate attack on cementitious materials, there is very little research addressing the sulfate attack arising specifically due to interactions between cement and radioactive waste. Frizon and Cau-dit-Coumes (Frizon and Cau-dit-Coumes, 2006) studied the impact of sulfates released from ion exchange resins into the cement matrix. They reported accelerated hydration of cement when mixed with sulfate solution with concentration 5.56×10^{-1}

mol/L. The action of sulfates led to the formation of delayed ettringite which expansion was not extensive during the experiment period. No research has been found addressing specifically thaumasite formation generating from sulfate nuclear waste.

6.9. Conclusions

Each underground repository for any type of radioactive waste has to ensure safe storage of the waste and hinder the release of radionuclides into the environment. To achieve that, the durability of the engineered barriers is crucial. Cement-based materials are used in several applications in underground repositories, as primary matrix for encapsulation of low- and intermediate-level waste and as [underground repositories may be in many cases very convenient for thaumasite formation, which poses the risk of thaumasite sulfate attack (TSA).

The paper summarized the up-to-date knowledge of the thaumasite sulfate attack on concrete in civil engineering industry and drew implications of TSA risk on cement-based materials used in radioactive waste disposal. The host rock of underground repositories and the surrounding groundwater may be rich in both carbonates and sulfates, especially in cases of clay, salt, limestone, dolomite etc. Also, the waste form itself often contains an abundance of sulfates and/or carbonates, such as evaporator concentrates, ion exchange resins, waste water from institutional washing machines etc. Temperatures below 15°C are often found in near-surface repositories at depths of several dozens of meters and the relative humidity is naturally very high in the underground environment. Therefore, the risk of TSA on cement-based materials used in underground repositories is high, however, there is very little investigation addressing the topic. Extensive research should be done clarifying and quantifying the impact of the TSA on cement-based materials in regard to the specific conditions of underground repositories: TSA mechanisms due to waste-cement interactions, TSA risk and mechanisms due to cement-host rock and surrounding groundwater interactions, possibility of TSA risk in low-pH concrete, risks of thaumasite and ettringite decomposition and recrystallization in areas with temperatures of 80 - 100°C and others.

7. Literature

Abdel Rahman, R.O., Ojovan, M.I., 2021. Toward Sustainable Cementitious Radioactive Waste Forms: Immobilization of Problematic Operational Wastes. Sustainability 2021, Vol. 13, Page 11992 13, 11992. https://doi.org/10.3390/SU132111992

Abubaker, F., Lynsdale, C., Cripps, J., 2014a. Laboratory study of the long-term durability of buried concrete exposed to Lower Lias Clay. Constr Build Mater 64, 130–140. https://doi.org/10.1016/J.CONBUILDMAT.2014.04.045

Abubaker, F., Lynsdale, C., Cripps, J., 2014b. Investigation of concrete-clay interaction with regards to the thaumasite form of sulfate attack. Constr Build Mater 67, 88–94. https://doi.org/10.1016/J.CONBUILDMAT.2013.10.033

Acher, L., Haas, J., Dannoux-Papin, A., Frizon, F., Dunstetter, F., Noirfontaine, M.-A. De, 2016. Influence of gamma radiation on cement hydrates, in: Mechanisms and Modelling of Waste/Cement Interactions. p. 50.

Adinarayana, K.N. V, Sasidhar, P., Balasubramaniyan, V., 2013. Modelling of calcium leaching and its influence on radionuclide migration across the concrete engineered barrier in a NSDF. J Environ Radioact 124, 93–100. https://doi.org/10.1016/j.jenvrad.2013.04.009

ANSI/ANS-16.1-2003 American National Standard Measurement of the Leachability of Solidified Low-Level Radioactive Wastes by a Short-Term Test Procedure, 2003.

Atkins, M., Glasser, F.P., 1992. Application of portland cement-based materials to radioactive waste immobilization. Waste Management 12, 105–131. https://doi.org/10.1016/0956-053X(92)90044-J

Bar-Nes, G., Katz, A., Peled, Y., Zeiri, Y., 2008. The mechanism of cesium immobilization in densified silica-fume blended cement pastes. Cem Concr Res 38, 667–674. https://doi.org/10.1016/j.cemconres.2007.09.017

Barnett, S.J., Halliwell, M.A., Crammond, N.J., Adam, C.D., Jackson, A.R.W., 2002. Study of thaumasite and ettringite phases formed in sulfate/blast furnace slag slurries using XRD full pattern fitting. Cem Concr Compos 24, 339–346. https://doi.org/10.1016/S0958-9465(01)00085-3

Bellmann, F., Stark, J., 2008. The role of calcium hydroxide in the formation of thaumasite. Cem Concr Res 38, 1154–1161. https://doi.org/10.1016/J.CEMCONRES.2008.04.005

Benard, P., Garrault, S., Nonat, A., dit Coumes, C.C., 2005. Hydration process and Rheological Properties of Cement Pastes Modified by Ortho-Phosphate Addition. J Eur Ceram Soc 25, 1877–1883.

Bensted, J., 2006. Thaumasyt-Część 1: Droga do powszechnie przyjętego zrozumienia * Thaumasite-Part 1: The route to current understanding*. Cement Wapno Beton 4, 165–178.

Bensted, J., 2003. Thaumasite—direct, woodfordite and other possible formation routes. Cem Concr Compos 25, 873–877. https://doi.org/10.1016/S0958-9465(03)00115-X

Bensted, J., Callaghan, I.C., Lepre, A., 1991. Comparative study of the efficiency of various borate compounds as set retarders of class G oilwell cement. Cem Concr Res 21, 663–668.

Benton, G.L.K.E.K., 1970. Mechanism of Seawater Attack on Concrete. Journal Proceedings 67, 187–192. https://doi.org/10.14359/7261

Ben-Yair, M., 1974. The effect of chlorides on concrete in hot and arid regions. Cem Concr Res 4, 405–416. https://doi.org/10.1016/0008-8846(74)90106-9

Bergström, U., Pers, K., Almén, Y., 2011. Svensk Kärnbränslehantering AB R-11-16 International perspective on repositories for low level waste. Stockholm.

Bernachy-Barbe, F., 2019. A data analysis procedure for phase identification in nanoindentation results of cementitious materials. Mater Struct. https://doi.org/10.1617/s11527-019-1397-y(0123456789().,-volV()0123456789().,-volV)

Blanco-Varela, M.T., Aguilera, J., Martínez-Ramírez, S., Puertas, F., Palomo, A., Sabbioni, C., Zappia, G., Riontino, C., Van Balen, K., Toumbakari, E.E., 2003. Thaumasite formation due to atmospheric SO2–hydraulic mortar interaction. Cem Concr Compos 25, 983–990. https://doi.org/10.1016/S0958-9465(03)00122-7

Bobrowski, K., Skotnicki, K., Szreder, T., 2016. Application of Radiation Chemistry to Some Selected Technological Issues Related to the Development of Nuclear Energy. Top Curr Chem 374, 147–194. https://doi.org/10.1007/s41061-016-0058-7

Bothe, J. V, Brown, P.W., 1998. Phase formation in the system CaO–Al2O3–B2O3–H2O at 23±1°C. J Hazard Mater 63, 199–210. https://doi.org/https://doi.org/10.1016/S0304-3894(98)00221-0

Bouniol, P., 2010. The influence of iron on water radiolysis in cement-based materials s. Journal of Nuclear Materials 403, 167–183. https://doi.org/10.1016/j.jnucmat.2010.06.020

Bouniol, P., Bjergbakke, E., 2008. A comprehensive model to describe radiolytic processes in cement medium 372, 1–15. https://doi.org/10.1016/j.jnucmat.2006.10.004

Bouniol, P., Guillot, W., Dauvois, V., Dridi, W., Caër, S. Le, 2018. Original behavior of pore water radiolysis in cement-based materials containing sulfide: Coupling between experiments and simulations. Radiation Physics and Chemistry 150, 172–181. https://doi.org/10.1016/j.radphyschem.2018.04.021

Bouniol, P., Lapuerta-Cochet, S., 2012. The solubility constant of calcium peroxide octahydrate in relation to temperature ; its influence on radiolysis in cement-based materials. Journal of Nuclear Materials 420, 16–22. https://doi.org/10.1016/j.jnucmat.2011.09.009

Bouniol, P., Muzeau, B., Dauvois, V., 2013. Experimental evidence of the influence of iron on pore water radiolysis in cement-based materials. Journal of Nuclear Materials 437, 208–215.

Brough, A.R., Katz, A., Sun, G.K., Struble, L.J., Kirkpatrick, R.J., Young, J.F., 2001. Adiabatically cured, alkali-activated cement-based wasteforms containing high levels of fly ash. Cem Concr Res 31, 1437–1447. https://doi.org/10.1016/S0008-8846(01)00589-0

Buxton, G. V, 2008. An overview of the radiation chemistry of liquids, in: Sciences, E.D.P. (Ed.), Radiation Chemistry: From Basics to Applications in Material and Life Sciences. pp. 3–16.

Bykov, G.L., Gordeev, A. V, Yurik, T.K., Ershov, B.G., 2008. Gas Formation upon gamma-Irradiation of Cement Material. Radiation Chemistry 42, 248–251. https://doi.org/10.1134/S0018143908030041

Cau-dit-Coumes, C., 2013. Alternative Binders to Ordinary Portland Cement for Radwaste Solidification and Stabilization. Springer New York, pp. 171–191. https://doi.org/10.1007/978-1-4614-3445-0_16

Cau-dit-Coumes, C., Courtois, E., Guy, C., Courtois, S., Prene´, S., 2003. Mise au point de ciments phosphocalciques – application au blocage de l'activite´ labile du combustible nucle´aire irradie´ en situation de stockage direct.; Ecole The´matique CNRS-ATILH Physique, Chimie et Me´canique des Mate´riaux Cimentaires, La Colle sur Loup.

Cau Dit Coumes, C., Dhoury, M., Champenois, J.-B., Mercier, C., Damidot, D., 2017. Combined effects of lithium and borate ions on the hydration of calcium sulfoaluminate cement. Cem Concr Res 97, 50–60. https://doi.org/10.1016/j.cemconres.2017.03.006

CEA, 2009. Nuclear waste conditioning.

Champenois, J.-B., Dhoury, M., Coumes, C.C.D., Mercier, C., Revel, B., Bescop, P. Le, Damidot, D., 2015. Influence of sodium borate on the early age hydration of calcium sulfoaluminate cement. Cem Concr Res 70, 83–93. https://doi.org/10.1016/j.cemconres.2014.12.010

Champenois, J.-B., Mesbah, A., Coumes, C.C.D., Renaudin, G., Leroux, F., Mercier, C., Revel, B., Damidot, D., 2012. Crystal structures of Boro-AFm and sBoro-AFt phases. Cem Concr Res 42, 1362–1370. https://doi.org/https://doi.org/10.1016/j.cemconres.2012.06.003

Chen, Q.Y., Tyrer, M., Hills, C.D., Yang, X.M., Carey, P., 2009. Immobilisation of heavy metal in cement-based solidification/stabilisation: A review. Waste Management 29, 390–403. https://doi.org/10.1016/j.wasman.2008.01.019

Choppin, G., Liljenzin, J.-O., Rydberg, J., Ekberg, C., 2013. Nuclear Power Reactors, in: Radiochemistry and Nuclear Chemistry. Elsevier, pp. 655–684. https://doi.org/10.1016/b978-0-12-405897-2.00020-3

Clark, L., Group., T.E., Great Britain. Department of the Environment, T. and the Regions., 1999. The thaumasite form of sulfate attack: risks, diagnosis, remedial works and guidance on new construction; report of the Thaumasite Expert Group. Dep. of the Environment Transport and the Regions, London.

Clark, L., Thaumasite Expert Group., 2002. Thaumasite expert group report: review after three years of experience. 41.

Collett, G., Crammond, N.J., Swamy, R.N., Sharp, J.H., 2004. The role of carbon dioxide in the formation of thaumasite. Cem Concr Res 34, 1599–1612. https://doi.org/10.1016/j.cemconres.2004.02.024

Cornelis, G., Johnson, C.A., Gerven, T. Van, Vandecasteele, C., 2008. Leaching mechanisms of oxyanionic metalloid and metal species in alkaline solid wastes: A review. Applied Geochemistry 23, 955–976. https://doi.org/10.1016/j.apgeochem.2008.02.001

Coumes, C.C.D., Courtois, S., Peysson, S., Ambroise, J., Pera, J., 2009. Calcium sulfoaluminate cement blended with OPC: A potential binder to encapsulate low-level radioactive slurries of complex chemistry. Cem Concr Res 39, 740–747. https://doi.org/10.1016/j.cemconres.2009.05.016

Coumes, C.C.D., Dhoury, M., Champenois, J.B., Mercier, C., Damidot, D., 2017. Combined effects of lithium and borate ions on the hydration of calcium sulfoaluminate cement, in: Cement and Concrete Research. pp. 50–60. https://doi.org/10.1016/j.cemconres.2017.03.006

Craeye, B., Schutter, G. De, Vuye, C., Gerardy, I., 2015. Cement-waste interactions : Hardening self-compacting mortar exposed to gamma radiation. Progress in Nuclear Energy 83, 212–219. https://doi.org/10.1016/j.pnucene.2015.03.019

Crammond, N.J., 2003. The thaumasite form of sulfate attack in the UK. Cem Concr Compos 25, 809–818. https://doi.org/10.1016/S0958-9465(03)00106-9

Csenteyi, L.J., Glasser, F.F.P., Csetenyi, L., Glasser, F.F.P., 1995. Borate retardation of cement set and phase relations in the system Na2O-CaO-B2O3-H2O. Advances in Cement Research 25, 19.

ČSN 73 1371: Non-destructive testing of concrete – Method of ultrasonic pulse testing of concrete, 2012.

ČSN EN 1015-11: Testing methods for mortar for masonry - part 11: Determination of compressive and flexural strength of hardened mortars, 2000.

ČSN EN ISO 12570 (730573) Tepelně vlhkostní chování stavebních materiálů a výrobků - Stanovení vlhkosti sušením při zvýšené teplotě, 2001.

ČSN EN ISO/IEC 17025: Všeobecné požadavky na kompetenci zkušebních a kalibračních laboratoří, 2005.

Czech Radioactive Waste Repository Authority (RAWRA), 2023. Operational radioactive waste repositories [WWW Document]. URL https://www.surao.cz/en/public/operational-repositories/ (accessed 9.23.23).

Davidovitz, J., Morris, M., 1988. The Pyramids: An Enigma Solved. Dorset Press.

de Groot, G.J., van der Sloot, H.A., 1992. Determination of leaching characteristics of waste materials leading to environmental product certification, in: Gilliam, T., Wiles, C. (Eds.), Stabilization and Solidification of Hazardous, Radioactive, and Mixed Wastes, 2nd Volume. pp. 149–170. https://doi.org/10/978-0-8031-5186-4

Demribas, A., Karslioglu, S., 1995. The effect of boric acid sludges containing borogypsum on properties of cement. Cem Concr Res 25, 1381–1384. https://doi.org/10.1016/0008-8846(95)00130-5

Dewynter, V., Chomat, L., Guillot, W., Amblard, E., Durant, D., Cornaton, M., Bourbon, X., 2017. Concrete radiolysis effect on steels corrosion and comparison with non-irradiated material, in: EUROCORR 2017 Conference, 20th INTERNATIONAL CORROSION CONGRESS, & Process Safety Congress 2017.

Dhir, R.K., Paine, K.A., Tang, A.M.C. (Albert M.C., University of Dundee. Concrete Technology Unit., 2005. CONCRETE BEHAVIOUR IN ENGINEERING BARRIERS FOR LOW AND MEDIUM RADIOACTIVE WASTE REPOSITORY: EXAMPLE OF El CABRIL, CORDOBA, SPAIN 186. https://doi.org/10.1680/ROCINF.34099.0001

Döbelin, N., Kleeberg, R., Doebelin, N., Kleeberg, R., 2015. Profex: a graphical user interface for the Rietveld refinement program BGMN 48, 1573–1580. https://doi.org/10.1107/S1600576715014685

Dyer, T., 2014. Concrete durability. CRC Press-Taylor & Francis Group.

El-Dakroury, A., Gasser, M.S., 2008. Rice husk ash (RHA) as cement admixture for immobilization of liquid radioactive waste at different temperatures. Journal of Nuclear Materials 381, 271–277. https://doi.org/10.1016/j.jnucmat.2008.08.026

El-Kamash, A.M., El-Naggar, M.R., El-Dessouky, M.I., 2006. Immobilization of cesium and strontium radionuclides in zeolite-cement blends. J Hazard Mater 136, 310–316. https://doi.org/10.1016/j.jhazmat.2005.12.020

Elleuch, L., Dubois, F., Rappeneau, J., 1972. Effects of neutron radiation on special concretes and their components. Special Publication of The American Concrete Institute 43 1071–1108.

Fernandez-Jimeneza, A., Macpheeb, D.E., Lachowskib, E.E., Palomoa, A., 2005. Immobilization of caesium in alkaline activated fly ash matrix. Journal of Nuclear Materials 346, 185–193.

Ferreira, E.G.A., Yokaichiya, F., Marumo, J.T., Vicente, R., Garcia-Moreno, F., Kamm, P.H., Klaus, M., Russina, M., Gunther, G., Jimenez, C.E., Franco, M.K.K.D., 2018. Influence of the irradiation in cement for the Brazilian radioactive waste repositories: Characterization via X-ray diffraction, X-ray tomography and quasielastic neutron scattering. Physica B Condens Matter 551, 256–261. https://doi.org/10.1016/j.physb.2018.01.018

Foct, F., Giandomenico, M.V. Di, Bouniol, P., 2013. Modelling of hydrogen production from pore radiolysis in cemented intermediate level waste water, in: Sciences, E.D.P. (Ed.), NUCPERF. pp. 0–7.

Frizon, F., Cau-dit-Coumes, C., 2006. Cementation of ILW ion exchange resins: Impact of sulfate ions released by radiolysis on hydrated matrix. Journal of Nuclear Materials 359, 162–173. https://doi.org/10.1016/J.JNUCMAT.2006.08.024

Fryda, H., Vetter, G., Ollitrault-Fichet, R., Boch, P., Capmas, A., 1996. Formation of chabazite in mixes of calcium aluminate cement and silica fume used for caesium immobilization. Advances in Cement Research 8, 29–39. https://doi.org/10.1680/adcr.1996.8.29.29

Fujiwara, K., Ito, M., Sasanuma, M., Tanaka, H., Hirotani, K., Onizawa, K., Suzuki, M., Amezawa, H., 2009. Experimental Study of the Effect of Radiation Exposure to Concrete. 20th International Conference on Structural Mechanics in Reactor Technology (SMiRT 20).

Galan, I., Steindl, F.R., Grengg, C., Dietzel, M., Mittermayr, F., 2023. On the hydration of ternesite and the formation of thaumasite. Cem Concr Res 172, 107212. https://doi.org/10.1016/J.CEMCONRES.2023.107212

García Calvo, J.L., Hidalgo, A., Alonso, C., Fernández Luco, L., 2010. Development of low-pH cementitious materials for HLRW repositories: Resistance against ground waters aggression. Cem Concr Res 40, 1290–1297. https://doi.org/10.1016/J.CEMCONRES.2009.11.008

Gaze, M.E., Crammond, N.J., 2000. The formation of thaumasite in a cement:lime:sand mortar exposed to cold magnesium and potassium sulfate solutions. Cem Concr Compos 22, 209–222. https://doi.org/10.1016/S0958-9465(00)00002-0

Goñi, S., Guerrero, A., Lorenzo, M.P., 2006. Efficiency of fly ash belite cement and zeolite matrices for immobilizing cesium. J Hazard Mater 137, 1608–1617. https://doi.org/10.1016/j.jhazmat.2006.04.059

Goto, S., Suenaga, K., Kado, K., Fukuhara, M., 1995. Calcium Silicate Carbonation Products. Journal of the American Ceramic Society 78, 2867–2872. https://doi.org/j.1151-2916.1995.tb09057.x

Gougar, M.L.D., Scheetz, B.E., Roy, D.M., 1996. Ettringite and C-S-H Portland cement phases for waste ion immobilization: A review. Waste Management 16, 295–303. https://doi.org/10.1016/S0956-053X(96)00072-4

Guerrero, A., Goñi, S., Allegro, V.R., 2009. Effect of temperature on the durability of class C fly ash belite cement in simulated radioactive liquid waste: Synergy of chloride and sulphate ions. J Hazard Mater 165, 903–908. https://doi.org/10.1016/J.JHAZMAT.2008.10.073

Hilloulin, B., Robira, M., Loukili, A., 2018. Coupling statistical indentation and microscopy to evaluate micromechanical properties of materials: Application to viscoelastic behavior of irradiated mortars. Cem Concr Compos 94, 153–165. https://doi.org/10.1016/j.cemconcomp.2018.09.008

Hilsdorf, H.K., Kropp, J., Koch, H.J., 1978. The Effects of Nuclear Radiation on the Mechanicals Properties of Concrete. American Concrete Institute Special Publication SP- 55 223–251.

Hlaváč, Z., Dewynter-Marty, V., Koťátková, J., Gulliot, W., Tutour, P. Le, 2018. Study of concrete radiation ageing, in: TINCE 2018. pp. 1–8.

ICHIKAWA, T., KOIZUMI, H., 2002. Possibility of Radiation-Induced Degradation of Concrete by Alkali-Silica Reaction of Aggregates. J Nucl Sci Technol 39, 880–884. https://doi.org/10.1080/18811248.2002.9715272

ICSD database FIZ Karlsruhe, 2018.

International Atomic Energy Agency, 2020. Design Principles and Approaches for Radioactive Waste Repositories, Nuclear En. ed. International Atomic Energy Agency.

International Atomic Energy Agency, 2013. The Behaviours of Cementitious Materials in Long Term Storage and Disposal of Radioactive Waste.

International Atomic Energy Agency, 2009. Classification of radioactive waste: general safety guide.

International Atomic Energy Agency, 2001. Handling and Processing of Radioactive Waste from Nuclear Applications.

International Atomic Energy Agency, 1996. International basic safety standards for protection against ionizing radiation and for the safety of radiation sources.

International Centre for Diffraction Data, 2019. JCPDS PDF-4 database.

Kaplan, M.F., 1989. Concrete radiation shielding. Harlow: Longman Scientific.

Khalil, M.Y., Merz, E., 1994. Immobilization of intermediate-level wastes in geopolymers. Journal of Nuclear Materials 211, 141–148. https://doi.org/10.1016/0022-3115(94)90364-6

Kirkegaard, P., Bjergbakke, E., Markert, F., 2014. CHEMSIMUL — a tool for simulating chemical reaction systems 1–14.

Kontani, O., Ishizawa, A., Maruyama, I., Takizawa, M., 2012. Evaluation of irradiation effects on concrete structure.

Koťátková, J., 2018. THE EFFECT OF SUPERPLASTICIZERS ON THE PROPERTIES OF GAMMA IRRADIATED CEMENT PASTES. Ceramics - Silikaty 306–310. https://doi.org/10.13168/cs.2018.0026

Koťátková, J., Kolář, K., Zatloukal, J., 2018. Setting and hardening conditions of cement pastes encapsulating evaporator concentrate, in: NUWCEM 2018 - Cement-Based Materials for Nuclear Wate. pp. 1–4.

Koťátková, J., Zatloukal, J., Kolář, K., 2020. Mechanical and setting/hardening conditions of cement pastes for evaporator concentrates incorporating admixtures, in: INTERNATIONAL CONFERENCE OF NUMERICAL ANALYSIS AND APPLIED MATHEMATICS ICNAAM 2019. AIP Publishing, p. 70004. https://doi.org/10.1063/5.0031157

Koťátková, J., Zatloukal, J., Reiterman, P., Kolář, K., 2017a. Concrete and cement composites used for radioactive waste deposition. J Environ Radioact 178–179, 147–155. https://doi.org/10.1016/j.jenvrad.2017.08.012

Koťátková, J., Zatloukal, J., Reiterman, P., Kolář, K., 2017b. Concrete and cement composites used for radioactive waste deposition. J Environ Radioact 178–179, 147–155. https://doi.org/10.1016/j.jenvrad.2017.08.012

Lafond, E., dit Coumes., C.C., Gauffinet, S., Chartier, D., Stefan, L.P., Bescop, P. Le, 2017. Solidification of ion exchange resins saturated with Na+ ions: Comparison of matrices based on Portland and blast furnace slag cement. Journal of Nuclear Materials 483, 121–131.

Leemann, A., Loser, R., 2011. Analysis of concrete in a vertical ventilation shaft exposed to sulfate-containing groundwater for 45 years. Cem Concr Compos 33, 74–83. https://doi.org/10.1016/J.CEMCONCOMP.2010.09.012

Lee, W.E., Ojovan, M.I., Jantzen, C.M., 2013. Radioactive waste management and contaminated site clean-up : processes, technologies and international experience, 1st ed. Woodhead Publishing.

Leitner, C., Neubauer, F., 2011. Tectonic significance of structures within the salt de-posits Altaussee and Berchtesgaden-Bad Dürrnberg, Northern Calcareous Alps. Austrian Journal of Earth Sciences 104, 2–21.

Lenoir, M., Grandjean, A., Ledieu, A., Dussossoy, J.L., Cau Dit Comes, C., Barre, Y., Tronche, E., 2009. Sulphate in Liquid Nuclear Waste: from Production to Containment|INIS, in: Proceedings of the GLOBAL 2009 Congress - The Nuclear Fuel Cycle: Sustainable Options and Industrial Perspectives.

Lichvar, P., Rozloznik, M., Sekely, S., 2013. Behaviour of Aluminosilicate Inorganic Matrix During and After Solidification of Radioactive Sludge and Radioactive Spent Resins and Their Mixtures. International Atomic Energy Agency, Waste Technology Section, pp. 1–16.

Lieber, W., 1973. Effect on inorganic admixtures on the setting and hardening of portland cement. Zement-Kalk-Gips 2, 75–79.

Łowińska-Kluge, A., Piszora, P., 2008. Effect of Gamma Irradiation on Cement Composites Observed with XRD and SEM Methods in the Range of Radiation Dose 0-1409 MGy. Acta Phys Pol A 114, 399–411. https://doi.org/10.12693/APhysPolA.114.399

Ma, B., Gao, X., Byars, E.A., Zhou, Q., 2006. Thaumasite formation in a tunnel of Bapanxia Dam in Western China. Cem Concr Res 36, 716–722. https://doi.org/10.1016/J.CEMCONRES.2005.10.011

Mallants, D., Ochs, M., Wang, L., 2016. Radionuclide and Metal Sorption on Cement and Concrete. Springer Verlag.

Maruyama, I., Ishikawa, S., Yasukouchi, J., Sawada, S., Kurihara, R., Takizawa, M., Kontani, O., 2018. Impact of gamma-ray irradiation on hardened white Portland cement pastes exposed to atmosphere. Cem Concr Res 108, 59–71. https://doi.org/10.1016/j.cemconres.2018.03.005

Maruyama, I., Kontani, O., Takizawa, M., Sawada, S., Ishikawa, S., Ishikawao, S., Yasukouchi, J., Sato, O., Etoh, J., Igari, T., 2017. Development of soundness assessment procedure for concrete members affected by neutron and gamma-ray irradiation. Journal of Advanced Concrete Technology 15, 440–523. https://doi.org/10.3151/jact.15.440

Masonnaye, J.M.C., 1993. Immobilization of borates and phosphates with saturated lime solutions. Solid State Ion 56, 133–139.

Mayberry, J.L., Huebner, T.L., Ross, W., Nakaoka, R., Schumacher, R., Cunnane, J., Singh, D., Darnell, R., Greenhalgh, W., 1993. Technical area status report for low-level mixed waste final waste forms. Volume 2, Appendices. https://doi.org/10.2172/10184155

Ma, Y., Hu, J., Ye, G., 2013. The pore structure and permeability of alkali activated fly ash. Fuel 104, 771–780. https://doi.org/10.1016/j.fuel.2012.05.034

McCulloch, C.E., 1985. Cements in Radioactive Waste Disposal: Some Mineralogical Considerations. Mineral Mag 49, 211–221. https://doi.org/10.1180/minmag.1985.049.351.08

McDowall, D.C., 1971. The effects of gamma radiation on the creep properties of concrete.

McNearney, S., Davidson, I., Mottershead, D., Brocklehurst, J.E., Kelly, B.T., 1971. The effects of reactor radiation on concrete.

Mittermayr, F., Baldermann, A., Kurta, C., Rinder, T., Klammer, D., Leis, A., Tritthart, J., Dietzel, M., 2013. Evaporation — a key mechanism for the thaumasite form of sulfate attack. Cem Concr Res 49, 55–64. https://doi.org/10.1016/J.CEMCONRES.2013.03.003

Neubauer, F., Schorn, A., 2011. Emplacement of an evaporitic mélange nappe in central Northern Calcareous Alps: Evidence from the Moosegg Klippe (Austria). Austrian Journal of Earth Sciences 104, 22–46.

Nobst, P., Stark, J., 2003. Investigations on the influence of cement type on thaumasite formation. Cem Concr Compos 25, 899–906. https://doi.org/10.1016/S0958-9465(03)00118-5

Nuclear Energy Agency (NEA), 2018. Microbial Influence on the Performance of Subsurface, Salt-Based Radioactive Waste Repositories. Boulogne-Billancourt, France.

Nuclear Energy Agency (NEA), 2014. Natural Analogues for Safety Cases of Repositories in Rock Salt: Salt Club Workshop Proceedings, in: Salt Club Workhop. Braunschweig, Germany, p. 269.

Ojovan, M.I., 2011. Handbook of advanced radioactive waste conditioning technologies.

Ojovan, N. V., Startceva, I. V., Barinov, A.S., Ojovan, M.I., Bacon, D.H., McGrail, B.P., Vienna, J.D., 2004. Product consistency test of fully radioactive high-sodium content borosilicate glass K-26, in: Materials Research Society Symposium Proceedings. Materials Research Society, pp. 339–344. https://doi.org/10.1557/proc-824-cc8.14

Oliver, W.C., Pharr, G.M., 1992. An improved technique for determining hardness and elastic modulus using load and displacement sensing indentation experiments. J Mater Res 7, 1564–1583. https://doi.org/10.1557/JMR.1992.1564

Pape, Y. Le, 2015. Structural effects of radiation-induced volumetric expansion onunreinforced concrete biological shields. Nuclear Engineering and Design 295, 534–548. https://doi.org/10.1016/j.nucengdes.2015.09.018

Pape, Y. Le, Giorla, A., Sanahuja, J., 2016. Combined Effects of Temperature and Irradiation on Concrete Damage. Journal of Advanced Concrete Technology 14, 70–86. https://doi.org/10.3151/jact.14.70

Park, S.-S., Kwon, S.-J., Jung, S.H., 2012. Analysis technique for chloride penetration in cracked concrete using equivalent diffusion and permeation. Constr Build Mater 29, 183–192. https://doi.org/10.1016/j.conbuildmat.2011.09.019

Pátzay, G., Weiser, L., Feil, F., Patek, G., 2011. Analysis and Selective Treatment of Radioactive Waste Waters and Sludges. Waste Water - Evaluation and Management. https://doi.org/10.5772/15457

Plecas, I, Dimovic, S., Smiciklas, I., 2009. Influence of bentonite and zeolite in cementation of dry radioactive evaporator concentrates. Appl Clay Sci 43, 9–12. https://doi.org/10.1016/j.clay.2008.07.003

Plecas, I., Dimovic, S., Smiciklas, I., 2009. Influence of bentonite and zeolite in cementation of dry radioactive evaporator concentrates. Appl Clay Sci 43, 9–12. https://doi.org/10.1016/j.clay.2008.07.003

Plecas, I, Dimovic, S., Smiciklas, I., 2006. Utilization of bentonite and zeolite in cementation of dry radioactive evaporator concentrate. Progress in Nuclear Energy 48, 495–503. https://doi.org/10.1016/j.pnucene.2005.12.001

Plecas, I., Dimovic, S., Smiciklas, I., 2006. Utilization of bentonite and zeolite in cementation of dry radioactive evaporator concentrate. Progress in Nuclear Energy 48, 495–503. https://doi.org/10.1016/j.pnucene.2005.12.001

Plecas, I., Pavlovic, S., Pavlovic, R., 2004. Leaching behavior of 60Co and 137Cs from spent ion exchange resins in cement–bentonite clay matrix. Journal of Nuclear Materials 327, 171–174. https://doi.org/10.1016/j.jnucmat.2004.02.001

Pospíšil, K., Frýbort, A., Kratochvíl, A., Macháčková, J., 2008. Scanning Electron Microscopy Method as a Tool for the Evaluation of Selected Materials Microstructure. http://tots.upol.cz/doi/10.5507/tots.2008.002.html 1, 13–20. https://doi.org/10.5507/TOTS.2008.002

Rahman, M.M., Bassuoni, M.T., 2014. Thaumasite sulfate attack on concrete: Mechanisms, influential factors and mitigation. Constr Build Mater 73, 652–662. https://doi.org/10.1016/J.CONBUILDMAT.2014.09.034

Rahman, R.O.A., Ibrahium, H.A., Hung, Y.-T., 2011. Liquid Radioactive Wastes Treatment: A Review. Water (Basel) 3, 551–565. https://doi.org/10.3390/w3020551

Rahman, R.O.A., Zaki, A.A., 2020. Comparative analysis of nuclear waste solidification performance models: Spent ion exchanger-cement based wasteforms. Process Safety and Environmental Protection 136, 115–125. https://doi.org/10.1016/j.psep.2019.12.038

Rakhimova, N., 2022. Recent Advances in Alternative Cementitious Materials for Nuclear Waste Immobilization: A Review. Sustainability 2023, Vol. 15, Page 689 15, 689. https://doi.org/10.3390/SU15010689

Rakhimova, N.R., Rakhimov, R.Z., Morozov, V.P., Potapova, L.I., Osin, Y.N., 2017. Mechanism of solidification of simulated borate liquid wastes with sodium silicate activated slag cements. J Clean Prod 149, 60–69. https://doi.org/10.1016/j.jclepro.2017.02.066

Ramachandran, V.S., Lowery, M.S., 1992. Conduction calorimetric investigation of the effect of retarders on the hydration of Portland cement. Thermochim Acta 195, 373–387. https://doi.org/10.1016/0040-6031(92)80081-7

Ramezanianpour, A.M., Hooton, R.D., 2013. Sulfate resistance of Portland-limestone cements in combination with supplementary cementitious materials. Materials and Structures/Materiaux et Constructions 46, 1061–1073. https://doi.org/10.1617/S11527-012-9953-8

Ramírez, S., Cuevas, J., Vigil, R., Leguey, S., 2002. Hydrothermal alteration of "La Serrata" bentonite (Almeria, Spain) by alkaline solutions. Appl Clay Sci 21, 257–269. https://doi.org/10.1016/S0169-1317(02)00087-X

Reches, Y., 2019. A multi-scale review of the effects of gamma radiation on concrete. Results in Materials 2, 100039. https://doi.org/10.1016/j.rinma.2019.100039

Romer, M., Holzer, L., Pfiffner, M., 2003. Swiss tunnel structures: Concrete damage by formation of thaumasite. Cem Concr Compos 25, 1111–1117. https://doi.org/10.1016/S0958-9465(03)00141-0

Rosseel, T.M., Maruyama, I., Pape, Y. Le, Kontani, O., Giorla, A.B., Remec, I., Wall, J.J., Sircar, M., Andrade, C., Ordonez, M., 2016. Review of the Current State of Knowledge on the Effects of Radiation on Concrete. Journal of Advanced Concrete Technology 14, 368–383. https://doi.org/10.3151/jact.14.368

Roux, C., 1989. Conditioning of Radioactive Concentrates with High Boron Content, Formulation and Characterization.

San, S., Li, N., Tao, Y., Zhang, W., Ching, W.Y., 2018. Understanding the atomic and electronic origin of mechanical property in thaumasite and ettringite mineral crystals. Journal of the American Ceramic Society 101, 5177–5187. https://doi.org/10.1111/JACE.15774

Schmidt, T., Polytechnique, É., De Lausanne, F., Le, P., 2007. Sulfate attack and the role of internal carbonate on the formation of thaumasite. https://doi.org/10.5075/EPFL-THESIS-3853

Shon, J.S., Lee, H.K., Kim, G.Y., Kim, T.J., Ahn, B.G., 2022. Evaluation of Disposal Stability for Cement Solidification of Lime Waste. Materials 2022, Vol. 15, Page 872 15, 872. https://doi.org/10.3390/MA15030872

Siemer, D.D., Olanrewaju, J., Scheetz, B., Grutzeck, M., 2001. Development of hydroceramic waste forms for INEEL calcined waste. Ceramic Transactions 119, 391–398.

Sims, I., Huntley, S.A., 2004. The thaumasite form of sulfate attack-breaking the rules. Cem Concr Compos 26, 837–844. https://doi.org/10.1016/J.CEMCONCOMP.2004.01.002

Singh, D., Barber, D., Wagh, A.S., Strain, R. V, Tlustochowicz, M., 1998. Stabilization and Disposal of Argonne-West Low-level Mixed Wastes in Ceramicrete Waste Forms. Energy Technology Division,Argonne National Laboratory.

Skalny, J., Marchand, J. (Jacques), Odler, I., 2002. Sulfate attack on concrete, 1st Editio. ed.

SKB, 2013. RD&D-programme 2013: Programme for research, development and demonstration of methods for the management and disposal of nuclear wastes.

Slater, D., Floyd, M., Wimpenny, D.E., 2003. A summary of the Highways Agency Thaumasite Investigation in Gloucestershire: the scope of work and main findings. Cem Concr Compos 25, 1067–1076. https://doi.org/10.1016/S0958-9465(03)00131-8

Sommers, J.F., 1969. Gamma Radiation Damage of Structural Concrete Immersed in Water. Health Phys 16, 503–508. https://doi.org/10.1097/00004032-196904000-00011

Soo, P., Milian, L.M., 2001. The effect of gamma radiation on the strength of Portland cement mortars. J Mater Sci Lett 20, 1345–1348.

Šoštarić, S.B., Neubauer, F., 2013. Principle rock types for radioactive waste repositories. Rudarsko Geolosko Naftni Zbornik 24, 11–18.

Sotiriadis, K., Nikolopoulou, E., Tsivilis, S., 2012. Sulfate resistance of limestone cement concrete exposed to combined chloride and sulfate environment at low temperature. Cem Concr Compos 34, 903–910. https://doi.org/10.1016/J.CEMCONCOMP.2012.05.006

Sun, Q., Li, J., Wang, J., 2011a. Effect of borate concentration on solidification of radioactive wastes by different cements. Nuclear Engineering and Design 241, 4341–4345. https://doi.org/10.1016/j.nucengdes.2011.08.040

Sun, Q., Li, J., Wang, J., 2011b. Solidification of borate radioactive resins using sulfoaluminate cement blending with zeolite. Nuclear Engineering and Design 241, 5308–5315. https://doi.org/https://doi.org/10.1016/j.nucengdes.2011.08.028

Sun, Q., Wang, J., 2010. Cementation of radioactive borate liquid waste produced in pressurized water reactors. Nuclear Engineering and Design 240, 3660–3664. https://doi.org/10.1016/j.nucengdes.2010.07.018

Szalo, A., Žatkulák, M., 2000a. Borate Compound Content Reduction in Liquid Radioactive Waste From Nuclear Power Plants With VVER Reactor, in: Nuclear Energy in Central Europe 2000. pp. 1–6.

Szalo, A., Žatkulák, M., 2000b. Borate Compound Content Reduction in Liquid Radioactive Waste From Nuclear Power Plants With VVER Reactor, in: Nuclear Energy in Central Europe 2000. Bled, Slovenia, pp. 1–6.

Terzijski, I., Kocáb, D., Štěpánek, P., Strnad, J., Girgle, F., Šimůnek, P., 2021. Development of Variants of High-Performance Self-Compacting Concrete with Improved Resistance to the Attack of Sulfates. Applied Sciences 2021, Vol. 11, Page 5945 11, 5945. https://doi.org/10.3390/APP11135945

Thaulow, N., Sahu, S., 2004. Mechanism of concrete deterioration due to salt crystallization. Mater Charact 53, 123–127. https://doi.org/10.1016/j.matchar.2004.08.013

Tian, B., Cohen, M.D., 2000. Does gypsum formation during sulfate attack on concrete lead to expansion? Cem Concr Res 30, 117–123. https://doi.org/10.1016/S0008-8846(99)00211-2

Tits, J., Wieland, E., Muller, C.J., Landesmann, C., Bradbury, M.H., 2006. A wet chemistry study of the strontium binding by calcium silicate hydrates. J Colloid Interface Sci 300, 78–87.

Toyohara, M., Kaneko, M., Mitsutsuka, N., Fujihara, H., Saito, N., Murase, T., 2002. Contribution to Understanding Iodine Sorption Mechanism onto Mixed Solid Alumina Cement and Calcium Compounds. J Nucl Sci Technol 39, 950–956. https://doi.org/10.1080/18811248.2002.9715281

Treatment and conditioning of radwaste in nuclear power plants, 2008.

Trtílek, R., 2017. Testing of solidification of semi-liquid radioactive waste.

Trudinger, P.A., 1971. Metals, minerals and microbes. Minerals Science and Engineering 3, 13–25.

Ulm, F.J., Constantinides, G., 2014. The effect of two types of C-S-H on the elasticity of cement-based materials: results from nanoindentation and micromechanical modeling. Cem Concr Res 34, 67–80.

Varlakov, A., Zherebtsov, A., 2021. Innovative and conventional materials and designs of nuclear cementitious systems in radioactive waste management. Sustainability of Life Cycle Management for Nuclear Cementation-Based Technologies 297–338. https://doi.org/10.1016/B978-0-12-818328-1.00004-6

Vejmelková, E., Pavlíková, M., Jerman, M., Černý, R., 2009. Free water intake as means of material characterization. Building Physics 33, 29–44.

Vodák, F., Trtík, K., Sopko, V., Kapičková, O., Demo, P., 2005. Effect of γ-irradiation on strength of concrete for nuclear-safety structures. Cem Concr Res 35, 1447–1451. https://doi.org/10.1016/j.cemconres.2004.10.016

Vodák, F., Vydra, V., Trtík, K., Kapičková, O., 2011. Effect of γ-irradiation on Properties of Harderned Cement Paste. Mater Struct 44, 101–107.

Wagh, A.S., Singh, D., Jeong, S.Y., Strain, R. V, 1997. Ceramicrete stabilization of low-level mixed wastes - a complete story.

Wagh, A.S., Singh, D., Patel, K., Jeong, S., Park, J., 1999a. Salt waste stabilization in chemically bonded phosphate ceramics.

Wagh, A.S., Strain, R., Jeong, S.Y., Reed, D., Krause, T., Singh, D., 1999b. Stabilization of Rocky Flats Pu-contaminated ash within chemically bonded phosphate ceramics. Journal of Nuclear Materials 265, 295–307. https://doi.org/10.1016/S0022-3115(98)00650-3

Warren, J.K., 2006. Evaporites: Sediments, resources and hydrocarbons. Evaporites: Sediments, Resources and Hydrocarbons 1–1035. https://doi.org/10.1007/3-540-32344-9

Wilson, J., Bateman, K., Tachi, Y., 2021. The impact of cement on argillaceous rocks in radioactive waste disposal systems: A review focusing on key processes and remaining issues. Applied Geochemistry 130, 104979. https://doi.org/10.1016/j.apgeochem.2021.104979

World Nuclear Association, 2023. Storage and Disposal Options for Radioactive Waste - World Nuclear Association [WWW Document]. URL https://world-nuclear.org/information-library/nuclear-fuel-cycle/nuclear-waste/storage-and-disposal-of-radioactive-waste.aspx

Xiang, L., Liu, X., Liu, P., Jiang, X., Dai, C., 2020. Mineralogical and hydraulic characteristics of mudstone in the Tamusu candidate area in northwest China for high-level radioactive waste geological disposal. Clay Miner 55, 71–82. https://doi.org/10.1180/CLM.2020.12

Xu, H., Deventer, J.S.J. Van, 2000. The geopolymerisation of alumino-silicate minerals. Int J Miner Process 59, 247–266. https://doi.org/10.1016/S0301-7516(99)00074-5

Zatloukalová, J., Dewynter-Marty, V., Zatloukal, J., Kolář, K., Bernachy-Barbe, F., Bezdička, P., Konvalinka, P., 2020a. Microstructural and micro-mechanical property changes of cement pastes for ILW immobilization due to irradiation. Journal of Nuclear Materials 540. https://doi.org/10.1016/j.jnucmat.2020.152346

Zatloukalová, J., Marty, V.D.-, Zatloukal, J., Kolář, K., Hlaváč, Z., Guillot, W., Konvalinka, P., 2021. Investigation of radiolysis in cement pastes immobilizing simulated evaporator concrentrates. Ann Nucl Energy 151. https://doi.org/10.1016/j.anucene.2020.107901

Zatloukalová, J., Marty, V.D., Zatloukal, J., Kolář, K., Hlaváč, Z., Konvalinka, P., 2020b. Mechanical properties of irradiated cement pastes for immobilization of evaporator concentrates. Progress in Nuclear Energy 127. https://doi.org/10.1016/j.pnucene.2020.103437